Theoretical Analysis of the Steam Pressure Exchange Ejector for an Automotive Air Conditioning Application

By David Gould

B.S. in Mechanical Engineering, May 2005 University of Vermont

Thesis submitted to

The Faculty of
The School of Engineering and Applied Science of The George Washington University in partial satisfaction of the requirement for the degree of Master of Science

August 31, 2009

Thesis directed by

Charles Garris Jr.

Professor of Mechanical and Aerospace Engineering

Acknowledgements

The completion of this thesis couldn't have been done without the guidance and support from my parents and my brothers. Their deep understanding on the many factors that are involved in the completion of the written work has been true testament of their love and patience.

A deep gratitude go to my research colleague and friend, Kartik Bulusu, for his support in developing the MATLAB simulation program and more importantly for keeping the research group's motivation and moral up through all the up and downs that associate with research. It has been a great privilege to work with research partner and friend, Kaustubh Chabukswar, for the mutual contributions on better understanding the physics behind the pressure exchange and ejector concept. I would like to thank my research advisor for his guidance while also providing us independence which is necessary in the learning process in the research field.

I would like also to thank Dr. Eskandarian of George Washington University's CEE Department for supporting the research through the Energy in Transportation Grant. Special thanks go to the GW department and machine shop staff for their flexibility in helping the propulsion research group and providing a close knit community and a reliable and whole heartedly support system. Special thanks go to BSST for providing technical data and specs on the 2005 BMW 530i sedan.

Theoretical Analysis of the Steam Pressure Exchange Ejector for an Automotive Air Conditioning Application

Abstract

The project conducted at The George Washington University is a computer simulation and theoretical analysis of the steam pressure exchange ejector air conditioning system for an automobile at various ejector efficiencies and modeled using the turbomachinery analog. The turbomachinery analog is an idealization of the pressure exchange ejector for thermally energized air conditioning applications. The system is well suited for capturing waste heat from the internal combustion engine exhaust. In particular, the ejector automotive air conditioning system is designed to replace the belt driven compressor and reduce the gasoline consumed and corresponding greenhouse gas emissions. The research involves comparing numerical results from an existing conventional automotive air conditioning system using refrigerant R-134a on an average midsized sedan with the steam pressure exchange ejector air conditioning system on the 2005 BMW 530i midsize sedan. The new air conditioning system contains the ejector and an additional loop consisting of exhaust gas heat exchangers, and a pump in exchange for the compressor. The inclusion of the ejector into the system will cause modifications in the system component design and size, especially in the condenser. Computer simulations consist of an ideal system analysis along with results from a more realistic system based on previous ejector efficiencies, system parameters, and generalized dissipations from equipment. Tests are conducted through computer simulations using MATLAB/Simulink. Further investigation compares the performance and capabilities of the conventional ejector with the pressure exchange ejector to better understand the fundamental differences.

Table of Contents

List of Figures

APPENDIX

List of Tables

Appendix Tables

List of Abbreviations

A/C	Air Conditioning
ASHRAE	American Society of Heating, Refrigeration, & Air Conditioning Engineers
BSST	Research and Develop Company in Thermoelectrics
BTU	British Thermal Unit
CFC	Chlorofluorocarbons
COP	Coefficient of Performance
DEWI	Direct Equivalent Warming Impact
DOE	U.S. Department of Energy
EPA	Environment Protection Agency
ECU	Automotive Engine Electric Control Unit
EU	European Union
EUDC	Extra Urban Driving Cycle
FDFI	Fluid Dynamic Flow Induction
GWP	Global Warming Potential
HEV	Hybrid Electric Vehicles
HFC	Hydrofluorocarbons
hp	Horsepower
IAPWS	Internal Association of the Properties for Water and Steam
$IEWI_m$	Indirect Equivalent Warming Impact (mass of A/C system)
$IEWI_o$	Indirect Equivalent Warming Impact (A/C system in operation)
ISC	Idle Speed Control
LMTD	Log Mean Temperature Difference
MPH	Miles Per Hour
NEDC	New European Drive Cycle
NREL	National Renewable Energy Laboratory
ODP	Ozone Depleting Potential
PE	Pressure Exchange
PHX	Primary Exhaust Heat Exchanger
PNGV	Partnership for New Generation of Vehicles
rpm	Revolutions Per Minute
SAE	Society of Automotive Engineers
SPR	Superheater Heat Exchanger
TEMA	Tubular Exchange Manufacturers Association
TEWI	Total Equivalent Warming Impact
TXV	Thermal Expansion Valve

List of Symbols

A	Heat transfer area, ft^2
A_{tcrss}	Tube cross-sectional area, ft^2
A_R	Equivalent Tube Area, ft^2
Aw	Tube wall area, ft^2
B	Vertical Baffle Spacing, in
cp	Isobaric specific heat of fluid, Btu/lbm °F
C	Tube Clearance, in
CL	Tube Layout Constant
Co	Shah's Correlation Convection number
C_{rto}	Ejector Compression Ratio
CTP	Tube Count Calculation Constant
D	Diameter, in
Deq	Equivalent Diameter of Shell Diameter, in
d	Tube diameter, in
d_h	Hydraulic diameter of flow passage, ft.
ê	Entrainment Ratio
E_{rto}	Ejector Expansion Ratio
f	Dimensionless Fanning friction factor
F_{CB}	Shah's Correlation's Convection Boiling Factor
F_{phx}	LMTD Counterflow Correction Factor
F_o	Shah's Correlation's Enhancement Factor
Fr	Shah's Correlation's Froude number
g	Gravity force, (32.2 ft/ sec^2)
G_{aircnd}	Air Mass Flux through Condenser, lb / sec ft^2
H	Convective heat transfer coefficient, Btu/ft^2 min °F
H_{air}	Air Convection heat transfer coefficient, Btu/ft^2 min °F
h_{cnd}	Condenser Height
H_{tcb}	Tube side Convective Boiling Heat Transfer coefficient, Btu/ft^2 min °F
I	Specific enthalpy of fluid, Btu/lbm
k	Thermal conductivity of fluid, Btu/hr ft °F
K_{FR}	Shah's Correlation Correction Factor
L_{cnd}	Length of Condenser

m Mass flow rate, lbm/min

N_T Number of Tubes in Shell & Tube Heat Exchanger

N_P Number of Passes in Shell & Tube Heat Exchanger

Nu Nusselt Number

P Pressure, lbf/ft^2

Pr Prandtl Number

P_{RT} Tube Pitch Ratio

ΔP Pressure drop, lbf/in^2

Q Heat transfer rate, Btu/min

Re Reynolds Number

St Stanton Number

T Absolute temperature, °F

Tb_{ptch} Tube Pitch, in.

T_M Mean Temperature Difference, °F

T_{LMTD} Log Mean Temperature Difference, °F

u_m Fluid mean velocity, ft/sec

U Overall heat transfer coefficient, Btu/ft^2 hr °R

V_m Fluid mean velocity, ft/sec

W Specific work, ft lbf/lbm

x Refrigerant quality, i.e., vapor mass fraction

Subscripts and Symbols

For thermal, fluid dynamic properties of steam, exhaust, and air in system follow this nonmenclature:

m_{abc} where:

'a' = type of fluid (air, ref [steam refrigerant], exh [exhaust])
'b' = location in system (cond [condenser], evap [evaporator], etc…)
'c' = fluid location in component (i [inlet] or o[outlet])

i.e. – $I_{refcondo}$ = enthalpy of steam refrigerant exiting the condenser

ρ Density, lb/ ft^3

μ Dynamic Viscosity lbm /ft s

σ Free Flow / Frontal Area Ratio

air Air

atm Atmospheric Conditions

boil	Normal boiling properties
blk	Bulk properties
c	Cold side fluid
cmp	Compressor
cndfan	Condenser Fan
cond	Condenser
evap	Evaporator
evapblwr	Evaporator Blower
exh	Exhaust Gas
fshell	Fouling Resistance in shell side
ftube	Fouling Resistance in tube side
h	Hot side fluid
humair	Humid Air
i	Inlet
ins	Inside Diameter
iscmp	Isentropic Compressor Process
istrb	Isentropic Turbine Process
liq	Liquid phase
mix	Mixed flow
o	Outlet
out	Outside Diameter
PHX	Primary Heat Exchanger
pmp	Pump conditions
prim	Preliminary Approximation
ref	Refrigerant
sat	Saturation
shell	Shell-side of Heat Exchanger
sec	Secondary
SPR	Superheater Heat Exchanger
steam	Steam Refrigerant
t	Tube-side of Heat Exchanger
trb	Turbine
vap	Vapor phase state
wall	Wall properties
vent	ventilation

Chapter 1 Introduction

The world has become increasingly aware of the detrimental environmental effects of burning fossil fuels for energy production. The rate of gasoline and energy consumption has been steadily increasing for the past 30 years due to population and economic growth but, more importantly, due to the continuing world dependence on fossil fuels. Improvements in the automotive industry on fuel economy efficiency would make a substantial environmental and economic impact on our society. According to Figure 1.1.1 from the US Department of Energy (DOE), two thirds of all oil consumed in the United States is from the transportation sector. The refining of oil to gasoline for automotive purposes accounted for two thirds of the 42 million barrels of oil per day consumed in the transportation sector in 2004(DOE, 2005). Other petroleum products commonly used for transportation include diesel fuel (used for trucks, buses, railroads, some vessels, and a few passenger autos), jet fuel, and residual fuel oil (used for tankers and other large vessels). Furthermore, personal and commercial automobiles including cargo trucks account for eighty percent of the transportation energy use (DOE, 2005). As noted, gasoline consumption for transportation purposes accounts for a large percentage of energy consumption and dependence on foreign oil. Modifications on the automotive vehicle to produce a more fuel efficient vehicle will have beneficial effects on the reducing oil consumption and the harmful environmental gas emissions.

The world has become progressively more aware of the detrimental environmental effects of fossil fuel burning and its role in the global warming phenomenon. Although the automotive air conditioning use in the U.S. is seasonal, reports reveal that around 23.5 gallons of gasoline for the average domestic vehicle's 696 yearly gallons of gasoline are consumed due to air conditioning (Bhatti, 1999).

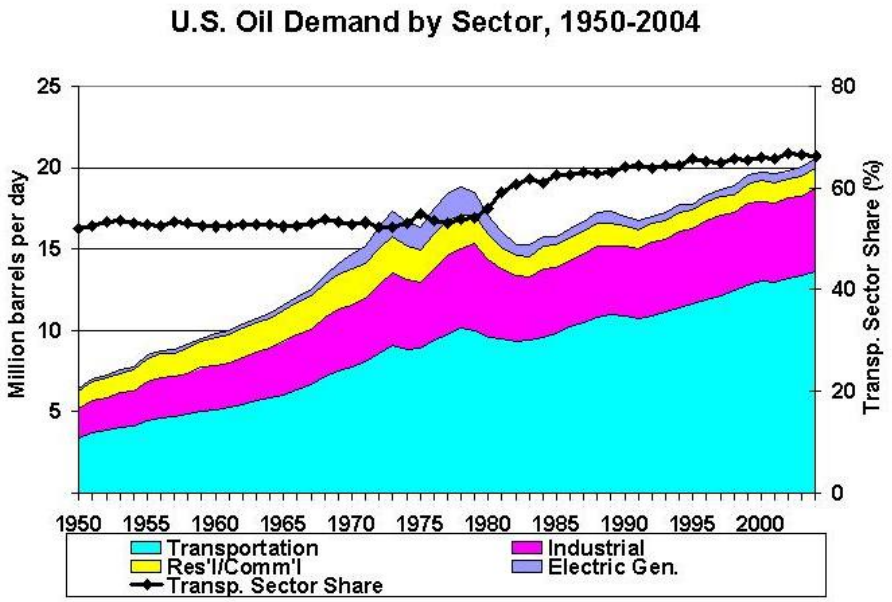

Figure 1.1.1 U.S Oil Demand based on Energy Use Sectors Source: 2005 *Annual Energy Review*

The new generation of hybrid vehicles and downsizing of internal combustion engines for better fuel economy has created a greater impact of the A/C system on the vehicle's total energy efficiency and emissions. Tests at the Clean Air Vehicle Technology Center have reported 28% loss in fuel economy for a light duty vehicle when the A/C system was on. The center also reported that the A/C system creates an 81% increase in nitrogen oxide emissions and a 30% increase in non methane hydrocarbons which are contributors to acid rain and global warming (Hendricks, 2001). Larger impact on the more energy efficient hybrid electric vehicles (HEV) was reported at the National Renewable Energy Laboratory (NREL). Tests conducted on the HEV Toyota Prius and Honda Insight at NREL reported 30-35% decrease in fuel economy when the A/C was on (Hendricks, 2001). Both tests reveal that there is room for improvement for energy efficiency in the automotive A/C industry.

The novel pressure exchange ejector invention by The George Washington University's Professor Charles Garris Jr. may aid in producing a more energy

efficient automotive air conditioning system. The research and theory is focused on using the pressure exchange ejector and a low power pump as a replacement for the compressor in the typical automotive vapor compression air conditioning system. Previous studies and results from the traditional automobile air conditioning systems and previous experiments of the conventional ejector air conditioning system will aid in the comparison with the innovative pressure exchange ejector air conditioning system.

The comparison between the innovative pressure exchange ejector and conventional air condition systems involves setting similar environment conditions of the automotive surroundings, vehicular speed, and cooling capacity. The collection of all these input variables are imported into a custom pressure exchange (PE) ejector air conditioning software algorithm designed in MATLAB where integrated fluid dynamics and heat transfer equations determine the system's coefficient of performance, energy use, pressure drops, heat exchangers' total surface area and volume. This air conditioning system consists of an additional loop with two waste heat recovery heat exchangers and a pump to power and energize the ejector's primary flow. The air conditioning loop in the system enters the secondary inlet of the ejector and consists of the typical components of an air conditioning system: condenser, throttling device, and evaporator. All components will be analyzed and monitored during simulations. The main objective of the MATLAB program is to monitor the properties of each component of the steam PE ejector A/C system as the ejector efficiency is modified. Sizing parameters of all the heat exchangers and required waste heat from the exhaust waste heat recovery loop will be one of the important factors in determining the lowest ejector efficiency attainable before failure based on the design conditions and cooling loads. Exhaust gas temperatures along the

exhaust system have been collected from two experimental and computer simulations tests on the 2005 BMW 530i sedan from BSST, a research and develop thermoelectric company (LaGrandeur, 2006). After designing the steam pressures and temperatures entering and exiting each component of the A/C system based on the cooling load and cabin and outside temperatures, the mass flows through each loop was determined at various ejector efficiencies. From these results, the heat demand to run the ejector was determined and increased as the efficiency decreased. The failure of the steam pressure exchange system was then discovered to occur at an ejector efficiency of 40.5% due to the ejector's excessive thermal heat demand from the engine exhaust system. The steam pressure exchange ejector A/C system at ideal conditions to 40.5% ejector efficiency are compared directly to the conventional R-134a vapor compression air conditioning system results produced by M.S. Bhatti of Delphi Thermal Systems where similar cooling loads, vehicle conditions, and environmental conditions were applied. An additional analysis was conducted on a 22.5% ejector efficiency which represents the average conventional ejector efficiency using theoretical results and the turbomachinery analog. Since the efficiency is below 40.5% the system for this condition assumes that the ejector's excessive thermal input demand could be provided from an additional heat exchanger recovering heat from the engine coolant. The additional conventional ejector analysis provided a baseline for the patented and limited experimented pressure exchange ejector. The three ejector efficiencies of 100% (ideal), 40.5%, and 22.5% are specifically analyzed for comparison to the conventional R-134a system based on coefficients of performance, energy savings, vehicle fuel economy, global warming impact, and equipment sizing and weight.

Chapter 2 Current Air Conditioning Technology

The novel pressure exchange ejector automotive air conditioning system is a combination of modifications to the conventional ejector and the automotive vapor compression air conditioning system. To better understand the final design of this two loop air conditioning system, this chapter will briefly detail the existing conventional automotive air conditioning (A/C) system and the conventional ejector automotive air conditioning system.

2.1 Automotive Air Conditioning System

The basic conventional air conditioning system for automobiles is a reverse Rankine vapor compression system consisting of five main components. The components in the system are the compressor, condenser, evaporator, expansion device, and an accumulator to assure the refrigerant entering the compressor is a vapor. A receiver/drier device downstream of the condenser may also be included if the expansion device is a thermostatic expansion valve which can only operate if liquid flow is passing through. Figure 2.1.1 details a typical automotive air conditioning system along with sensors to help better control and adjust to changing refrigerant conditions and outside environment. The compressor is belt driven by the vehicle's engine and begins the air conditioning process by increasing temperature and pressure of the refrigerant vapor. The increase of vapor pressure causes an increase to the refrigerant condensation temperature. The refrigerant vapor is transferred into the condenser which is generally located under the car hood and in the front section of the car to optimize on the wind created when the car is in motion; referred to as ram air.

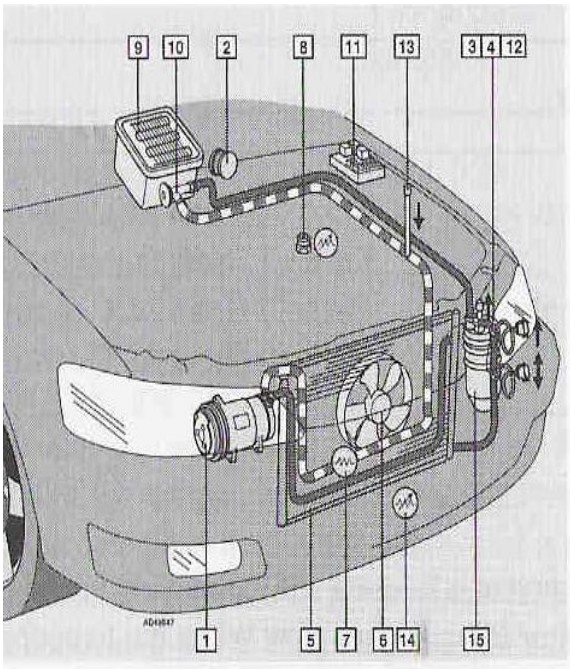

No.	Components
1	A/C compressor clutch
2	A/C/heater blower motor
3	A/C refrigerant high pressure switch
4	A/C refrigerant triple pressure switch
5	Condenser
6	Engine coolant blower motor
7	Engine coolant blower motor resistor
8	Engine coolant temperature (ECT) sensor
9	Evaporator – behind fascia
10	Expansion valve
11	Fuse box/relay plate
12	High pressure service connector
13	Low pressure service connector
14	Outside air temperature sensor – under front bumper
15	Receiver-drier

Figure 2.1.1 Typical Automotive Air Conditioning system run by a compressor driven vapor compression cycle including all the accompanying components (Autodata Ltd).

A condenser or joint purposed radiator/condenser fan is used to cool and condense the refrigerant vapor when the vehicle is not in motion. The requirement to condense the refrigerant vapor into liquid in the condenser is through a refrigerant condensation temperature higher than the ambient air temperature. During this process, the ambient air is absorbing the heat as it passes through the condenser and rising in temperature. Negligible pressure drop occurs in the refrigerant condensation process where refrigerant pressure and corresponding condensation temperature remain constant which allow for a consistent high temperature difference between the air and refrigerant temperatures for optimal heat transfer. Since the condenser is generally placed right in front of the radiator, a system design constraint is that the automotive condenser and engine cooling radiator must use the same air for cooling. Depending on the engine load and engine rpm, the air temperature rise through the

condenser is limited by the engine heat rejection requirement which as a result limits the effectiveness of the condenser. Once the liquid refrigerant leaves the condenser, the system reduces the pressure of the liquid using an expansion device such as the thermostatic expansion valve or capillary orifice tube in order to lower the boiling point temperature of the refrigerant as it enters the evaporator. The refrigerant boiling point pressure is critical in order to achieve a corresponding boiling temperature at or below the desired cabin cooling temperature. The expansion process allows for optimum absorption of heat from the refrigerant's latent heat of vaporization. The liquid located in the evaporator piping absorbs heat from air recirculated from the cabin and/or the air vented from the exterior. This warm air is blown across the evaporator blower and its heat is absorbed by the liquid refrigerant and causes the refrigerant to change phase into a low-pressure refrigerant vapor. The air having its heat removed is blown into the vehicle interior cabin. The temperature difference between the refrigerant and the surrounding air is a key factor in optimizing on heat transfer. Typical refrigerant such as R134a contain non-pressurized boiling temperatures of -5.8° F (–21°C). This refrigerant is required to be pressurized above atmospheric pressure through the evaporator in order to raise its boiling temperature above the freezing point of water 32°F (0°C). The reason for the requirement is to prevent condensate from freezing on the exterior surface of the evaporator. Evaporators contain methods of draining the water vapor from the air that condenses on the exterior evaporator surface. Condensate or ice on the exterior surface of the evaporator would block air flow from the evaporator blower creating a decrease in heat transfer and air flow and resulting in poor evaporator performance.

Proper vapor compression cycle design optimizes the pressure of the refrigerant to control the refrigerant evaporation and condensation temperatures. The

greater the difference between these controlled temperatures with the surrounding air temperature, the higher the heat transfer rate and heat exchanger efficiency.

The rate of heat transfer for convection is analyzed using Newton's law of convection and Fourier's law for conduction where both are dependent on the temperature gradient.

$$q = h\ A\ (T_{refi} - T_{airi}) \qquad 2.1.1$$

Fourier's Law of conduction:

$$q = k\ A\ (T_i - T_o) \qquad 2.1.2$$

The automobile's limitation of space underneath the hood has forced engineers to reduce the physical size of the condenser. Thus, as a result the efficiency of the air conditioning system is reduced to avoid altering the body's infrastructure or creating a negative effect on other components of the drive train system. The high temperatures underneath the hood during the hot summer months and the battle for cool air between the engine coolant radiator and air conditioning (A/C) condenser have created a compromised location for the condenser. In both cases, the radiator and condenser need to take advantage of the ram air while also not diminishing the aerodynamics of the vehicle. The majority of the automotive companies have placed the A/C condenser in the front of the car and right behind the front bumper as shown in Figure 2.1.1. The engine radiator is stacked behind the condenser and allowing the same ram air to pass through. This location optimizes the access of direct forced convection from the ram air created by the moving car. However since the two heat exchangers are stacked one behind the other, the condenser is limited to raising the temperature of the passing air of 20 –25 degrees Fahrenheit under medium to high engine load and 50-70°F during low engine load or idling (Bhatti, 1999). These

constraints allow sufficient heat transfer between the air and the radiator downstream from the A/C condenser

The air conditioning industry has developed a dimensionless performance parameter in order to compare one system with another. That parameter refers to the coefficient of performance (COP) where the refrigerant cooling capacity is compared with the work needed to achieve that cooling. There are two typical types of COP with one defined as the ratio of cooling to the work done on the refrigerant and referred to as the cycle coefficient of performance (COP_{cycle}). The other type, referred to as system coefficient of performance (COP_{system}), is the ratio of cooling to the total work done as a system including the fan and blower work needed for convection heat transfer from the air. Section 6.2 describes more in detail of the variables involved in the COP analysis. The cycle coefficient of performance calculation is shown in Equation 2.1.3 where its value decreases as more work is needed from the compressor.

$$COP_{cycle} = \frac{Q_{evap}}{W_{cycle}} \qquad 2.1.3$$

$$COP_{system} = \frac{Q_{evap}}{W_{system}} \qquad 2.1.4$$

Traditionally a competitive COP_{cycle} for an automotive air conditioning system ranges from 1 to 3 in using a variety of alternative refrigerants like R-134a, R-152a, and hydrocarbons such as propane and ammonia (Ghodbane,1999). Section 2.1.5 details the thermodynamic and environmental evaluation behind the universal use of R-134a for automotive air conditioning application and its high global warming potential that has been neglected as a concern for the past 30 years (Koban, 2007). The recent increasing environmental global warming concern of refrigerant emissions has caused the slow transitional banning process of the R-134a for air conditioning

and refrigeration use in Europe (Ghobane, 1999). This has created new innovative air conditioning systems and refrigerants as potential replacements. These alternative air conditioning systems are described in further detail in Section 2.1.7 with a direct comparison of global warming impact (GWP) between all alternative A/C systems and the steam pressure exchange ejector A/C system in section 6.2.4.

2.1.1 Compressor

In the conventional automotive air conditioning system, the driver of the system lies in the compressor which takes the low pressure refrigerant vapor from the evaporator and pressurizes it to higher pressure to attain a higher condensation temperature. Once the pressure is met, the refrigerant is released into the condenser to be cooled at constant pressure. For non-electric vehicles, the compressors used are mechanically driven by the engine through a belt as displayed in Figure 2.1.2. For hybrid electric vehicles, compressors are usually powered by electric motors. Further components such as the water pump for engine cooling and alternator for recharging the engine battery are belt driven and add to engine load on the vehicle. When the engine is running, the mechanically driven compressor is engaged through a magnetic clutch that is turned on by the passenger. This action enables the drive plate to attract towards the drive belt pulley and is held as one unit. So as the A/C system provides cool air to the cabin, the compressor rotational speed matches the engine rotational speed. As a result the compressor is designed primary to meet the cooling demands at low engine rpm and loses efficiency at higher engine rpm where the compressor rotational speed exceeds what is needed for the cooling load. Compressor fuel efficiency has improved through the development of a variable capacity compressor with a control valve that varies its intake and outtake volumes based on the demands of cooling system. This also reduces the wear of the magnetic clutch plate and

continuous on/off cycles that a non-variable compressor performs. Mechanical compressors contain three main styles based on how it mechanically compresses the vapor refrigerant: reciprocating (crank and axial piston), rotary (vane) , and oscillating (scroll type – helix) where the rotary vane are most commonly used compressor for automotive air conditioning applications and can be designed as a variable capacity type (Daly, 2006). The isentropic efficiencies for each compressor varies based on different mechanical design where scroll compressors range in 65 to 75 % efficiency. The high speed centrifugal compressor provides a 75 to 85% efficiency range while the low speed reciprocating compressor ranges from 60 to 70 % efficiency (Bhatti, 1999).

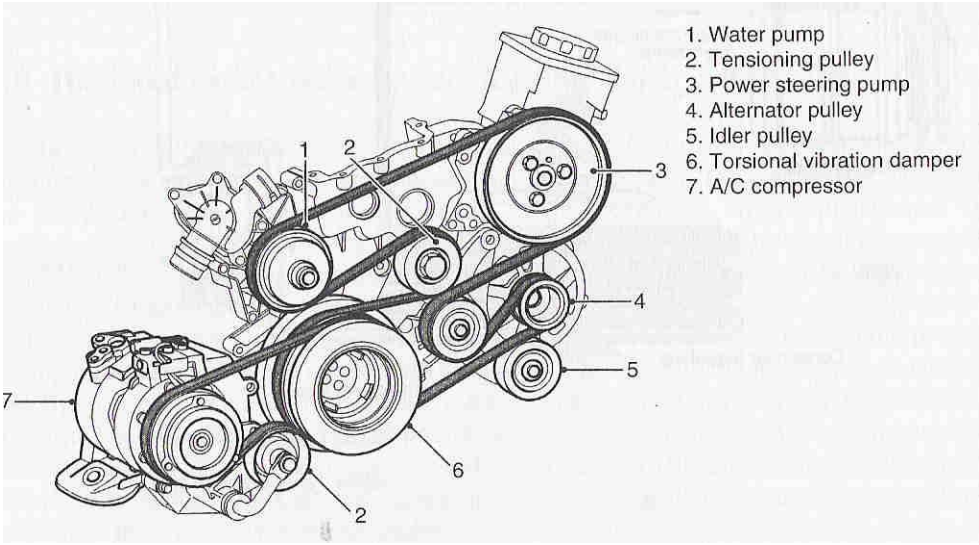

Figure 2.1.2.Typical schematic of vehicle engine's belt driven components including conventional A/C compressor (Daly, 2006).

2.1.2 Condenser Design and Fan

The ideal condenser is designed to provide adequate surface area to fully condense the refrigerant and avoid any refrigerant pressure drop in the process. Condensers are generally made from aluminum for its high thermal conductivity, light

weight properties, low corrosive nature with the outside environment, and high resistance to chemical reactions with the refrigerant and oil mixtures. The design consists of an array of tubes and fins where tubes are used to carry the refrigerant through the heat exchanger and the fins add surface area to increase the heat transfer rate between the refrigerant and outside medium. The four main condenser and evaporator designs are serpentine fin, tube and plate, tube and coiled fin, and parallel flow. The serpentine design is the only design that does not split the refrigerant flow into many streams to increase the surface area contact with refrigerant but still manages to fully condense at the exit of the condenser. The parallel flow design contains a similar serpentine design but its design splits the flow into horizontal stacked tubes and allows the flow to mix vertically at the ends. The design contains two large vertical tube header at both ends to collect mixed flow and split the flow again by sending it across a new set of stacked vertically inline horizontal tubes underneath the first stack. A typical parallel flow condenser contains a three stack of a set of horizontal tubes. The tube and plate and the tube and coiled fin design is of serpentine nature but splits the flow into 2 or 3 serpentine tubes with fins attached perpendicular to horizontal flow of the refrigerant.

Fans existing in the automotive radiator/condenser cooling applications are of radial design and electrically driven through an electric motor. The rotating speed of the motor and hence the fan, is controlled by varying the current supplied. A combination of external and internal sensors measure the outside air temperature and humidity and the refrigerant temperature and pressure inside the condenser to relay a calibrated electric signal to adjust the radiator/condenser fan speed accordingly to the demand.

2.1.3 Evaporator and Blower

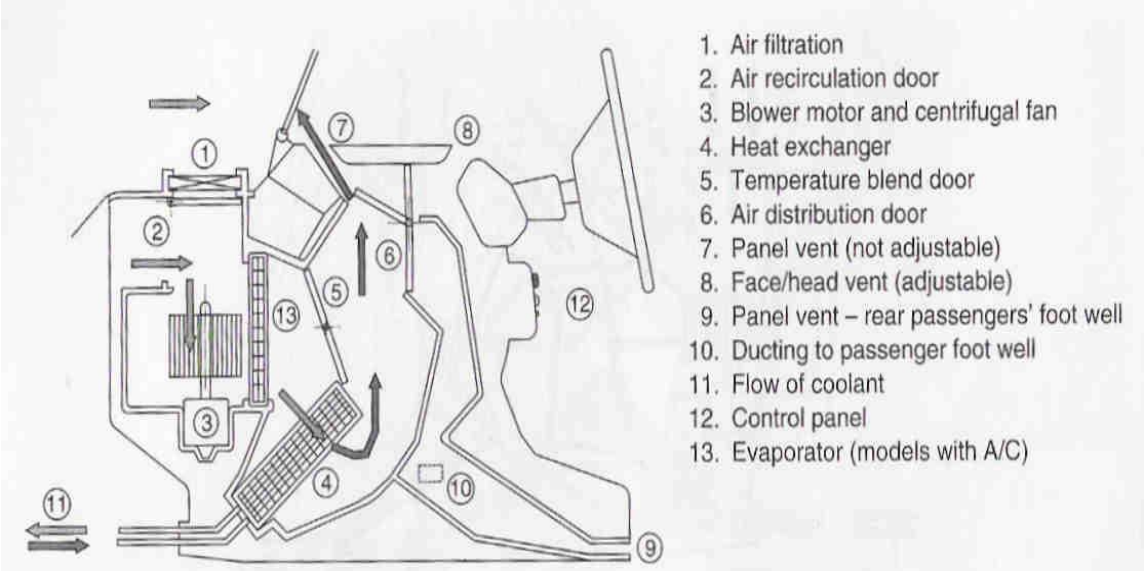

Figure 2.1.3 Schematic of the Automotive Ventilation System used for heating and cooling purposes located at the dashboard and front hood of the vehicle (Daly, 2006).

The evaporator design is similar to the condenser design and Section 2.1.2 can be used as reference to its design. The only difference between the two is that the evaporator is slightly smaller in width and height to fit inside the front hood and dashboard interface. In order to provide enough surface area for heat transfer, the evaporator compensates the loss of frontal area with added core thickness.

The evaporator blower consists of the centrifugal fan design shown in Figure 2.1.3 in order to redirect from outside downward moving vented air just outside the car's windshield. The redirection of the air flow is shown Figure 2.1.3 as the air is blown perpendicular to fan's rotating axis and across the evaporator. Pollen filters and carbon filters are implemented in the vent to purify the air and remove spores, pollen, and dust. As seen in the figure, the heater also lies in the same vent for heating purposes and for mixed temperatures of 65-75°F where sensors in the vent monitor air leaving the evaporator. The sensor signals the hot coolant to pass through the heater if

the air leaving the evaporator is too cold. Air distribution through control doors and vents allow mixing of the cold air across the evaporator and warm air from the heater to reach the desired median air temperature. The front air entering vents and rear air exiting vents also contain an air quality sensor that would signal the control unit to close if exhaust fumes or poor air quality was entering. Recirculated air would then be used to cool the cabin. Humidity sensors are also incorporated to control whether the vented or recirculated air is used to cool the cabin. Figure 2.1.4 details the flow passage of hot air entering the sedan that is to be cooled and the typical locations of vents of where the cool air blown into the cabin. The schematic also shows the location of the vents at the rear windshield that let the initial hot humid air out.

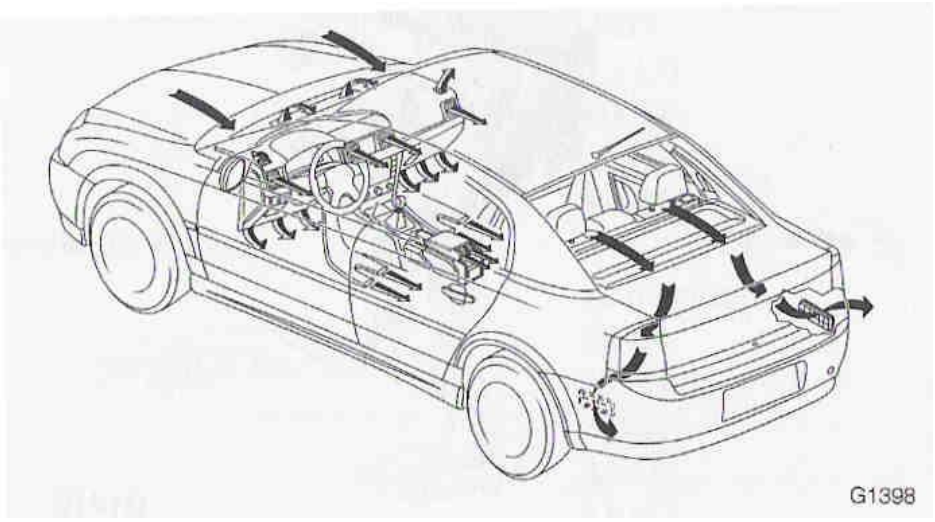

Figure 2.1.4 Schematic of the interior cabin ventilation system for a typical sedan (Daly, 2006)

2.1.4 Regulating Equipment and Expansion Device

The key component of the refrigerant's cooling capacity is the expansion device that reduces the pressure of the high pressure liquid refrigerant exiting the condenser. As mentioned earlier, lowering the refrigerant pressure also lowers its boiling temperature which allows utilization of its latent heat of vaporization to absorb heat from the air. The control of volume and mass flow rate of the refrigerant entering the evaporator is through one of two types of expansion devices; the expansion valves and capillary orifice tube. The expansion devices must control and monitor three important functions.

- Separate high pressure liquid refrigerant from condenser exit from the low pressure refrigerant in evaporator.
- Meter mass flow rate of refrigerant to match cooling load needed from evaporator
- Ensure refrigerant leaving evaporator is fully evaporated and/or superheated

Both the thermostatic expansion valve (TXV) and capillary orifice tube are used as the control valve and monitor the transient conditions of the refrigerant under various loads and environments. The two devices however monitor the condition through two different means. The thermostatic expansion valve monitors the temperature of the refrigerant exiting the evaporator and adjusts the refrigerant flow rate through a sensor expansion valve to make sure the refrigerant fully evaporates as it exits the evaporator. The variable capillary orifice tube uses condenser pressure and temperature readings to adjust its valve opening for adequate flow rate.

The TXV however is sensitive to saturated vapor in the refrigerant flow and typically a receiver/drier is place in between the condenser and the TXV. The

receiver/drier is a cylindrical shaped device with desiccant and filter at the bottom to collect any dirt or moisture from the refrigerant flow. Its main objective is to make sure that only liquid refrigerant exits. Certain receiver/driers are connected to condenser piping where inadequate cooling in the condenser may exist. The uncondensed refrigerant vapor in the receiver/drier is redistributed back into the condenser for it to be fully condensed.

The key to preventing damage to the compressor is providing lubricant oil mixed with the vapor refrigerant to permit excessive wear and premature failure of the compressor vanes. Another important condition is ensuring that the refrigerant is completely in vapor state to prevent liquid refrigerant from damaging the compressor. The accumulator is incorporated to prevent those situations from occurring and contains a desiccant to absorb any moisture and filter particles from the refrigerant. The accumulator also contains a bleed hole of very small quantities of refrigerant mixed with 3% in mixed total volume of lubricating oil to ensure lubricant oil is entering the compressor (Daly, 2006).

The conventional automotive air conditioning system using a compressor contains pressure relief valves in the accumulator and receiver/drier for safety precautions. The precaution is from the potential occurrences over time of a clogged pipe developed from accumulation of non-condensables, particulates, and rust from inside the pipe that would create excessive pressure build up in the system. These valves would aid in preventing a ruptured pipe that would result in potential damage to the vehicle and could create a serious accident. The valves approximately release at 500 to 580 psi. These valves are the last resort aside from other safety measures implemented in the system.

The thermostatic expansion valve is more suitable for the steam ejector A/C system since the system for its better control of the refrigerant pressure and temperature entering and exiting the evaporator. An orifice valve would have less flexibility and control of the varying cooling loads. A thermostatic expansion valve (TXV) that closely monitors the evaporator conditions would be a better match for system and a precautionary receiver/dryer may also be implemented.

The conventional air conditioning system is comprised of variety of sensing control units that enable quick response to changes in temperature and desires from the passenger in order to meet precise cooling loads and air temperature. The steam ejector A/C system plans on using the same sort of sensors to control and monitor the transient load and environment. For the scope of this preliminary theoretical analysis of steam pressure exchange ejector, the sensors are not described in detail and wouldn't be implemented until after experimental tests are conducted.

2.1.5 History and Selection of Refrigerant

The history of automotive refrigerants dates back in the early 1930s when Thomas Midgley introduced the first chlorofluorocarbon (CFC), R12 (CCl_2F_2), into the commercial industry that revolutionizes the refrigeration system industry. By 1939, Cadillac was putting in prototype air conditioning systems in their luxury vehicles. Expansion of A/C systems in automobiles grew to one million by 1959. The onset of the ozone depletion theory in 1974 where R12 was one of the leading contributors, forced DuPont, one of the leading refrigerant producing companies, to look into alternative refrigerants. In 1976, DuPont produced a hydrofluorocarbon called tetrafluoroethane, (CH_2FCF_3) HFC 134a, also known as R-134a, which is now one of the most commercialized refrigerants used today. The ozone depletion theory didn't draw concluding evidence and policy attention until 1987 during the Montreal

Protocol when they declared 50% decrease in production of chlorofluorocarbons (CFC). By then over seven-two percent of new manufactured vehicles contained air conditioning systems using R12 refrigerant. Modifications on the system's components and material selection have been made to incorporate HFC 134a into the R12 system since R134a is corrosive to certain plastics parts. Unlike R12, HFC 134a contains no chlorine to deplete the ozone when emitted into the atmosphere.

The discovery of R-134a has brought little or no harm for the ozone layer but it unfortunately contributes to global warming that has been an increasing contributor to climate change. Global warming occurs from gases (referred to as greenhouse gases) released in the atmosphere that are more transparent to the incoming solar rays than the thermal radiation emitted by the earth surface. These greenhouse gases trap the earth's thermal infrared radiation created by sun and raise the temperature of the earth's surface. The primary and majority greenhouse gas emitted is carbon dioxide and is used as measurement reference for other types of greenhouse gases. Other gases that are also used in refrigeration and air conditioning are chlorofluorocarbons (CFCs), hydrochlorofluorocarbons (HCFCs) and hydrofluorocarbons (HFCs). The quantification of emissions is classified using the term global warming potential (GWP) with reference of 1 GWP equal to 1 kg of CO_2 emitted into the atmosphere. The global warming potential for R-134a is 1300 which means that 1 kg of R-134a gas emitted into the atmosphere is equivalent to 591 pounds (1300 kg) of carbon dioxide gas emitted (Daly, 2006). The total global warming impact of running an automotive air conditioning system is a combination of direct emissions due to leakages, indirect emissions due to fuel consumption of running the system, and the effect of the extra weight to carry it around. Direct emissions are a result of flexible hosepipes' poor connections, deteriorating compressor shaft seals, and any

production, recovery, recycle or disposal processes. This direct and indirect emissions concept has become widely used in evaluating the environmental effect of refrigerant systems and is referred to as the total equivalent warming impact (TEWI).

The European Union has decided to phase out R-134a by 2011 due to its high GWP and a complete ban by 2014 to 2017. The United States and other automotive industries, under pressure through the Society of Automotive Engineers (SAE), are strongly considering the phasing out R-134a and implementing alternative fluorochemical refrigerants with a low global warming potential and zero ozone depletion potential such as HFO-1234yf (tetrafluoropropane). Similar to hydrocarbons, the setback that has limited it growth is its slightly higher flammability.

Replacing the universal R-134a must meet certain criteria in order to be considered a viable alternative. The four main criteria are its physical, thermodynamic, safety, and environmental impact properties showcased in Table 2.1.1. Some of R-134a physical properties that are a disadvantageous besides being a greenhouse gas are:

- Only miscible with synthetic polyalkylglycol (PAG) lubricant for compressor use
- Attacks and corrodes metals and certain plastics
- Has explosive properties
- Odorless and absorbs moisture
- Heavier than air when gaseous and can create suffocation

Many hydrocarbons such as propane and ammonia have similar thermodynamic and physical properties along with better environment properties with lower GWP and lower atmospheric life span but unlike R-134a they are flammable and contain 10 times the heat of combustion. The flammability and explosive

properties are strong factor in the selection and approval from Society of Automotive Engineer and Car Manufacturer standards. This holds especially true based on the safety of the passengers who may be smokers and always at risk of an accident when they get in the car. A refrigerant that is flammable or explosive would increase its severity risk to the passengers. Automakers are reluctant to use hydrocarbons even with matching or better COP than R-134a due mainly to liability reasons.

Table 2.1.1 Environmental and Thermodynamic Properties of Refrigerants

Refrigerant	R-134a	R-152a	R290 Propane	R-718 Steam
Chemical Formula	CH_2FCF_3	CH_2CHF_2	$CH_3CH_2CH_3$	H_20
Molecular Mass	102.1	66.1	44.10	18
Normal Boiling Point (°F)	-15	-11.2	-43.80	212
Lubricant	POE/PAG	N/A	Mineral Oil	N/A
Atmospheric Life	14	2	<1	<1
Ozone Depletion Potential	0	0	0	0
Lower Flammability (% in air)	None	4.80	2.10	None
Heat of Combustion (Btu/lb)	1806	7481	21625	N/A
Global Warming Potential	1300	121	11	0
Latent Heat of Vaporization (Btu/lb) @ 40 F	84.1	129.75	156.74	1070.9
Vapor Specific Volume (ft^3/lb) @40 F	0.95	1.66	1.35	2445
Vapor Specific Heat (Btu/lb- F) @ 40 F	0.217	0.251	0.451	0.452
Latent Heat of Condensation (Btu/lb) @ 100 F	71.2	115.48	132.92	1037
Liquid Density (lb/ft^3) @ 100 F	71.94	54.03	29.58	61.2
Liquid Specific Heat (Btu/lb- F) @ 100 F	0.36	0.43	0.67	1

One of the main reasons that steam was selected as the refrigerant for the pressure exchange ejector automotive air conditioning system is that it is a renewable and clean refrigerant with no environment impact. Steam also contains certain physical and thermodynamic properties that exceed R-134a and other properties that are a disadvantage. The use of steam eliminates any flammability or explosive concerns and the only corrosive property is that it is a catalyst medium for oxidation and reduction reactions in rusting. The thermodynamic property of its latent heat of vaporization and condensation is more than ten times that of R-134a and having twice the specific heat in the vapor and liquid phase enhances it heat transfer properties. The only concern with the thermodynamic properties of steam is that for the vapor compression cycle air conditioning system, steam needs to be in the vacuum pressure for both the evaporator and condenser. This requirement forces its specific volume in vapor state to be extremely high as shown in Table 2.1.1.

However steam's high specific volume leaves it susceptible to a less compact system with large heat exchangers to compensate for it. However with its high heat transfer rate with its high latent heat of vaporization and condensation minimizes the mass flow rate and hence the volumetric flow rate passing through. This along with a slightly higher powered condenser fan and evaporator blower will help minimize the increased size of the heat exchangers.

2.1.6 Climate Comfort – Temperature and Humidity

Comfort for vehicle passengers is a combination of the temperature and humidity in the cabin. The human body is constantly perspiring and uses evaporation of the sweat produced to cool the body. Convection of the air absorbs and removes the heat from the skin and any perspiration aids in adding humidity into the air. Since the specific heat of the less dense water vapor is on average twice the specific heat of

air, mixed humid air creates lower heat transfer rate between the skin and air creating discomfort for the body. The evaporator aids in the convection process with cooler blown air and removal of humidity of the cabin air as its water vapor condenses on the evaporator's cold refrigerant's heat exchanger (Daly, 2006).

The American Society of Heating, Refrigeration, and Air Conditioning Engineers (ASHRAE) was developed a standard for evaluating human comfort based on temperature and humidity. The conclusion are reports detailing the comfort zone of 67°F to 82°F based on relative humidity, season, clothing worn, activity levels and other factors (Office of Atmospheric Programs, 2002) . It is recommended to maintain an absolute humidity ratio of 0.012 of pound mass of water vapor to pound mass of air for comfort and a relative humidity of less than 60% to prevent microbial growth for the cool air. The variety of factors involved that can be modified for comfort are beyond the scope of this thesis but the recommended conditions fall in the simulated conditions in the designed steam ejector A/C system.

2.1.7 Alternative Air Conditioning Systems

The phasing out of R-134a from the European Union and its European markets based the concerns about the refrigerant's GWP have created new types of unconventional air conditioning systems that will provide additional competition to the steam pressure exchange ejector air conditioning system. The U.S. has not decided on phasing out the refrigerant and may take measures to improve a better leak-free system instead. A list of possible alternatives are (Daly, 2006):

- CO_2 (R-744) based Heating and Cooling System
- Absorption Refrigeration
- Secondary Loop System (R-152)
- Air Cycle Refrigeration (R-729)

The CO_2 transcritical refrigeration and heat pump system for both cooling and heating the vehicle cabin is being implemented in certain vehicles in Europe. The requirement for transcritical conditions for carbon dioxide are extreme high pressure of up to 2320 psi and low side of 1740 psi to run vapor compression cycle. Thicker piping and stronger fittings are required which add weight and cost. This also leaves vulnerability to leaks and high risks of further passenger injury during accident if system is ruptured.

Absorption refrigeration contains a similar vapor compression cycle with condenser, evaporator, and expansion system but uses a pump and a liquid transport medium that is mixed with the vapor refrigerant leaving the evaporator to absorb heat and convert mixed solution into liquid. The mixed solution of the liquid medium and refrigerant are pumped to higher pressure as opposed to using a compressor with vapor refrigerant in the conventional system which requires more energy. The drawbacks lie in the expensive equipment and heat to separate the solution back to pure refrigerant and transport medium after it is pumped. The common refrigerants using water as a transport medium are ammonia and lithium bromide and contain hazardous properties that require safeguard measures. Ammonia is toxic at low concentrations and lithium bromide is corrosive to most common materials and as a result the absorption cycle requires added cost and complexity to control these issues.

The third alternative air conditioning system is described as a Secondary Loop System which contains a similar vapor compression cycle using R-152a but replaces the evaporator with a chiller to cool a second loop that uses brine under pressure from two different pumps. The second loop also contains two front and a rear coolers with no expansion device, to provide more cooling at different areas of the vehicle. The advantages of multiple coolers provide quicker response time to cooling needs and the

primary loop require half the refrigerant charge of R-134a under the same specifications to run the system. Figure 2.1.6 details the Secondary Loop System using R-152a and its added components. The main drawbacks to the system are the cost and weight of the added pumps and coolers to system. Furthermore, the pumps and compressor from primary loop cumulatively would increase the energy and fuel consumption of system. Lastly, the system primary loop would use a hydrocarbon like R-152a which is flammable.

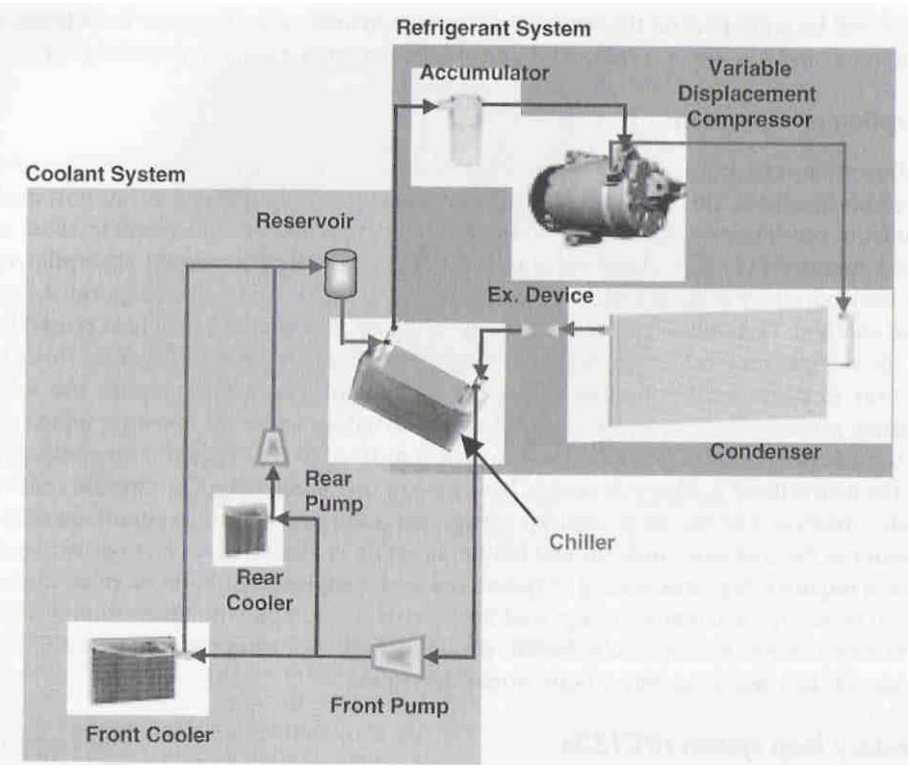

Figure 2.1.6 Secondary Loop A/C Loop using R-152a and brine with front and rear cooler and pumps (Daly, 2006)

The last system referred as Air Cycle Refrigeration uses air is an open ended A/C system that operates on a turbomachinery concept and draws the air from the cabin and pressurizes it. The air's temperature and pressure rises and flows through a heat exchanger to lose some heat with the outside environment. The compressed air is

then isenthalpically expanded using a turbine and reduces its temperature and pressure and blown into the cabin as cool air. The turbine is also connected to the compressor to recover some energy during the expansion. The system does not operate similar to vapor compression cycle and doesn't optimize on refrigerant's latent heat of vaporization and condensation. The poor thermal properties of air's specific heat require high pressurization from the compressor creating a low COP and high energy consumption to provide cool air.

Chapter 3 Conventional and Pressure Exchange Ejector

3.1 Conventional Ejectors

At the turn of the 20th century, the use of ejector refrigeration was commonly used due to its simplicity, low cost, and versatility with a variety of refrigerants. Ejectors are often considered an alternative to the conventional refrigeration system due its ability to utilize wasted heat and ability to discharge large volumes of compressed mixed flow. However, its low coefficient of performance offset those advantages and results in more energy input into the ejector and a larger condenser to handle the higher thermal load in the vapor compression cycle. These disadvantages have encouraged engineers to look into a mechanically driven single loop system for a better performing refrigeration and air conditioning cycle. The improvements of the compressor efficiency and use of fossil fuels to convert its chemical combustion energy to mechanically drive the compressor led to the phasing out of the ejector for small scale air conditioning and refrigeration applications. Larger scale industrial systems continue to use the ejector refrigeration systems due to the utilization of waste heat from steam created by fossil fuel burning from other industrial mechanical driven systems.

The conventional ejector in an air conditioning or refrigeration system has been designed to transfer heat and pressure from a higher pressure primary flow to a secondary flow of lower energy and pressure. In ejector air conditioning and refrigeration, the secondary flow is the refrigerant exiting the evaporator and has exhausted its pressure to lower its evaporation temperature to provide cooling. The secondary vapor flow is required to be re-pressurized in the vapor compression cycle in order to raise its condensation temperature. The resultant outcome from the

conventional ejector is a mixed fluid of primary and secondary flows at an intermediate pressure and temperature.

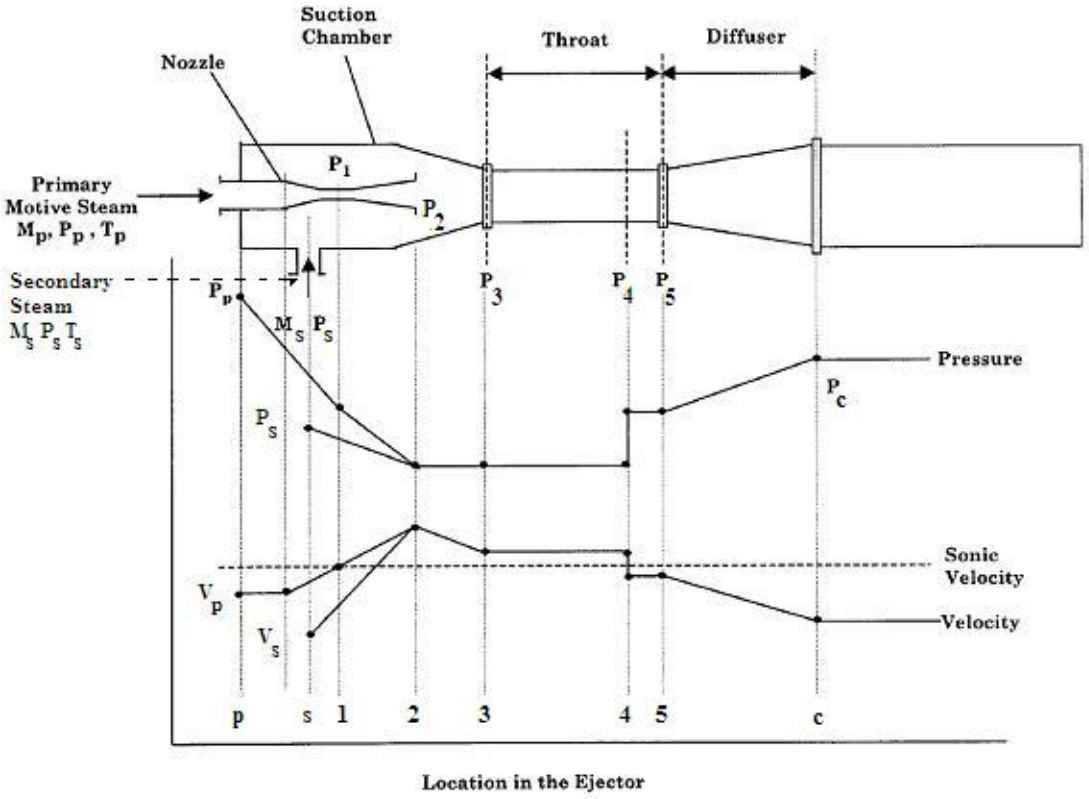

Figure 3.1.1 Pressure and Velocity Profile of primary and secondary flow through conventional ejector (El-Dessouky, 2001).

There are four sections of the ejector system, the nozzle, a cylindrical suction chamber (plenum), the diffuser throat section, and the subsonic diffuser. The fluid mechanics behind pressurizing the secondary flow is to first convert the pressurized primary flow into a supersonic flow through a converging and diverging nozzle in the plenum region. This diverging nozzle section decreases the primary flow's pressure through expansion in order to increase its velocity. The expansion process lowers the pressure at the nozzle exit detailed at state 2 in the ejector pressure profile in Figure 3.1.1. The low pressure and primary flow's high velocity draws, or entrains the

secondary flow into the plenum and diffuser. The entrainment process is a result of friction and shear stresses acting at the interface between the two streams. The entrainment ratio refers to the mass flow rate of the secondary flow induced into the ejector over the primary mass flow rate. The turbulent shear stresses created by the high velocity primary flow and entrained secondary flow begin the mixing process and exchange of momentum. Figure 3.1.1 details the pressure and velocity profiles along the length of the conventional ejector. The analysis of the partially mixed flow leaving the suction chamber and entering the throat can be split into two separate models. The throat area can be considered as a constant area model or a constant pressure model. The constant pressure model is applied in Figure 3.1.1 as seen with constant pressure between state 3 and 4 in the ejector model. Constant pressure models are predominantly used in most literature due to its favorable comparison with experimental data (El-Dessouky, 2001). As the two fluids are mixing and approaching the diffuser, a strong normal shock occurs at point 4 in Figure 3.1.1 that increases the pressure while decreasing its velocity. The location of the shock wave is dependent on the back pressure created by the condenser along with the design of the ejector. This strong shock converts some of the dynamic pressure back to static pressure, shown from P_4 to P_5 in Figure 3.1.1. This is a highly dissipative and irreversible process to raise the flow's static pressure. Finally, the mixed flow passes through the diffuser to regain static pressure while decreasing velocity. The suction chamber, throat, and diffuser configuration in the figure is similar to the supersonic converging and diverging nozzle but slightly larger. As the mixed primary and entrained secondary flow enter the diffuser at supersonic speeds, the reverse effect occurs where the flow regains static pressure and decreases velocity down to subsonic speed.

The fluid dynamic equations involved in calculating the predicted exit pressure, mass flow rate, and entrainment ratio from a specifically designed conventional ejector are described in previous literature (Sun and Eames, 1995 and El Dessouky, 2001). The means by which pressure and temperatures are calculated are through steady state fluid dynamic equations for supersonic and subsonic compressible flow. The area ratios between the throat area for both the supersonic nozzle and diffuser are critical in determining the mach number of the primary flow exiting the nozzle and volume of mixed flow discharged into the condenser. The total ejector efficiency for conventional ejectors used in previous literature is based on fluid dynamic equations on compressible flow and is a product of the frictional losses in the nozzle, throat section, and diffuser area (El-Dessouky, 2001).

The terminology used in the conventional ejector analysis are:

the entrainment ratio which is the ratio of the secondary mass flow rate divided by the primary mass flow,

$$\hat{e} = m_{primary} / m_{secondary} = m_{refexh} / m_{refevp}$$

the compression ratio defined as:

$$C_{rto} = P_{mix} / P_{secondary} = P_{refcond} / P_{refevp}$$

And finally the expansion ratio expressed as:

$$E_{rto} = P_{secondary} / P_{primary} = P_{refevp} / P_{refexh}$$

The boundary conditions involved in this mathematical model include:

- The ejector flow is one dimensional, adiabatic, and at steady state conditions.
- Primary and secondary flows contain the same specific heat and their inlet velocities are negligible.

- The mixed flow through the diffuser compresses with the resultant exit velocity considered insignificant.
- Mixing of the motive primary and entrained secondary flows occur in the suction plenum and diffuser throat.
- Frictional losses are defined from isentropic efficiencies of the nozzle, diffuser, and mixing throat.
- Primary and secondary flow are under saturated conditions.

The process of energy transfer in the conventional ejector is through fluid to fluid interaction of momentum exchange and mixing at steady flow conditions. The combination of turbulent mixing and a strong normal shock for the conventional ejector creates a highly dissipative and a low compression performance device. The ejector design is critical to produce the specific compression and entrainment ratio based on inlet primary and secondary flow pressures. Any variations in inlet pressures for the specific ejector design that would cause an increase in mass flow rate in system could potential reach a critical point of choked flow which precipitously decreases its efficiency and coefficient of performance. The critical point where choked flow occurs is when high primary flow increases its mass flow across the diffuser throat region to the point where minimizing the back pressure at exit has no effect on the mass flow rate leaving the ejector. Choked flow when created causes the mass flow rate to remain constant through the throat region and diminishing the ejector's entrainment capabilities resulting in a drastic decline in efficiency.

3.2 Description of Pressure Exchange Ejector

The pressure exchange ejector contains the additional term "pressure exchange" due to its mechanism of taking one body of fluid that is being expanded and exerted a pressure force at the moving interface with another body of fluid to compress it. This direct fluid to fluid contact is done by reversible work without mechanical assistance gives the opportunity to gain efficiency and performance in comparison to the conventional ejector.

The pressure exchange ejector detailed in Figure 3.1.2 differs from the conventional ejector with its additional axially centered rotor and corresponding crypto-steady frame of reference. The term crypto-steady flow refers to a flow which was steady in a special moving frame of reference, but was non-steady in the laboratory frame of reference (Zhang, 2007). The role of the rotor is solely intended to generate rotating fluid interfaces between the primary and secondary flows. The supersonic primary flow will impinge upon the canted vanes designed on the rotor causing the rotor to spin at high rotational speeds (Garris, 1998). The rotor is designed to be free spinning. Similar to the turbomachine, high rotational speeds are required due to the fact that the rate of energy transfer is proportional to the speed of the interface.

The improvement of less dissipative oblique shock structures as opposed to conventional ejector's turbulent mixing and normal shock structure provides an increase in efficiency. Rotating primary and secondary flow interfaces form over the rotor vanes which resemble blades in a turbomachine and are referred to as 'psuedoblades.' will form over the vanes and a series of expansion fans and compression waves will cause the secondary flow to expand into the interstices between the oblique-vane-shock structures (Garris, 1997). Once the secondary flow

lies inside the interstices and rotating alongside the rotor, the momentum and energy are exchanged between the primary and secondary flow through pressure exchange. Added pressurization of the secondary fluid occurs as the psuedoblades are pushed out radially while in rotation and is compressed by surrounding primary flow compressing it against the radial wall. The flows continue past the rotor and are mixed in the diffuser at constant pressure. The diffuser also reduces to mixed discharge velocity to subsonic speeds while regaining some static pressure in return. The device is discussed in further detail in written patent (Garris, 2009) and previous literature (Zhang, 2007)

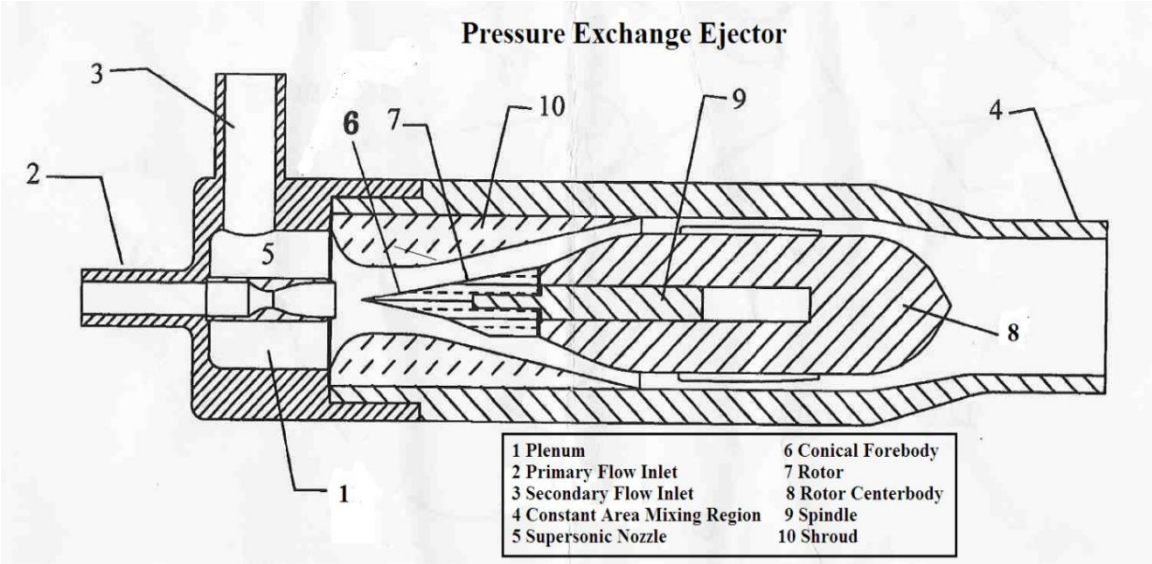

Figure 3.1.2 Schematic of Patented Pressure Exchange Ejector (Garris, 1997)

The coefficient of performance and efficiency of the pressure exchange ejector is greatly dependent of the flow induction, pressure exchange, and heat transfer between the two flows. The entrainment ratio and compression ratio are one of the limiting fluid dynamic factors that reduce efficiencies for the conventional ejector. The use of the turbomachinery analog for the pressure exchange ejector and also the

conventional ejector can be used to simulate thermodynamic performance of the ejector.

The concept of applying the turbomachinery analog for the thermodynamic analysis of the pressure exchange ejector is based on similar fluid mechanical process where the high pressure and high energy fluid exhausts its energy to reenergize and pressurize another fluid. The interaction between the high pressure motive primary steam and the low pressure secondary steam is considered a fluid dynamic flow induction (FDFI) device since it involves the direct transfer of energy and momentum between two fluids through fluid dynamic contact. The high energy primary flow converts from high pressure to high velocity as it passes through the supersonic nozzle and creates flow induction to entrain the secondary flow. In the case of the conventional ejector, the entrainment created brings the two fluids together into the diffuser where irreversible turbulent mixing occurs followed by a normal shock which is highly dissipative and inefficient. The simplicity and low cost and maintenance of the device is an advantage to the mechanical compressor. However, the conventional ejector's low efficiency and performance is not comparable to the mechanical compressor.

As previously discussed, the energy transfer process of both ejectors, the conventional and pressure exchange ejector, can be represented by the turbomachinery analog. The primary flow passing through the turbine provides the energy to compress and thermally energize the secondary flow which passes through the compressor. As shown in Figure 4.1.4, the turbine drives the compressor through a common shaft. In reference to the secondary flow, the work done on it can be interpreted as entering a compressor that is being powered by the turbine process in the primary flow. The combination of a turbine that powers a compressor either

through a direct shaft or other mechanically coupled system. The integration of the turbomachine characteristics into the ejector analysis is referred to as the turbomachinery analog. Figure 4.1.4 details the location of turbine process of the primary flow through the supersonic nozzle along with location of compression process of the secondary flow.

The pseudoblades in a pressure exchange ejector are set precisely as vanes in a turbomachine. As such, the ultimate level of performance that any flow induction device can obtain is that of isentropic turbomachinery. It is well known that ejectors can be represented as a mechanically coupled turbine-compressor combination (Kamara, 2005). The turbine is energized by the primary fluid, which then drives the compressor receiving the secondary fluid. The compressor and turbine discharge to a common manifold shown in Figure 3.1.3 as the mixer. If the turbine and the compressor operate isentropically, the level of performance for the turbomachine is at its highest theoretical peak. This ideal condition is an important figure of merit to determine the ejector's optimal performance. However in order to approximate the real performance of the ejector, the turbomachinery analog is adjusted with modifications of the turbine efficiency and compressor efficiency. The ideal condition and modifications of the turbine and compressor efficiencies were used in the approach of this thesis to determine the influence of the ejector efficiency on the implemented automotive air conditioning system. The efficiencies used in the analysis serve to establish desired goals for the PE ejector in order for it to be competitive in the automotive A/C application. The ejector efficiency can be similarly expressed as the multiplication of turbine and compressor efficiency,

$$\eta_{ejector} = \eta_{compressor}\,\eta_{turbine} \qquad 3.2.1$$

where turbine and compressor efficiency are defined as the ratio of actual work and its theoretical isentropic process:

$$\eta_{\text{compressor}} = \frac{\dot{m}_{\text{sec}} (I_{4_{\text{iscmp}}} - I_3)}{\dot{m}_{\text{sec}} (I_{4_{\text{cmp}}} - I_3)} = \frac{(I_{4_{\text{iscmp}}} - I_3)}{(I_{4_{\text{cmp}}} - I_3)} \qquad 3.2.2$$

$$\eta_{\text{turbine}} = \frac{\dot{m}_{\text{prim}} (I_1 - I_{4_{\text{trb}}})}{\dot{m}_{\text{prim}} (I_1 - I_{4_{\text{istrb}}})} = \frac{(I_1 - I_{4_{\text{trb}}})}{(I_1 - I_{4_{\text{istrb}}})} \qquad 3.2.3$$

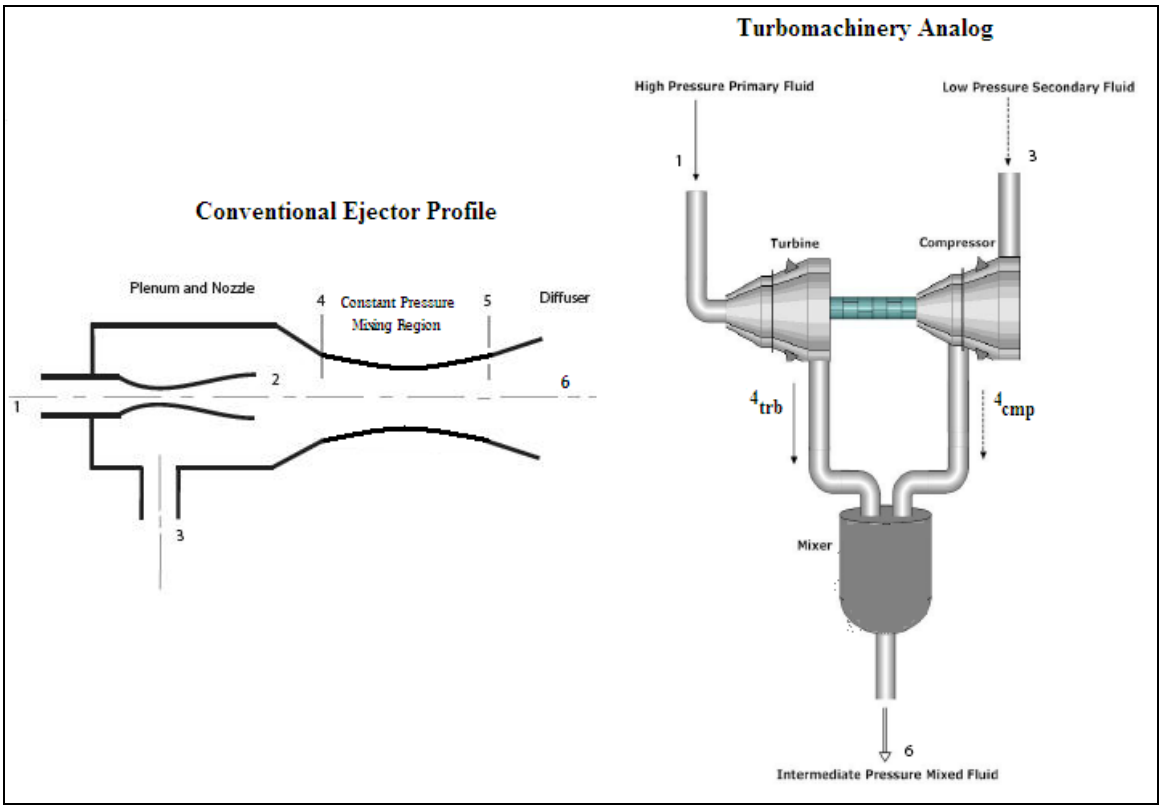

Figure 3.1.3 Conventional Ejector and Turbomachinery Correlation Diagram (Bulusu, 2008)

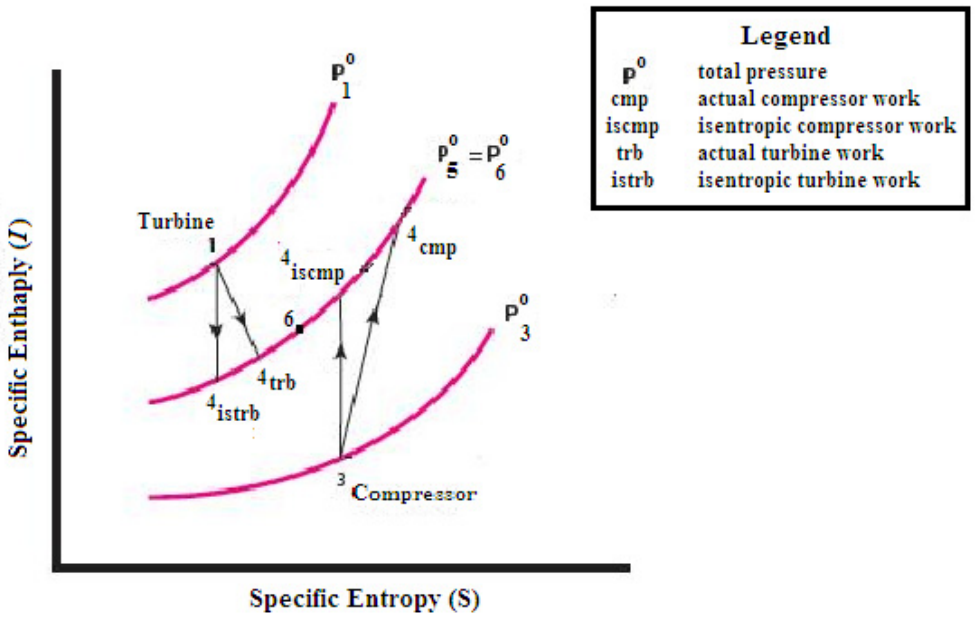

Figure 3.1.4. Mollier Chart diagram of Turbomachinery Analog analysis for ejector

The exit pressure was predetermined through the back pressure created by the set saturation pressure and temperature for the condenser. The corresponding mixed flow enthalpy at the ejector exit was determined through the conservation of mass and the conservation of energy between the two fluids entering the ejector at different mass flow rates and enthalpies. The mixed flow enthalpy was calculated using the energy equation below under adiabatic conditions with no work being done on the system.

$$m_{prim}\,(I_{4_{turb}}) + m_{sec}\,(I_{4_{cmp}}) = (m_{prim} + m_{sec})\,I_5 = (m_{mix})\,I_6 \qquad 3.2.4$$

with the condition of $I_5 = I_6$ for the energy transfer across the diffuser between the two fluids under isenthalpic process at constant total pressure. Figure 3.1.4 details the turbomachinery isentropic and actual work process and the mixing of the two fluids in the diffuser using the mollier chart.

With the known steam exit pressure and calculated enthalpy, the exit temperature of the mixed steam vapor flow was calculated. The steam exit temperatures for the ejector were designed for the superheated region to avoid having saturated steam in the supersonic nozzle and plenum region during the primary flow's expansion. Saturated steam would create oxidation and may cause performance problems with the rotor bearings of the pressure exchange ejector. Due to the space limitations in an automobile along with steam's high specific volume at vapor state, high temperature superheated steam were reached to maximize the enthalpy value and minimize the steam volumetric flow rate entering the pressure exchange ejector. The low volumetric flow rate is a key component in keeping the ejector and heat exchangers compact in design.

The predetermined steam inlet and outlet pressures and temperatures through the steam pressure exchange ejector A/C system was developed by combining conventional ejector experimental values detailed in Tables A.1, A.2, and A.3 in Appendix A and looking into pressure ratios required for implementing an steam ejector vapor A/C system with high condensation temperatures for an air cooled condenser. The future goals are to design the ejector through compressible and supersonic flow calculations for proper diameters, lengths, area ratios and test the design the prototype experimentally and computationally.

3.4 Applications of Pressure Exchange Ejector

The pressure exchange ejector similar to the conventional ejector has a variety of applications. The pressure exchange ejector can be used in refrigeration and air conditioning systems, absorption cycles (Balasubramaniam, 1975). Applications also extend out to desalination and water purification systems along with thrust

augmentation systems, and supercharging enhancement systems for exhaust intake for internal combustion engines. The conventional ejector for the majority of these applications has been theoretically and numerically analyzed along with some experimental results. The potential for added efficiency and performance from the pressure exchange ejector and the growing environmental and energy consumption concerns give the patented invention potential for implementation into these applications.

3.5 Previous Ejector Systems for Automotive Air Conditioning (A/C)

The concept of using the conventional ejectors for automotive applications has been conducted through experimental testing in Everitt (1999) and theoretically in Balasubramaniam (1975). Previous researchers and experimentalist have attempted to implement the conventional ejector with an additional primary loop pressurized through a low powered pump and thermally energized from either a boiler or heat exchanger inside the engine coolant system and/or exhaust gas piping.

Balasubramaniam combined a theoretical analysis of engine cooling jacket waste heat and exhaust gas waste heat recovery concept for the ejector air conditioning system. The design also was designed to provide engine cooling with or without the A/C system turned on. The complexity of the design is showcased in Figure 3.5.1 where a series of heat exchangers are used for both engine cooling jacket and exhaust gas waste heat recoveries are implemented. The system also contains a pair of recuperators to exchange heat through single phase heat transfer between engine coolant and A/C refrigerant. The project was viewed from an energy management perspective and the specific design, sizing, and weight of the many heat exchangers used in the system design were beyond the scope of the project.

The Balasubramaniam design and his better fuel economy results showed promise and validity for a more technical and experimental look into the system. One of the major concerns not addressed in the report however is the space and resultant weight required for the system that are key to automotive air conditioning application. A further in depth analysis of the technical design would aid in the feasibility of the system especially with completely modifying the engine cooling system infrastructure. Since the conduction of this new conventional ejector A/C design was in the 1970s, the primary refrigerant, Freon-11 used in the analysis has already been phased out due its high ozone depleting potential (ODP).

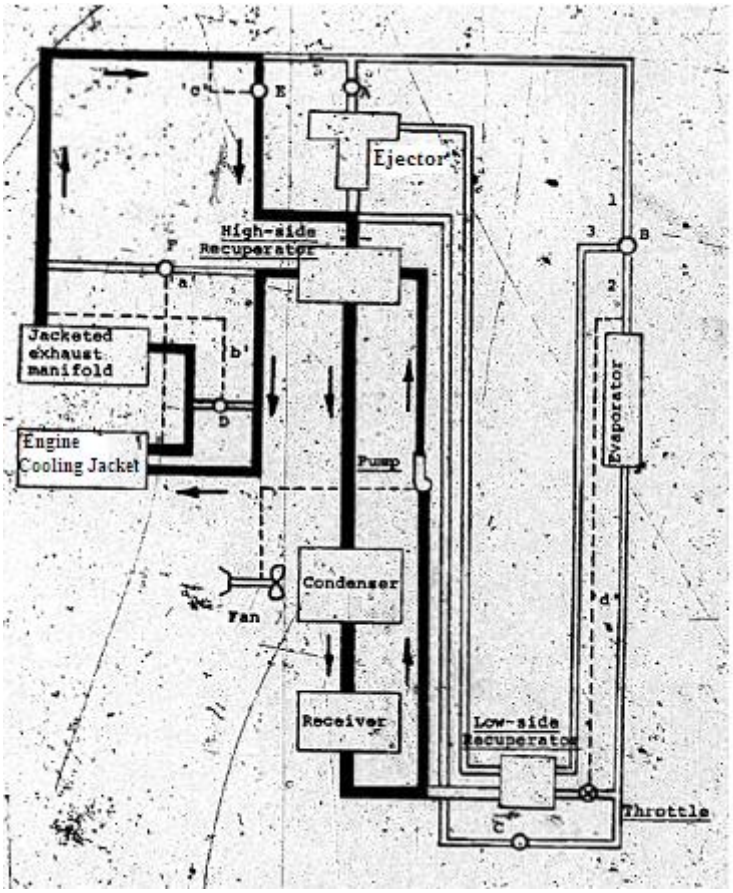

Figure 3.5.1 Schematic of a duel automotive conventional ejector A/C and engine coolant system designed by Balasubramaniam in1975.

Everitt and Riffat conducted experiments for a steam conventional ejector A/C system by using simulated system with the typical vehicle A/C components mounted on a test bench inside a wide tunnel to mimic the vehicle motion (Everitt, 1999). The exhaust waste heat recovery was closely matched with a boiler placed in primary flow loop. The system parameters of the steam refrigerant were set with inlet primary pressures entering at different saturation temperatures while the secondary flow temperature and pressure coming from evaporator were kept constant. Each set of trials consists of constant pressure and temperatures for the mixed flow exit and secondary flow inlet while entrainment ratio, exit ejector pressures and temperatures were controlled by varying the primary inlet pressure and temperature. The secondary saturated steam inlet from evaporator varied to determine the overall coefficient of performance and choked flow parameters to determine the range of efficiency for the ejector. It was concluded under the design conditions that lowering the condenser pressure and temperature aids in raising the COP_{cycle} and entrainment ratio. The ejector specific design contains a critical condenser pressure for the ejector back pressure to limit the increasing COP_{cycle} and entrainment ratio results. Lowering the back pressure beyond a critical point creates a choked flow that produces constant mass flow rate through the diffuser and a steady decrease in performance. Table A.1 in Appendix A details two operating conditions in their experimental analysis by varying the condenser saturation temperature at 68° F and 77° F. They reported a maximum COP of 0.4 with the inclusion of the thermal input as work input from the boiler. The COP in this analysis along with the steam PE ejector can be looked at two different manners depending on the inclusion or exclusion of an independent source of engine waste heat as a work input for the refrigerant cycle. This issue is discussed in future sections in Chapter 6. For direct comparison with the PE ejector, the

turbomachinery analog was applied to the conventional ejector used in this system and discovered that the efficiency for the different set of trials ranged from 15 to 22%. This information along with Tables A.2-A.4 of the different designed conventional ejectors, aided in determining the average efficiency of a conventional ejector using steam in both the secondary and primary flow inlet.

The major concerns for this steam conventional ejector air conditioning system in the automotive application are the low ejector efficiencies and large ejector lengths. Steam under vacuum conditions in the examples above and in previous literature produce a very low efficiency. As a result, higher energy input is required in the primary flow through the ejector either by increased mass flow rate or high enthalpy through increased pressure or temperature of the primary flow. The mixed flow leaving the ejector is either at a higher mass flow rate or enthalpy as it enters the condenser. The consequence is a larger heat rejection needed from the condenser and forcing the condenser to be larger than the conventional air conditioning or refrigeration condenser. Another consideration is the ejector's specific design that limits the inlet primary pressure and mass flow rate range based on secondary flow conditions and desired exit pressure. Excessive primary mass flow rate through the ejector chokes the flow and the resultant entrainment of the secondary flow decreases which detrimentally degrades the performance of the ejector. The use of steam as a refrigerant for air conditioning and refrigeration systems require the vapor compression cycle to be at vacuum pressure throughout the cycle. Steam contains a high specific volume at vacuum pressure and requires larger piping than the typical hydrocarbon or hydrofluorocarbon refrigerants causing a slight increase in the size of the condenser and ejector.

The conventional ejector design contains a high length to throat diameter ratio in order to provide enough axial distance for the secondary and primary flow to interact and mix. The length of the conventional ejector based on recommendations from ASHRAE(1979) are:

- Ejector Mixing Region 6-10 throat diameters long, averaging at 7
- Constant Pressure or Area Region requires 3-5 throat diameters length to accommodate shock pattern and its axial movement under load
- Subsonic Diffuser at the exit has an axial length of 4-12 throat diameters

Taking the three ejector design parameters listed below and adding the minimums and maximums together, the range of the ejector lengths is a minimum of 13 times the throat diameter to a maximum of 27 times the throat diameter

Steam also contains a high freezing temperature of 32°F that becomes an issue during the winter months. The risk of rupturing pipes and tubes in the A/C system during the winter months would be a concern for the durability of the system. The high freezing temperature and specific volume disadvantages have caused automotive companies to look elsewhere for refrigerants such as R-134a with a freezing temperature of -142°F. A solution to the freezing problem is to contain an expandable reservoir connected to the system for the steam to automatically drain after the A/C system is turned off. This would allow for the water to freeze in the winter months without damaging the system. A reservoir would benefit also in checking water level and refilling system with cleaner water. A reservoir however would require a delayed response to recharge the system's pressure and steam flow. To reduce the delayed time, the reservoir would be located in between the condenser outlet and the location where the two flows split to the pump and expansion device.

Last of all, the previous experiments also contain weight and complexity concerns based on their design. The systems mentioned above use a low powered pump to produce low pressure for the primary flow entering the ejector and result in low ejector exit pressures with a condensation temperature too low to be air cooled by the warm outside air. This resulted in their design to add further complexity, weight, and energy consumption by requiring additional piping and pump for a water cooled condenser. This added pump and piping along with the additional exhaust waste heat primary loop diminishes any cost effectiveness and energy savings. The goal of the pressure exchange ejector A/C system is provide a higher ejector exit pressure and corresponding condensation temperature to use an air cooled condenser and utilize the ram air or radiator fan to provide cooling. The consequence of higher ejector exit pressure is providing higher primary pressure at the ejector inlet. The source of the high pressure refrigerant is from a more powerful pump than in the previous experiments that will reduce using water cooled condenser and its required pump and piping which reduce the complexity, weight, and space of the system.

After looking into the previous automotive conventional ejector A/C system and seeing the energy consumption savings and better fuel economy savings listed in the reports, a theoretical analysis of energy management along with a heat exchanger design of the system with a potentially more efficient ejector in the pressure exchange ejector would make for a more deliverable and feasible analysis of the system. The goal of the steam PE ejector A/C system is to take a step further in the analysis with a more technical analysis to cover size and weight of components along with the vehicle fuel economy, energy savings and conservation, and environmental emissions study.

Chapter 4 Pressure Exchange Steam Ejector Auto Air Conditioning Analysis

4.1 Two Loop Ejector Air Conditioning System Model

An automotive ejector air conditioning system utilizing the pressure exchange ejector or the conventional ejector requires specification of operating parameters which affect the performance of the system. This system focuses on the automotive applications which differ from residential air conditioning applications in that the system is more sensitive to size and weight. The ejector A/C system contains the typical vapor compression refrigeration loop found in the existing automobile but also contains a second loop of a pump and a heat exchanger to recover waste heat from the engine exhaust system. The vehicle internal combustion engine for the typical midsize sedan uses around 30% of the combusted gasoline to propel or provide ancillary energy to the car. The rest of the 70% is wasted heat to be removed from the engine (Hendricks, 2001). The exhaust gas carries away around half of the wasted heat while the rest is absorbed by the engine coolant to cool the engine. The steam PE ejector system using waste heat as a thermal source has two locations to recovery waste heat. Recovering waste heat from the engine coolant system would add complexity to the two loop system as shown in Balasubramaniam's system especially with the engine continuously needing to be cooled while the air conditioning system is only a seasonal commodity. This design is more applicable and feasible in the year round tropical and warm weather regions where A/C would be used more than two seasons of the year. Running the A/C piping alongside the engine coolant to exchange is a possibility to preheat the steam but the engine coolant temperatures of below 300°F are not high enough to evaporate and superheat the steam refrigerant to 530°F in the

PE ejector A/C system design. Instead of adding piping or heat exchanger just to preheat the steam around the space limited engine compartment, the engine cooling system was left out in the waste heat recovery loop of the PE ejector A/C system. The engine exhaust system contains all the thermal properties and available waste heat to superheat the steam with exhaust gases leaving the engine exhaust manifold at 1300°F (LaGrandeur, 2005). The exhaust length and less space constraint allow for adequate spacing and surface area for heat transfer between hot exhaust gas and the steam refrigerant.

There are various geometric parameters and design considerations for the exhaust gas heat exchangers, pump, evaporator, and condenser in order to potentially retrofit an existing automobile or apply the system to a new model. These constraints are mentioned for each component of the A/C system while also trying to keep the system competitive in the market and feasible with weight and size.

The components of the steam ejector A/C system are superimposed on the BMW 530i detailed in Figure 4.1.1 along with phase state of the steam refrigerant throughout the two loop ejector A/C system. In order to optimize use of steam's latent heat of vaporization and condensation during heat transfer, the steam refrigerant is kept below atmospheric pressure through both the condenser and evaporator. Vacuum pressure for vapor steam creates a high specific volume that will be a critical factor in determining the size of the evaporator. Since the additional waste heat recovery adds refrigerant mass flow rate into the system, there is a substantial increase in the amount of heat rejected in the condenser which requires a larger condenser than the conventional mechanical A/C systems.

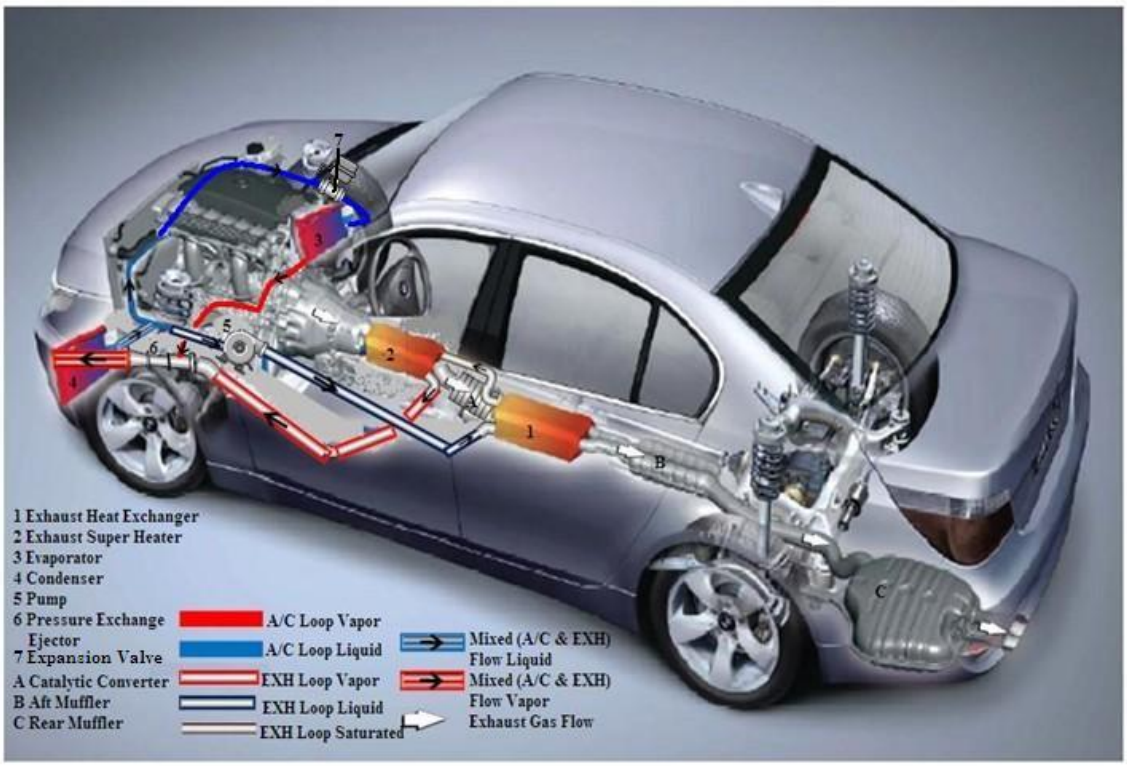

Figure 4.1.1 Full Diagram of Ejector Air Conditioning System on the BMW 530i sedan with Air Conditioning (A/C) loop and Exhaust (EXH) loop. (Courtesy of BSST and BMW).

The exhaust system contains constraints that are not to be overlooked during the design and operation of the heat exchangers. The biggest constraint is the catalytic converter requiring an exhaust gas temperature to be 582°F (300°C) or higher to effectively operate. This constraint obviates the initial idea of the evaporation and superheat of the steam refrigerant through using one shell and tube heat exchanger. This restraint requires the system to have two shell and tube heat exchangers. The primary heat exchanger (PHX) located furthest downstream of the two heat exchanger in relation to the vehicle engine and its exhaust system shown in Figure 4.1.2 was designed to heat the steam to 0.70 quality vapor state. The steam refrigerant would

then enter the superheater (SPR) and superheat to 530°F at 60 psia. Figures 4.1.2 and 4.1.3 detail the steam pressure and temperature through each air conditioning component. Conventional and pressure exchange ejectors once designed, have a very limited range with varying inlet and outlet pressure ratios and mass flow rates (Eames, 1995). As a result, pressure ratios and corresponding saturation temperatures were kept constant for both the high and low cooling loads. The designed ejector air conditioning system contains a low cooling air temperature of 50°F and controls can be administered to provide mixing of warmer ambient air of 60°F through engine coolant mentioned and graphically shown in Section 2.1.3. The condenser air temperature outside at set at 100°F and above which requires a steam refrigerant condensation temperature above that.

This analysis assumes that the refrigerant mass flow is compressible and steady state through the entire system.

Outside air and inside the car cabin are considered incompressible and at steady state flow and treated as an ideal gas for determination of thermal properties.

In all the heat exchangers, the heat transfer rate between the two fluids was calculated using the log mean temperature difference (LMTD). Bulk temperatures were used to determine specific thermal and fluid properties for both fluids along with heat exchanger wall temperature. Design parameters for each heat exchanger were kept constant in order isolate the desired changing variable. These parameters shall be discussed individually in future sections covering specific heat exchangers

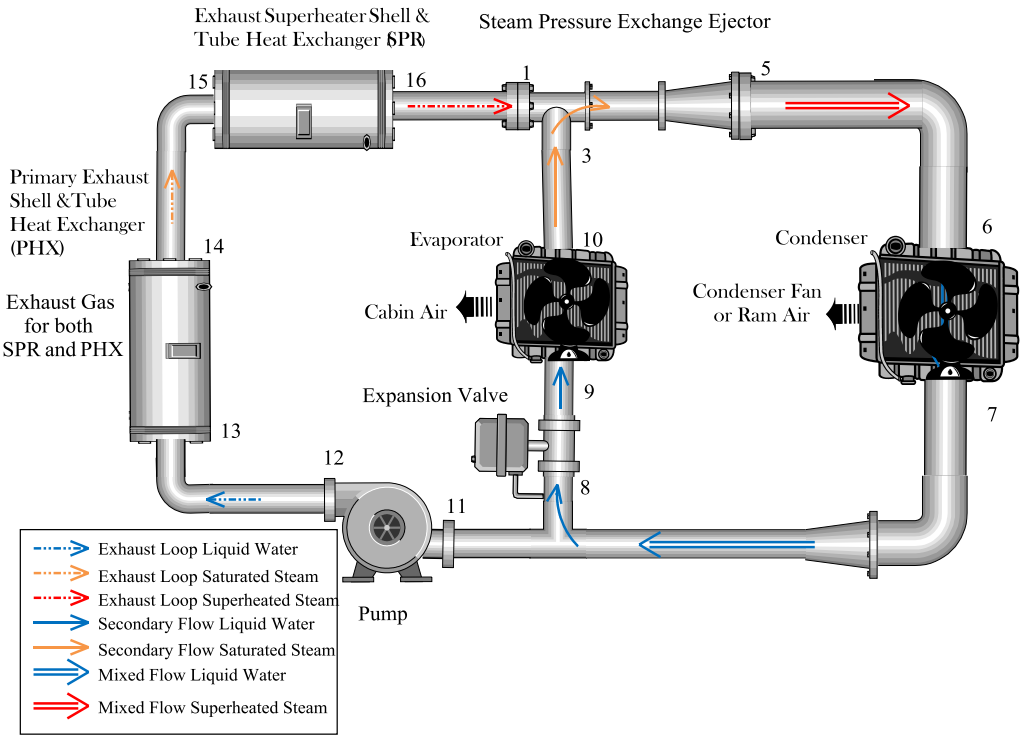

Figure 4.1.2 General Schematic of the Steam Pressure Exchange Ejector A/C System

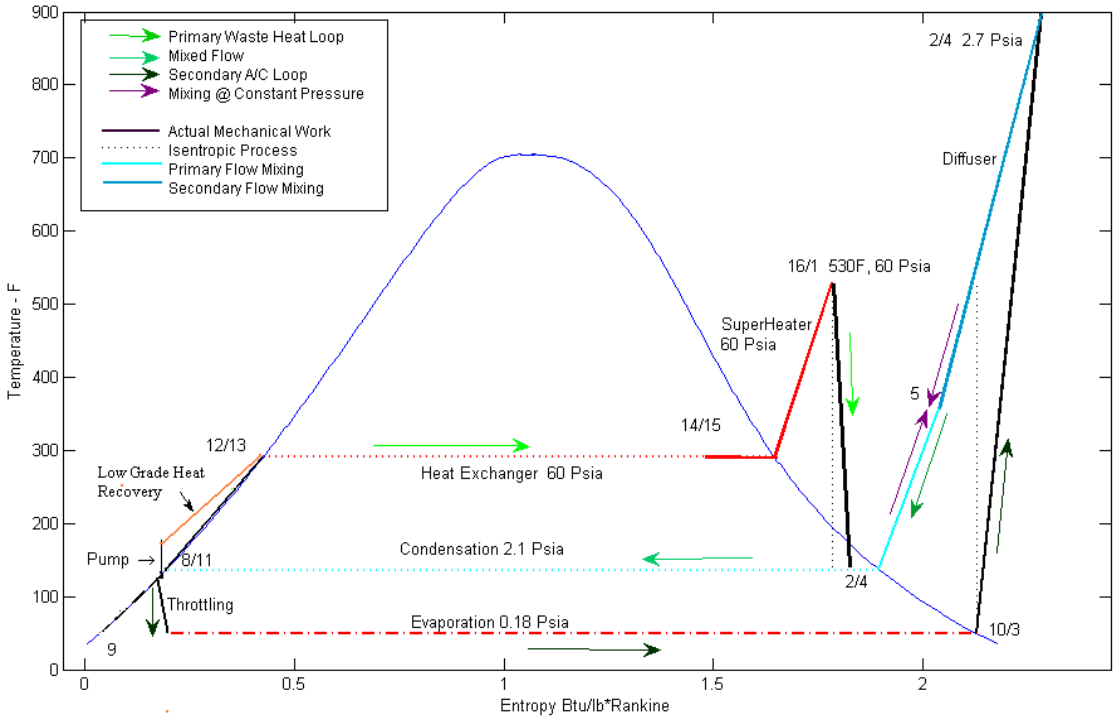

Figure 4.1.3 Temperature Entropy (TS) Chart monitored using MATLAB of the steam refrigerant in the PE ejector A/C system.

Further system parameters were set during the varying ejector efficiency simulations:

• The pump and ejector in the system are adiabatic with respect to the outside surroundings.

• Air, exhaust gas, and steam refrigerant flows are steady.

• The mass flow rate through the evaporator was kept constant for the constant low or high cooling load.

• Evaporator and condenser sizing was predetermined by (Kays, 1984) at slightly larger size and kept constant.

• Primary flow through the nozzle in turbomachinery analysis and the primary flow nozzle efficiency was assumed to be 90% (Fox, 2003).

• Temperature or pressure drops in piping between A/C components were considered negligible.

• During sizing and rating of exhaust heat exchangers, the lengths of the heat exchangers were kept constant.

4.1.1 Refrigerant Selection

A goal for the ejector air conditioning system is to contain a refrigerant that is environmentally friendly with zero ozone depleting potential (ODP) and low global warming potential (GWP) which are abiding to the Environmental Protection Agency (EPA) and European Union (EU) Standards. With our new ejector refrigeration design, the absence of a compressor dismisses the requirement of the refrigerant to be mixed with lubricating oil that is used to preserve the compressor vanes and prevent it from overheating. The R-134a refrigerant in the compressor driven A/C system require synthetic oils such as polyalkylene glycol (PAG) and polyolester (POE) to

provide lubrication. The absence of needing lubricating oil in the ejector air conditioning system will ease up on the restrictions in the selection process. In addition the fluid needs to be non-corrosive to metal, rubber, and plastic when it travels through all those materials in the cycle. Non-flammable and non-toxic properties would make for a safer refrigeration cycle. Lastly and probably the most important aspect in order to be considered in the free market, the mechanical and heat exchange components need to be cheap to produce, use, and dispose (Daly, 2006). The selection of steam as the refrigerant contains the low ODP and GWP standards although according to the EPA, water vapor is most dominant and abundant greenhouse gas in the atmosphere even compared to carbon dioxide. However, water vapor is not classified with a global warming potential due to its short life in the atmosphere. Water vapor is not well mixed (varies spatially 0-2%) in the atmosphere and automatically regulated in the atmosphere through precipitation (Office of Atmospheric Programs, 2002).

4.1.2 Condenser Design and Computer Simulations

The exhaust gas waste heat recovery loop is the driving force for the ejector air conditioning system but as a result it adds mass flow to the system and consequently more heat into the condenser. This in turn requires a larger condenser in the space restricted area in front of the car. The condenser frontal area of the length and width has been set constant and similar to the existing BMW 530i while the new design offers an extra row of tubes shown in Figure 4.1.4b to double the number of tubes and add surface area and thickness to accommodate for the larger mass flow rate and heat rejection. The design of the air cooled finned circular tube condenser is similar to the existing condenser and taken from previous design templates (Kays, 1984). The condenser design below in Figure 4.1.5 contains the various geometric parameters (A-

E) to conduct convection and conduction heat transfer calculations. The geometric parameters shown in Figure 4.1.5 are based from surface area ratios between the fins, condenser core, and a total surface area to total volume ratio referred to as compactness ratio. The surface area ratios aid in determining the hydraulic diameter and the free flow area for airflow through the condenser. These parameters aid in determining the pressure drops across the condenser along with calculating the air convention heat transfer coefficient detailed in Appendix B.2.

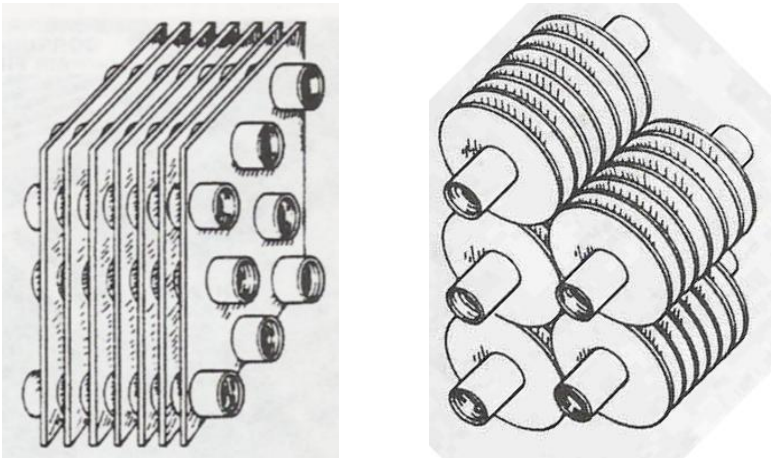

(a) (b)

Figure 4.1.4. Schematic of two types of air cooled compact heat exchangers (Kays, 1984). a) Plate-finned circular tube heat exchanger. (b) Coil-finned circular tube heat exchanger

Another addition to the condenser is the existing radiator/condenser fan to accommodate for the larger heat rejection load. The use of the fan is required in both the conventional and the ejector air conditioning system when the user demands low to high cooling loads in the cabin in cases when the car is idling, moving at slow speeds through traffic or climbing hills. Most vehicles contain a fan that cools both the radiator and A/C condenser along with the front section of the engine block as shown in figure 4.1.6a. The positioning of the condenser is set in front of the radiator where air flow is created through the condenser and radiator through induction. Shrouds are also constructed parallel to the flow to enhance the direction of flow and

reduce backflow. The fan air flow rate is designed to accommodate proper cooling for the radiator and condenser by factoring the sum of pressure losses across the radiator and condenser. The static pressure drop across the fan is function of the fan's performance and the system resistance curves.

The condenser/radiator fan is very sensitive to the pressure drop across the condenser, the type C geometric design was selected for its high hydraulic diameter and lower surface area to volume ratio to minimize the pressure drop across the condenser. Figure 4.1.7 details the pressure drop of air across the four different condenser design templates when applied to the same volumetric air flow rate. Type C in the finned circular tube condenser design provided the lowest pressure drop and was selected as the condenser to be used in analysis. The least compact condenser in model C provides the largest free flow/ frontal area ratio to aid in lowering its pressure drop. Analysis was conducted to determine whether selecting a less compacted condenser would fail and grow too big in size in order to handle the high heat rejection requirement under the assigned operating condition. Chapter 6 details the results of using Model C in the analysis of varying ejector efficiency at low and high cooling loads.

Fig. 10-89 Finned circular tubes, surface CF-9.05–3/4J. *(Data of Jameson.)*

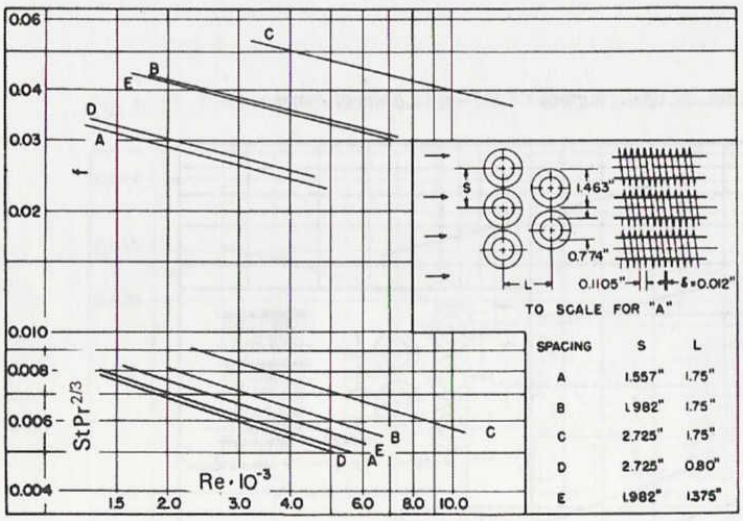

SPACING	S	L
A	1.557"	1.75"
B	1.982"	1.75"
C	2.725"	1.75"
D	2.725"	0.80"
E	1.982"	1.375"

Tube outside diameter = 0.774 in = 19.66 x 10^{-3} m

Fin pitch = 9.05 per in = 356 per m

Fin thickness = 0.012 in = 0.305 x 10^{-3} m

Fin area/total area = 0.917

	A	*B*	*C*	*D*	*E*	
Flow passage hydraulic diameter, $4r_h$ =	0.01681	0.02685	0.0445	0.01587	0.02108	ft
=	5.131 x 10^{-3}	8.179 x 10^{-3}	13.59 x 10^{-3}	4.846 x 10^{-3}	6.426 x 10^{-3}	m

Free-flow area/frontal area, σ =	0.455	0.572	0.688	0.537	0.572	
Heat transfer area/total volume, α =	108	85.1	61.9	135	108	ft^2/ft^3
=	354	279	203	443	354	m^2/m^3

Note: Minimum free-flow area in all cases occurs in the spaces transverse to the flow, except for *D*, in which the minimum area is in the diagonals.

Figure 4.1.5 Preliminary Condenser design used in the modified steam ejector air conditioning system. Condenser type C model was selected (Kays, 1984).

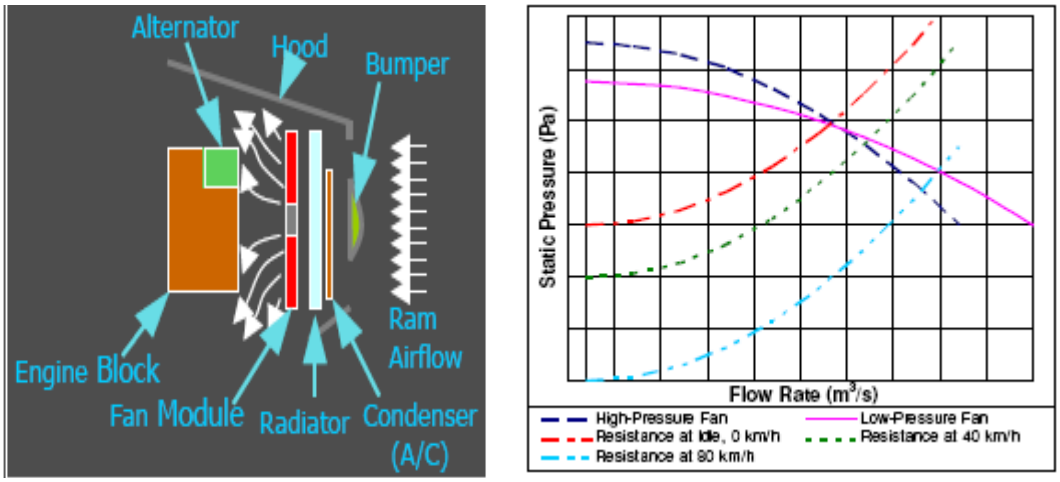

a) b)

Figure 4.1.6 a) Schematic of the engine compartment of a typical sedan. b) Axial fan performance example based on static pressure and system resistance. (Gifford 2006)

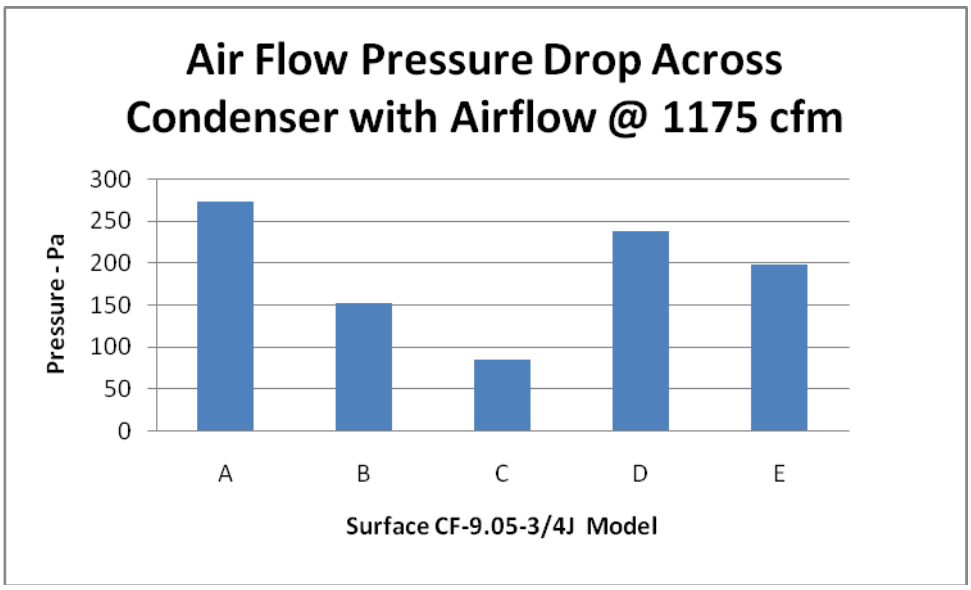

Figure 4.1.7 Air flow pressure drops with equal condenser volume and 1175 cubic feet per minute air volumetric flow rate from models shown in figure 4.3.2.

The critical condition that would require the most demand from the system would be a high cooling load during the idling conditioning where all components are

put under high load. Since the car is idling there is little or no convection heat transfer for the condenser, the condenser temperature sensors would trigger a high power load on the condenser fan and blower fan. Furthermore, the engine idling generates below average amount of heat and waste heat exchangers where only high efficient ejector of above 65% would be capable of provide those cooling needs. For the analysis between the steam pressure exchange ejector system and Bhatti R-134a system, the idling condition was simulated at low cooling load for a more realistic ejector efficiency application. Their results are compared in further detail in future chapters on their effectiveness and performance.

The process by which the design parameters and sizing of the heat exchanger involves taking basic preliminary steps to piece together all the factors that contribute to its performance. The first step is determining the desired cooling capacity for the system and the desired inlet and outlet temperature between the two fluids. For this experiment, the cooling capacity typical for the midsize sedan range from 1 to 2 tons (300 Btu/min – 600 Btu/min) based on the temperature difference between outside air and cabin air along with the desired setting dictated by passenger(s) in the car. Much of the outside and vehicle conditions set in the analysis are determined from Delphi's R-134a automotive A/C system analysis conducted by M.S. Bhatti.

4.1.3 Evaporator

The evaporator used in automotive air conditioning applications is similar to the condenser but tends to slightly smaller in volume because the heat rejection in the condenser is much larger than the heat absorbed in the evaporator. With the lower mass flow rate entering the evaporator compared to the mixed flow entering in the condenser for the steam ejector system, the heat rejected in the condenser is an order of magnitude larger. In terms of heat load, the evaporator size is not as critical factor

to system. However, the vapor steam refrigerant under vacuum conditions contains an intensely high specific volume in comparison to the other refrigerants as shown in Table 4.1.1. The high specific volume physical property leaves the evaporator with parameter that requires larger tubing and surface area. The steam's high latent heat transfer rate during its large latent heat of vaporization aids in lowering the surface area and volume size required from the evaporator

The evaporator design selected after many trials is the plate finned tube heat exchanger with serpentine flow of stagger vertical flow at the ends and horizontal flow across the length of the heat exchanger in Figure 4.1.8. The stagger pattern as oppose to the typical inline serpentine design adds thickness to the heat exchanger to be used with larger plate fins for added surface area. The heat transfer procedure and calculations used for this evaporator and the condenser in the steam pressure exchange ejector A/C system analysis are described in detail in Appendix B.

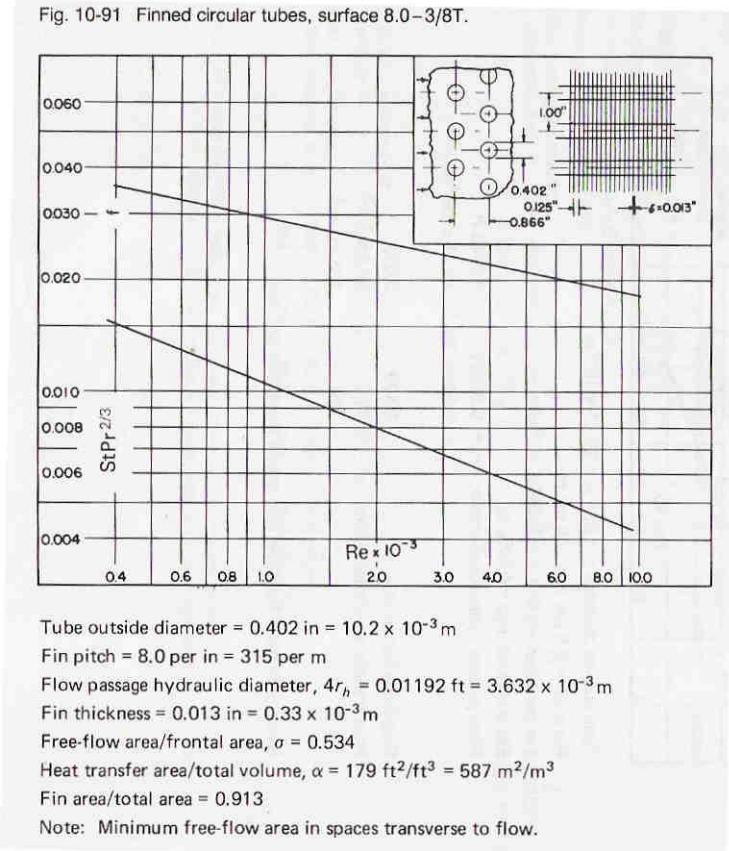

Figure 4.1.8 Evaporator design used in the steam ejector air conditioning system (Kays, 1984)

4.1.4 Pump

The exhaust loop pump to charge up the primary flow refrigerant provides the potential for consuming less energy in comparison to using a compressor. A smaller amount of energy is required to pressurize the liquid by a pump as opposed to the refrigerant vapor pressurized in a compressor is due to its lower specific volume. The pump unlike the compressor would be electrically driven either through the car battery or directly from the alternator. The option to use a mechanically belt driven pump is possible but the advantages of using an electrical driven pump outweigh it. The electrical pump in series thermoelectric sensors along the A/C system would result in a quicker and accurate response to cooling demand. Disconnecting the direct

connection to engine rpm like in the belt driven pump would eliminate the excessive load created at high engine rpm. The pump's low power load is low enough not to create a strain in the battery or alternator and the ability to easily electrically control the pump will create a more efficient system. A suitable pump for the application is a positive displacement 3 chamber diaphragm pump used for commercial RVs for providing pressurized water to kitchen and sink compartments in the vehicle. The pump specifications of electrical load controlled and providing up to 100 psi liquid water pressure at 0.84 gallons per minute. The pump work is determined thermodynamically through known inlet pressure and temperature leaving the condenser. From those values the steam's pump inlet enthalpy is determined and setting the pump exit pressure and temperatures allows the calculation of the exit enthalpy. The conditions designed for the pump are an inlet pressure of 2.7 psi at saturated liquid water state at 137°F and an exit pressure of 60 psi with a marginal increase of temperature at 150°F based on 80% efficient pump.

$$W_{pmp} = m_{refpmp} (I_{refpmpo} - I_{refpmpi})$$

The inlet and outlet temperatures and pressures are kept constant with the only changing variable in pump equation during varying ejector efficiency or cooling load conditions is the exhaust steam refrigerant mass flow rate. It is shown in the future results that at low ejector efficiency at specific cooling loads, the mass flow rate increases in order to compensate for the increase in primary flow's thermal input demand for the inefficient ejector.

4.1.5 Low Grade Waste Heat Recovery in Exhaust Insulated Piping

The steam refrigerant leaving the pump at 60 psi with minimal enthalpy rise from the inlet is designed to recover heat from the exhaust pipe through conduction as it travels parallel with it on its destination to the first heat exchanger. The inlet path of

the refrigerant piping in the exhaust loop begins at the pump located adjacent to the engine and travels three quarters the length of the exhaust system in order to reach the first heat exchanger. The design of aligning the refrigerant piping and the exhaust pipe parallel to each other near the exhaust manifold is to utilize the heat conduction between the two metal pipes as exhaust gas passes through inside the exhaust pipe at temperatures over 900°F (LaGranduer, 2004). The design uses the potential of recovering more waste heat that would normally be dissipated to the surrounding air. The amount of waste heat recovered is assumed to cover the enthalpy rise required from the pump exit enthalpy to enthalpy inlet of the primary heat exchanger referred to as low grade heat recovery in Figure 4.1.3. Insulating the refrigerant pipe and exhaust pipe further downstream of the exhaust manifold may be considered if piping at that location does not attain the desired steam refrigerant temperature rise of 150°F to 297°F. Another option is extending the refrigerant piping along the exhaust pipe and past the primary heat exchanger and recovering heat at the end of exhaust where for the BMW 530i the exhaust gas and wall temperatures are at least 300°F during idling conditions could also be extended along the exhaust pipe. The options explained above would add minimal frictional losses with the added length of refrigerant piping and with the high pipe temperatures of 900°F near the exhaust manifold, the pipe in that section would need to be steel in order to structurally withstand the high temperatures. The last option that would significantly modify the exhaust system is to insert the smaller sized refrigerant pipe inside the exhaust pipe and have the pipe travel to the primary heat exchanger and use the exhaust gas convection heat transfer to aid in heating up the refrigerant. The design solution with verified results is beyond the scope of this thesis and this section only describes ways of recovery waste heat that would provide the desired result. Experimental testing or

computation fluid dynamic software containing all the system parameters, engine performance, and air conditioning conditions will best determine the best option or options that will provide the desired waste heat recovered before entering the primary heat exchanger.

4.1.6 Exhaust Gas Shell and Tube Heat Exchangers

The exhaust waste heat recovery, mentioned in the earlier sections, had to be split up into two heat exchangers due to the presence of the catalytic converter lying right in the middle of exhaust system due to its required operating temperature of 582°F (300°C) or above (Heisler, 1997). The heat exchangers were set as shell and tube heat exchangers with the same material and configuration in Table 4.1.1. The first heat exchanger referred to as primary heat exchanger (PHX) handles the majority of steam evaporation to 0.7 vapor quality. The superheater (SPR) provides the rest of the heat to fully vaporize the steam and superheat it to 530°F. Since the steam refrigerant is designed to be superheated before entering the primary flow side of the ejector, the position of PHX is located downstream of the catalytic converter while the SPR lies upstream of the converter.

4.1.6.1 Design and Constraints

The design feature for the exhaust heat exchanger takes advantage of the high temperatures of the exhaust gas and the existing length of the automobile's exhaust system. The exhaust system runs three quarters the length of the car and for the 2005 BMW 530i sedan shown in Figure 4.1.10, it measures to around 11 feet. This allows a substantial amount of distance and area to recover heat from the engine's exhaust gas. A two tube pass and one shell pass shell and tube heat exchanger with a longitudinal baffle shown in figure 4.1.9 were designed for PHX and SPR heat exchangers. The benefit on the length of the shell and tube system is that it allows the heat transfer

process between the two fluids with less interior tubes and smaller shell diameter. At the tail end of the exhaust system, a muffler is required which limits the PHX length to 3.25 feet based on data shown in Figures 4.1.10 and 4.2.3 at the end of section 4.2. The spacing between the exhaust manifold and catalytic converter limits the superheater's length to 2.8 feet.

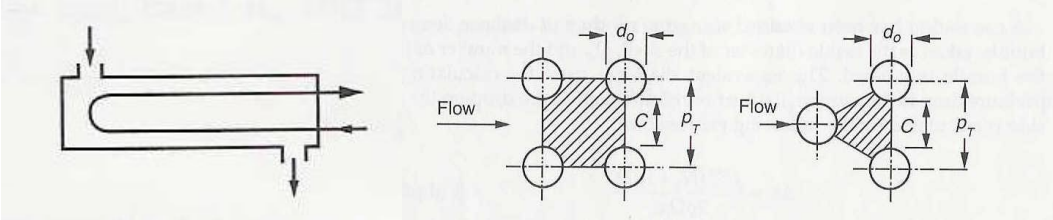

Figure 4.1.9 Diagram of One Shell and Two Tube Pass System for the Shell and Tube Heat Exchanger along with the Square and Triangle Tube Layouts. (Kakac, 2002)

The general rule for optimizing the geometric parameters of the shell and tube exchangers is to set the shell diameter to tube length ratio between 1/5 to 1/15 (Kakac, 2002). The conclusion was to contain two heat exchangers (PHX and SPR), to transfer enough heat from the exhaust gas to the steam refrigerant for phase change from sub cooled liquid to super heated steam. The actual diameter sizes for both heat exchangers also have a maximum limit due to the fact that it lies along the automobile's undercarriage where a certain clearance from the road is needed to prevent scraping and damaging the shell and tube heat exchangers especially from speed humps and speed bumps. According to the National Highway Safety Administration and the European Union, the average range for the automotive ground clearance for the exhaust system is between 10.25 and 11.8 inches (Heinz, 1998). The tests from Car and Driver Company in appendix B.3.1 on the BMW 530i show a ground clearance of 3.9 inches. This clearance doesn't give much space with speed humps and bumps along speed sensitive roads and neighborhoods ranging from 2.5

inches to 3.5 inches in height. Figure 4.1.10 shows that the low ground clearance is due to the low side and front paneling while the top of the exhaust system lies at the center of tire diameter which is 12.85 inches off the ground. A nine inch shell diameter heat exchanger would equate to about 3.8 to 3.9 inch ground clearance. To prevent risk of scraping and damaging the heat exchangers while traveling over uneven terrain or speed bumps, the front and rear suspension need to be raised 3 inches to give the set maximum limit of nine inch heat exchanger diameter with a 6.85 inch ground clearance. The handling and aerodynamic changes of the vehicle due to the raised automobile's center of mass would be minimal.

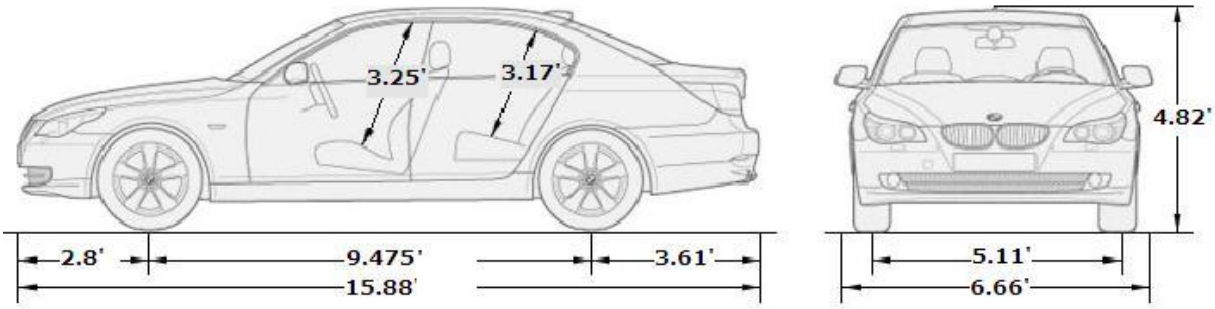

Figure 4.1.10 BMW 530i Full Body Drawing Schematic (Courtesy of BMW)

4.1.6.2 Shell-side and Tube-side Design

The shell and tube exhaust heat exchangers for both the PHX and superheater contain unknown geometric parameters such as the shell diameter size of the cylindrical shaped heat exchanger, diameter and number of tubes inside, and velocity of the steam refrigerant inside the tubes. For the tight spacing application, the shell and tube heat exchanger tube layout was set to a square tube layout with only two tube pass to maximize the potential number of tubes and in return minimize the shell diameter. The number of shell passes was set to one to minimize the exhaust pressure drop and back pressure. The tube pitch in the Figure 4.1.9, P_T, is designed so that the pitch ratio, $P_{RT} = P_T / d_{tout}$, is between 1.25 and 1.5 in order to keep the tube sheet that

hold up the tubes structurally stable (Kakac, 2002). For this application, the pitch ratio was set at 1.25 to maximize the number tubes inside the shell. Appendix B.4 and B.5 describe in detail the process by which preliminary geometric approximations using the Kern Method determined the initial unknown variables of tube-side refrigerant velocity, shell diameter, and number of tubes. These results were used in the heat transfer calculations of the shell-side and tube-shell convection and conduction coefficient properties from the log mean temperature difference method (LMTD). From this data the overall heat transfer coefficient and total surface area were calculated. These results were verified by working backwards using the LMTD method equations described in Appendix B.4 to solve for the initial unknown variables that the Kern Method approximated. If the approximations didn't match the LMTD results for the initial unknown shell diameter variable to within 2 percent, the approximations were then modified and LMTD heat transfer calculations were performed again until there was convergence.

Table 4.1.1 Shell and Tube Heat Exchanger design for both PHX and SPR Exhaust Heat Exchanger with recommendations and referencing from Kakac (2002)

Heat Exchanger Design and Material Selection

Tube inside	0.75 in.
Tube outside	0.68 in.
Square tube	1 in.
Number of	2
Baffle Spacing	0.45 * Shell
Baffle Cut	25%
Number of	2
Number of	1
Tube Material	Copper
Shell Material	Aluminum

4.1.7 Allocation of Streams for Shell and Tube Heat Exchangers

As the exhaust gas transfers heat to the steam refrigerant in the shell and tube heat exchanger, a decision needs to be made on which fluid flows through the tube and which travels through the shell. The steam refrigerant will flow through the tube and the exhaust gas flow across the shell. The considerations that helped determine this conclusion are (Kakac, 2002):

- The high pressure fluid is better fit to flow through the tube due to the tubes small diameter and only would the tube side channels and connections and not whole heat exchanger need to be designed to withstand high pressure
- The corrosive fluid must flow through the tubes otherwise both the shell and tubes will be corroded. Furthermore, it's more economical to manufacture special corrosive resistant alloys for the tubes than for the shell.
- The fluid with the lower heat transfer coefficient should flow on the shell side since it is easy to manufacture and design outside finned tubes.
- The fluid with lower mass flow rate should lie on the shell side since turbulent flow can be obtained at lower Reynolds number for better heat transfer coefficient on the shell side.
- The advice to have the more seriously fouling fluid flowing through the tube due to the easy removal and cleaning of the tubes as oppose to cleaning the shell.

All considerations except for the last one favor using steam refrigerant as the tube side fluid and exhaust gas for the shell side. Unfortunately for the last

consideration, the cleaning procedure will need an added effort if too much exhaust soot builds up.

Fouling is the accumulation of deposits and any undesired substances on a surface. The process of fouling occurs both in the interior piping and exterior surfaces of the heat exchanger. These unwanted deposits degrade the interior and exterior surface's heat transfer performance and over time clog up the piping and increase the pressure drop across the heat exchanger. As a result, more pumping power and larger heat exchanger surface area need to compensate for this added resistance. For our purposes involving three different heat exchangers, the condenser, evaporator, and exhaust heat exchanger, fouling factors for the evaporator and condenser will be similar due to fact that both are air cooled and contain high motive air as its secondary fluid. However, the exhaust gas heat exchanger will have exhaust gas and shell and tube design that will forecast a different fouling factor. There are different variables and fundamental processes involved in fouling and are described more in detail in previous literature (Kakac, 2004). The category by which all three heat exchangers fit under are particulate fouling which is from deposits and dust and crystallization fouling from inorganic salts in the steam refrigerant.

The heat exchanger analysis has included the fouling factor to closely match this resistance of the heat transfer process. Table 4.1.2 showcases the fouling resistance factor for both engine exhaust gas and steam (nonoil bearing) refrigerant.

Table 4.1.2 Fouling Resistance for Industrial Fluids from *Standards of the Tubular Exchanger Manufacturers Association* (TEMA 1988) With permission from Tubular Exchanger Manufacturers Association

TEMA Design Fouling Resistance for Industrial Fluids

Industrial Fluids	R_f (ft^2 -hr- °F / Btu)
Manufactured Gas	0.0100
Engine Exhaust Gas	0.0100
Steam (nonoil bearing)	0.0005
Exhaust Steam (oil bearing)	.0015 - .002
Refrigerant vapors (oil	0.0020
Compressed Air	0.0100
Ammonia Vapor	0.0100
CO_2 Vapor	0.0100
Chlorine Vapor	0.0020
Coal Flue Gas	0.0100
Natural Gas Flue Gas	0.0500

4.2 Analytical Procedure

The theoretical and numerical analysis of the automotive air conditioning system is conducted into the two sections. The first section is the theoretical pressure exchange steam ejector automotive air conditioning system analysis with various ejector efficiencies and assigned inlet and outlet refrigerant pressures and temperatures for each component in the system. The refrigerant pressures and temperatures are chosen for the condenser and evaporator to maximize the steam's latent heat transfer between the air and refrigerant. The role of the exhaust gas heat exchanger and the pump is to provide enough energy and mass flow rate to the primary flow inlet of the pressure exchange ejector to recharge the low pressure secondary flow. This primary flow loop is critical to minimize work done by the pump for it will need to be driven by either the car's engine belt drive. The pressure

differences between the primary and secondary flow for the pressure exchange ejector are designed for the optimization of the heat transfer and thermodynamics of the air conditioning system. The pressure exchange ejector analysis is considered an adiabatic process between the two fluids and uses the turbomachinery analog.

The conditions mentioned above and earlier in this chapter were inputted into the MATLAB algorithm with an iterative loop that would decrease the ejector efficiency from ideal (100%) to 22.5 % at 5% increments. The turbine for the primary flow was set at 100% for the ideal condition and then 90% for the rest of the iterations. The compressor for the secondary A/C loop was set at 100% for the ideal condition and then decreased at 5% increments down to 22.5%. The software had precautionary coding to tell the user if too much waste heat is needed from system than is available or in the case of the waste heat recovery heat exchangers or condensers if too much surface area is required.

The second half of the automotive air conditioning analysis is determining the capabilities of a standard conventional steam ejector. With experimentation of the conventional ejector from previous research, a range of pressure differences, entrainment ratios and compression ratios between the primary and secondary flow have been measured. Mentioned further in detail in Chapter 6, these measurements were used to calculate the experimental and theoretical ejector efficiency using the turbomachinery analog. Under the same conditions of cooling load, environment and vehicle conditions as the pressure exchange ejector A/C system, the low ejector efficiencies in the turbomachinery analog produced by experimental conventional ejector were implemented in the analysis. It was concluded that the calculated efficiencies of 20% and below would need more exhaust waste heat than what was available but was data collected and including in the analysis. This information helps

set a limit on the optimization of using steam as a refrigerant for the automotive air conditioning system with the existing ejectors on the market and will be compared with the theoretical capabilities of the pressure exchange ejector.

4.2.1 Implementation of Auto A/C System using MATLAB

The use of MATLAB software for the analysis of the automotive air conditioning provides ease in keeping track of all the thermodynamic and heat transfer variables with the changing car environment or ejector efficiency. The software allows for a customization of the system especially since it is a two loop air conditioning system. Little design modifications were made with the typical evaporator but the sizing and piping for the condenser, exhaust gas heat exchanger and superheater were made according to match the needed overall heat transfer rate. As shown in Figure D.1 in Appendix D, the algorithm behind the steam ejector air conditioning system reveals how the MATLAB program transfers the conditional fluid thermal properties and variables between sub functions.

The most critical sub function in the MATLAB program is the steam thermal and fluid dynamics properties function. This function written is capable of determining a variety of steam thermal properties based on known temperatures, pressures, and qualities such as enthalpy, entropy, saturation temperatures, viscosities, and thermal conductivity (Holmgren, 2006). It is also capable of finding enthalpy with just using known temperature and entropy if pressure is unknown. Holmgren developed the program using data from the 1997 steam and water data formulation from the International Association of the Properties for Water and Steam (IAPWS). The program can attain steam or water thermal properties in the temperature range of 32°F - 3632°F with pressure range from 0.089 to 1450.4 pound per square inch.

Appendix C shows the thermal properties used from the XSteam function and the known variables needed to find the thermal property.

4.2.2 BMW 530i Sedan Exhaust System Analysis

The waste heat recovery analysis used in the steam pressure exchange ejector air conditioning unit is derived from experimental results from an automotive waste heat thermoelectric project on a 2005 BMW 530i inline six cylinder sedan model conducted from BSST with consultation and data from BMW (LaGrandeur, 2006). The group's objective was to produce electricity from waste heat with thermoelectric materials and in doing so collected thermal and fluid properties of the exhaust system at different engine loads, speeds, and rpm for the BMW 530i. The data collected was a combination of experimental sensors measurements on the BMW 530i exhaust along with computer simulations from Advisor, a MATLAB program, developed by the National Renewable Energy Laboratory (NREL). According to LaGrandeur's report, the Advisor model demonstrated within 2% agreement to BMW tested fuel economy performance for the drive cycles and a 5% agreement to exhaust gas temperatures. This collection of data in the diagrams below were used to simulate the implementation of the new and modified steam ejector air conditioning system for an inline six cylinder gasoline internal combustion engine sedan at various speeds and engine loads. Further details on the calculations and equations used to connect BSST data with the vehicle conditions are described in Appendix B.3. In Figure 4.2.1, the New European Drive Cycle (NEDC) was used for this analysis (also known as MVEG-A cycle) which is the emissions certification in Europe consisting of four ECE-15 driving cycles and an Extra Urban Driving Cycle (EUDC) at the end (Pesaran, 2005). The ECE-15 and EUDC cycles that make up the NEDC are the standard driving modes for urban city driving in Europe. BSST's computer

simulations on the BMW 530i sedan in Figure 4.2.2 aided in providing exhaust temperatures along length of the exhaust system for the idle and 50 mph conditions in Figure 4.2.3.

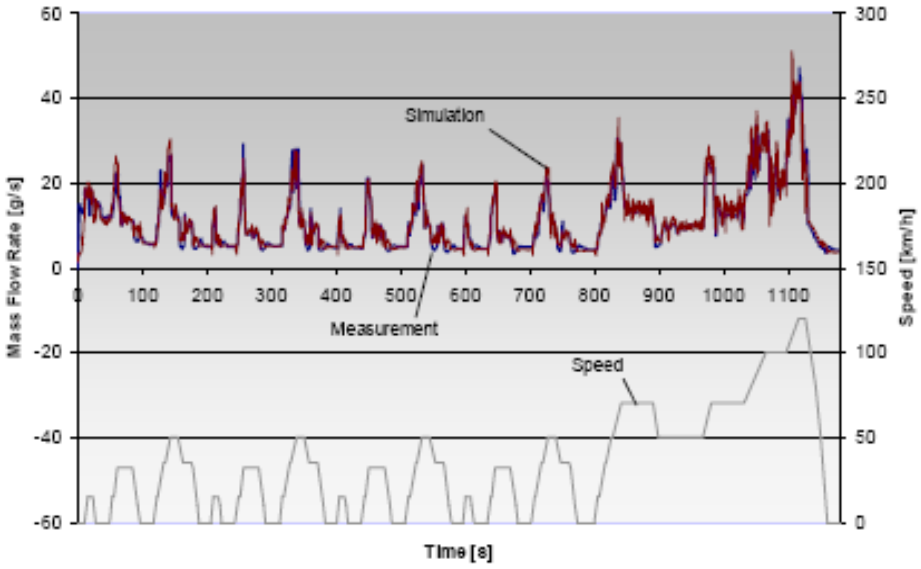

Figure 4.2.1 BMW 530i exhaust gas mass flow rate during New European Drive Cycle (NEDC) (LaGrandeur, 2006)

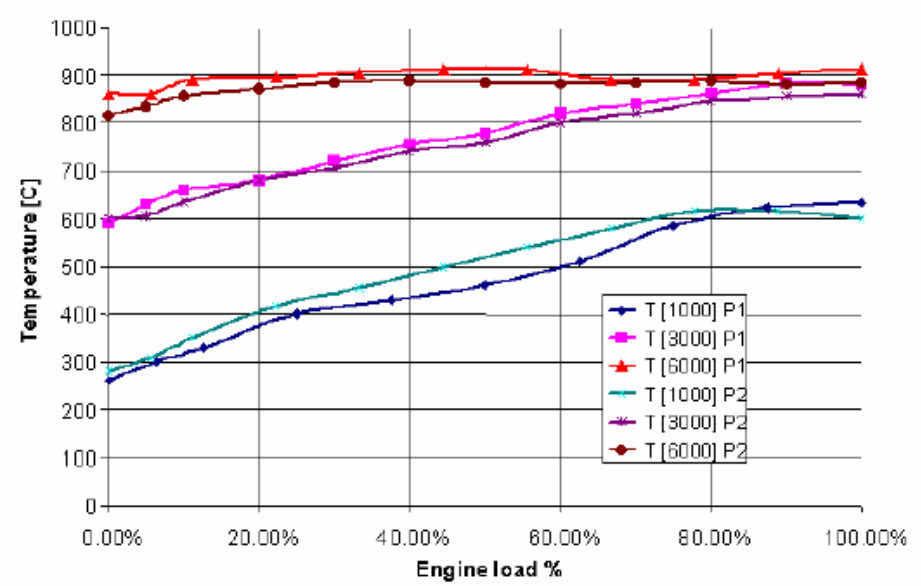

Figure 4.2.2 Exhaust gas temperatures in front (P1) of and behind (P2) the catalytic converter for various engine speeds (1000, 3000, 6000 RPM). (LaGrandeur, 2006)

The comparison between Bhatti's R134a system and the steam ejector air conditioning system were performed at idling and 50 mph conditions. The steam ejector air conditioning system requires corresponding exhaust gas thermal properties to match the idling and 50 mph engine conditions. The exhaust gas temperatures for the primary heat exchanger were approximated using a combination of data from Figure 4.2.1 and 4.2.2 based on the engine's load and rpm in the idling and moving state. After attaining the specifications of the BMW 530i drive train and transmission along with its coefficient of drag and rolling resistance, the 50 mph condition was set at 3000 rpm with the unknown engine load calculated using the total drag of the car and added auxiliary equipment that run off the engine belt drive or the car's battery. Since the 50 mph condition is considered cruising speed condition in Bhatti's analysis, the manual six speed engine is set on the sixth gear. The idling condition was set at 1000 rpm engine speed at 10% engine load to account for running auxiliary electric loads of 1500 W (85.3 Btu/min) from the battery such as lights, radio, etc. Appendix B.3 describes the equations and technical information behind all the concluding calculations. Figure 4.2.3 details the location of the shell and tube heat exchanger along with the piping and other air conditioning components which aid in approximating the exhaust gas temperature entering the heat exchanger.

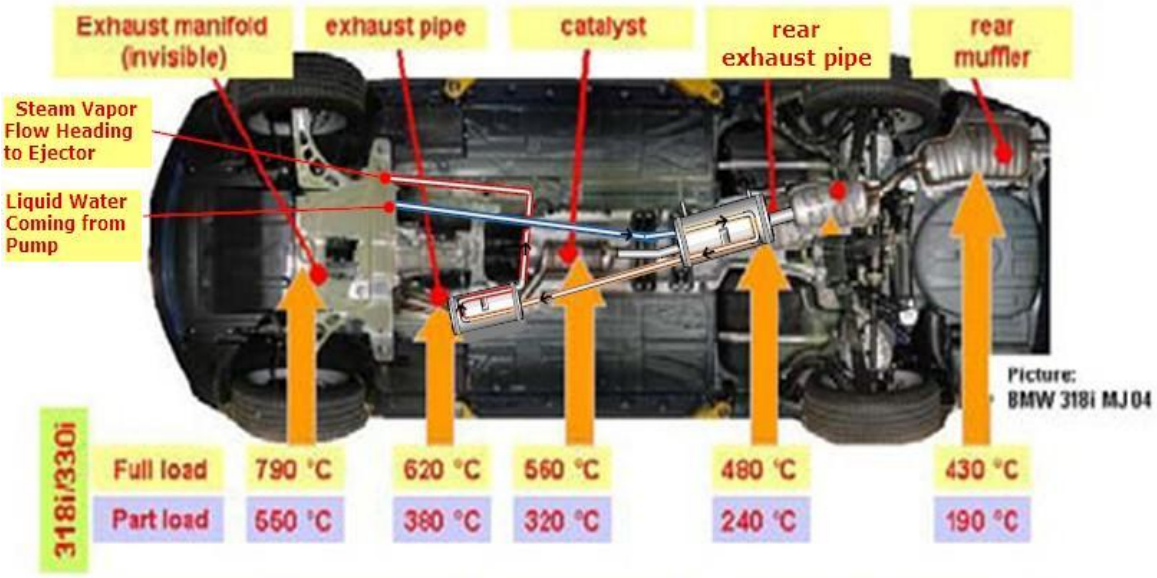

Figure 4.2.3 Modified Exhaust System for BMW 530i for Steam Ejector A/C System (LaGrandeur, 2005)

Chapter 5 Description of Delphi R-134a Conventional A/C System

5.1 Background of Delphi R-134a Air Conditioning System Model

The previous study conducted by M.S. Bhatti on behalf of Delphi Thermal Systems was an attempt to enhance the efficiency and performance of the existing automotive air conditioning system (Bhatti, 1999). The system was a typical vapor compression refrigeration system using refrigerant R-134a in a midsize sedan. The simulations conducted were under two conditions of the vehicle idling with a cooling load of 1 ton and the other condition of the vehicle traveling at cruising speed of 50 mph at 2 tons. Both conditions had similar outside environmental conditions but different desired cooled air temperatures for inside the vehicle. The idling condition at 1 ton cooling contained a desired air temperature of 70°F while the 50 mph condition at 2 ton cooling set the air temperature at 50°F. The simulation results to produce these desired results are detailed in Table A.4 in Appendix A. The report also describes the thermodynamic and heat transfer equations used in the heat exchanger simulation and are referenced in certain sections of this thesis.

The compressor being belt driven off the vehicle engine is in direct proportion to the engine rpm of 1000 and 2000 between the two conditions. Drive ratios for the compressor belt pulley system range from 0.89:1 to 1.41:1 based primarily on providing cooling capacities for low engine speed during idling. Consequently, the cooling capacity in the direct engine driven unit will increase steadily with engine speed. This provides a more transient refrigerant pressure and temperature output in the compressor. For high cruising speeds or acceleration, the compressor being driven off the belt can inadvertently consume up to 8 hp with a potential cooling

capacity of up to 4 tons (Balasubramaniam, 1975). The advantages of the belt driven system is flexibility at higher engine speeds of providing high cooling capacity if desired. The disadvantage of this flexibility is limited control of energy consumption since cooling capacities in vehicles only range from 1 to 2 tons of refrigeration (Balasubramaniam, 1975). Variable capacity compressors have been implemented in certain vehicles to match mass flow rates necessary for desired cooling capacity and reduce the compressor energy consumption. However for Bhatti's analysis, the compressor volumetric capacity is fixed which consumes more energy and creates a higher refrigerant mass flow rate and refrigerant pressure and temperature leaving the compressor than necessary. Bhatti details a theoretical ideal case in the analysis of fictitious belt driven compressor that can vary its volumetric capacity, control and modify compressor rpm speed to match the cooling load in which in return produces a 32% better isentropic efficiency. The result revealed half of the compressor rpm required and 1/10 of the energy consumed showing that the existing compressor has belt drive inefficiencies with limited control of matching the specific cooling capacity needed for the desired cooling load. One of the advantages of the steam pressure exchange ejector A/C system is the use of a low powered pump of less than 1 hp that is low enough to be electrically driven by the car battery or alternator as detailed in Figure A.5 and A.6 in Appendix A. An electric driven pump can be controlled through the thermoelectric sensors to match the cooling load capacity required with the corresponding pump impeller rpm and minimize excessive power use of the pump. The thermoelectric sensors would be similar to ones used for the trigger and controlling the radiator fan and are described more in detail in the next chapter.

Bhatti's main concern in his analysis was to show the energy efficiency and COP improvements for an enhanced R-134a A/C system. The lack of design

information of the fans, heat exchangers, and compressor analyzed in his report did make the design of the steam pressure exchange ejector system slightly more difficult and independent. Furthermore, all automotive air conditioning design companies and manufacturers do not provide design information for propriety reasons. BMW and Delphi who are used in this comparison refused to provide any design specifications on their air conditioning systems. The specifications of the blower and radiator fan were omitted in the Bhatti report but did detail the power consumed and corresponding air volumetric flow rate by the blower through the evaporator and radiator fan through the condenser for both the idle and 50 mph condition. The power consumed for the radiator/condenser fan was not included in the A/C energy balance calculations because it is considered to be used primarily for the radiator.

5.2 Automotive R-134a A/C Operating Conditions

The analysis conducted by M.S. Bhatti on behalf of Delphi Thermal Systems uses two specific conditions to compare the baseline R-134a A/C system with an enhanced R-134a A/C system along with the ideal version with 100% efficiency from compressor, radiator/condenser fan, and blower. The 68% compressor efficiency was declared the baseline compressor efficiency for the conventional automotive R-134a vapor compression A/C system (Bhatti, 1999). In this thesis, Bhatti's baseline R-134a A/C system is used for the comparison with the steam ejectors' A/C system.

Table A.4 describes in detail all the environmental and vehicle conditions involved in Bhatti and steam ejector A/C systems analysis. Table A.4 also contains the thermodynamic calculations of heat absorbed and rejected from the evaporator and condenser along with the power inputs required for the blower and compressor. The table showcases the effectiveness of the evaporator and condenser and the

amount of sensible and latent heat transfer which resulted from the designed simulated system. The table showcases the steam ejector A/C system calculations at 40.5% ejector efficiency compared with Bhatti's A/C system with 68% compressor efficiency.

Chapter 6 Comparison of the Automotive Conventional R-134a and the Steam Ejector A/C Models

6.1 Pressure Exchange vs. Conventional Ejectors Auto A/C System

The theoretical analysis of the pressure exchange ejector using the turbomachinery analog can be better referenced with its potential based off the performances from previous conventional steam ejectors and automotive conventional ejector systems. Since there has been limited experimental and computational testing on the pressure exchange ejector, this comparison provides a baseline for the novel pressure exchange ejector to improve upon. The design of the pressure exchange ejector is beyond the scope of this thesis and the conventional ejectors compared in this analysis are chosen based on similar pressure and temperature inlet conditions and corresponding mixed exit temperatures and pressures leaving the ejector. An accumulation of experimental results from previous conventional steam ejectors tests are detailed in the appendices (El-Dessouky, 2001). Table A.2 in the Appendix details the list of ejectors and their measured pressure readings at the inlets and exit of the steam ejector. All experiments listed were tested with inlet vapor flows at saturation pressure and temperature and using that information the steam inlet enthalpies for both the secondary and primary flow were determined. These inlet enthalpies were then used as inlets in the turbomachinery analog shown in Figure 6.1.1 as state 1 for primary flow and state 3 for secondary flow. The ejector exit pressure readings along with the condition used in the El-Dessouky experiments of mixing of the two fluids at constant pressure in the diffuser mixing region allowed for the calculation of the isentropic turbine and compressor enthalpy exit at state 4_{istrb} and state 4_{iscmp}.

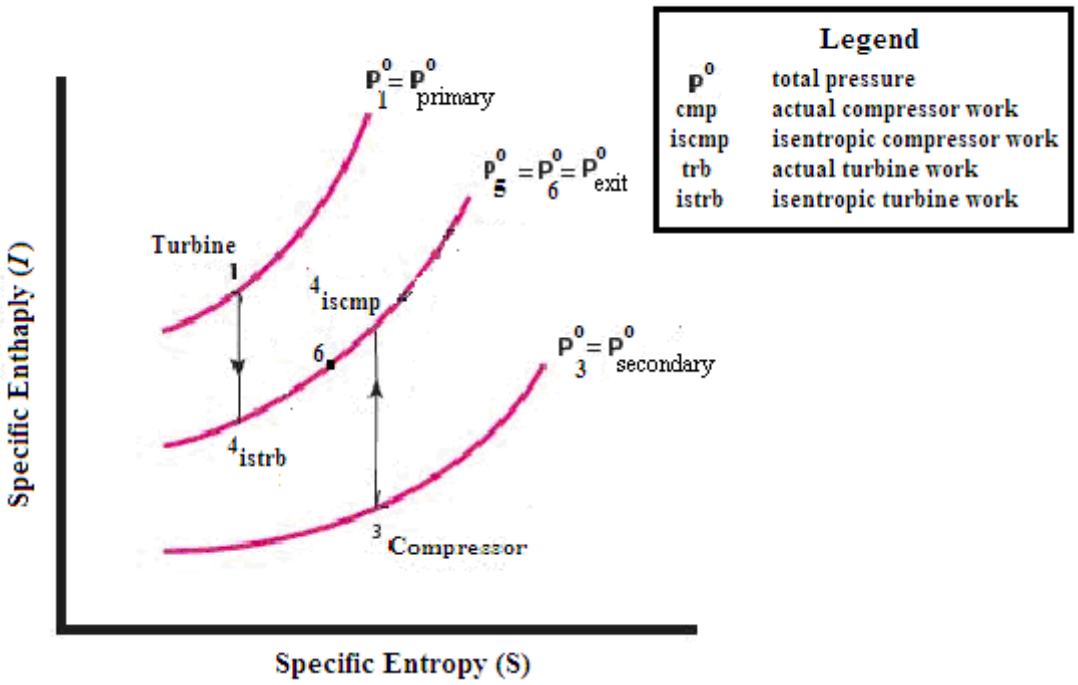

Figure 6.1.1 Schematic of Turbomachinery Analog using MATLAB for conventional ejector with mixing of two fluids at constant pressure to state 6.

Under adiabatic conditions and using the conservation of energy, the energy to compress the secondary flow is from the expansion process of the high pressure primary flow. This condition implies the actual work of the primary flow turbine process is equal to actual work done of the secondary flow compressor process shown in equation 6.1.0. Applying the ejector efficiency equation mentioned earlier in Chapter 3 and setting the actual compressor and turbine work equal to each other in equation 3.2.2 and 3.2.3, the ejector efficiency equation in 3.2.1 can be simplified to equation 6.1.1.

$$\eta_{ejector} = \eta_{compressor}\,\eta_{turbine} \qquad 3.2.1$$

$$\eta_{\text{compressor}} = \frac{\dot{m}_{\text{sec}} (I_{4_{\text{iscmp}}} - I_3)}{\dot{m}_{\text{sec}} (I_{4_{\text{cmp}}} - I_3)} = \frac{(I_{4_{\text{iscmp}}} - I_3)}{(I_{4_{\text{cmp}}} - I_3)} \quad 3.2.2$$

$$\eta_{\text{turbine}} = \frac{\dot{m}_{\text{prim}} (I_1 - I_{4_{\text{trb}}})}{\dot{m}_{\text{prim}} (I_1 - I_{4_{\text{istrb}}})} = \frac{(I_1 - I_{4_{\text{trb}}})}{(I_1 - I_{4_{\text{istrb}}})} \quad 3.2.3$$

$$\dot{m}_{\text{prim}} (I_1 - I_{4_{\text{trb}}}) = \dot{m}_{\text{sec}} (I_{4_{\text{cmp}}} - I_3) \quad 6.1.0$$

$$\eta_{\text{ejector}} = \dot{m}_{\text{prim}} (I_1 - I_{4_{\text{trb}}}) = \dot{m}_{\text{sec}} (I_{4_{\text{cmp}}} - I_3)$$

6.1.1

The entrainment mass flow ratio listed in Table A.3 were experimentally measured and used for the calculation of the ejector efficiency in equation 6.1.1. Table A.3 showcases the steam conventional ejector's wide range of efficiency of 5% to 18% that could potentially be used for steam refrigeration and air conditioning systems. Further analysis was conducted with tests by Eames to compare the ejector efficiency using the turbomachinery analog between the experimental and the theoretical results (Eames, 1995). The results comparing the top half of Table A.3 with Table A.4 show a decrease in efficiency difference from the experimental to theoretical with an average difference of 40% decrease with a range from 27% to 60%. The theoretical ejector efficiency averaged at 22.5% from Eames' three trials in Table A.4. This average result was used as the average theoretical efficiency of the steam conventional ejector and baseline for the pressure exchange ejector to improve upon.

The experimental steam conventional ejector A/C systems simulated for automotive applications conducted by Everitt and Raffit were also analyzed using the

turbomachinery analog where ejector efficiency ranged from 15% to 23% (Everitt,1999). This showed improvement from the individual steam conventional ejector efficiencies in Tables A.3.

Further conclusion and comparison to the conventional with the pressure exchange ejector is the difference in primary flow inlet conditions. The conventional ejectors in the past have used saturated steam at lower enthalpies to run the ejector. The pressure exchange (PE) ejector was thermodynamically designed to receive superheated steam for two important reasons. The first reason is to avoid the production of steam below the saturated line when the primary flow is expanded. This could create potential oxidation issues with the rotor bearings used in the PE ejector. The second reason for primary superheated steam is creating a higher enthalpy for the primary's turbine process in the turbomachinery analog. The result of a higher enthalpy is a lower primary mass flow rate through the ejector to power the secondary flow's compressor process in the ejector. The lower mass flow thermodynamically creates a higher entrainment ratio than a PE ejector using primary saturated steam at lower inlet enthalpy. Figure A.2 details the difference in entrainment ratios from conventional ejectors and the PE ejector at different calculated efficiencies based on the theoretically designed or experimentally tested inputs and outputs of the ejector using the turbomachinery analog and equation 6.1.1. There is a drastic difference in trends of the experimental and theoretical conventional ejector results and the PE ejector. The reason for this dissimilarity is the different primary flow inlet conditions and the fact that conventional ejector design and experimental results are derived primarily from compressible and supersonic and subsonic fluid dynamic equations. The turbomachinery analog used primarily for the design of the pressure exchange ejector in the A/C system is a thermodynamically idealization of the ejector under

adiabatic conditions to the outside surrounding and does not factor in subsonic and supersonic fluid dynamic equations used in the conventional ejector design.

6.2 Conventional R-134A vs. Pressure Exchange Ejector A/C System

The comparison between Bhatti's R134a conventional automotive air conditioning system and steam ejector air conditioning system involved matching the same cabin cooling capacity and environmental parameters listed in Table A.4. As detailed in Table A.4, the pressures, temperatures, and mass flow rates of the two different refrigerants at various points in system are drastically different where R-134a requires high pressure and steam refrigerant lies in vacuum pressure for the A/C loop. Factors such as the size of the interior area of the car, solar radiation, and the amount of glass area and people inside were beyond the scope of this analysis. The use of the Bhatti's high and low cooling load range of 1 ton to 2 ton of refrigeration is derived to correspond to the extremity of those factors and is a typical cooling load range for a midsize automobile (Bhatti, 1999). Theoretical computer simulations using MATLAB and XSteam function for steam thermal properties detailed in Appendix C will be based on those estimated heat loads.

The comparison is also conducted by varying the steam pressure exchange ejector efficiency from ideal conditions to 22.5% which is the approximate average theoretical efficiency of the steam conventional ejector using Eames results in Table A.4. The A/C unit at 40.5% ejector efficiency is critical to the analysis due in part to the calculation that the engine exhaust system at idle and 50 mph does not generate enough waste heat to provide the thermal inputs required by the ejector. Figure A.3 of the temperature vs. entropy (TS) chart and Figure A.4 of the ejector's Mollier Chart under the turbomachinery analog show the added work required by the compression process as the ejector efficiency decreases. As a result, the primary flow's turbine

process is required to drive the compression process and demands more thermal input from the exhaust waste heat recovery loop. Systems with ejector efficiencies below 40.5% such as the conventional ejector at 22.5% can work if the waste heat from the engine cooling system is considered and utilized. A system with waste heat recovery from engine cooling and exhaust system has been address in previous literature (Balasubramaniam, 1975) but is beyond the scope of this project. Further analysis were conducted on the steam PE ejector A/C system between ideal (100% efficient) condition to 22.5% ejector efficiency at idle condition and 50 mph condition to view and analyze the trends of certain variables in the system that are dependent on the ejector efficiency. On the other side of the comparison is the work done by M.S. Bhatti for a conventional R-134a A/C system with a belt driven compressor at 68% isentropic efficiency under the same operating conditions. The areas covered in the comparison of the two A/C systems and detailed in this chapter are the coefficients of performance, energy savings between one over the other, effects of the vehicle fuel economy, total weight of the systems, and the global warming impact of running each system.

6.2.1 A/C Performance Comparison

One of the important discoveries in the theoretical analysis of the steam PE ejector A/C system is determining when the increasing thermal input demand from the decreasing ejector efficiency exceed the engine waste heat created by the vehicle during the idle and 50 mph condition. Taking into consideration the maximum exhaust waste heat recovered under idle and 50 mph conditions to drive the steam ejector air conditioning system along with the demands of the desired air conditioning cooling load, the calculation of the minimum pressure exchange ejector efficiency to run each condition was determined. The engine exhaust waste heat system and

corresponding exhaust gas temperatures mentioned in Chapter 4 is, in general, a transient environment based on two parameters: the engine load and engine rpm. Interpolation from Figure 4.2.2 and other BSST recorded measurements were used to match exhaust gas temperatures with engine conditions (LaGrandeur, 2004). Figure 6.2.1 details the trend of the exhaust waste heat demand with decreasing ejector efficiency showing that at a 41% ejector efficiency requires the maximum available exhaust waste heat under idle condition and 40% ejector efficiency for 50 mph condition. The left-most measurement of 22.5% ejector efficiency is equivalent to the theoretical average efficiency of conventional steam jet ejector from Eames theoretical and experimental analysis. This measurement is to provide a reference to the existing conventional ejectors and their theoretical maximum performance. Obviously, the amount of waste heat needed to run the conventional ejector A/C system with 22.5% ejector efficiency shown in Figure 6.2.1 is nearly doubled of what is available from the engine exhaust system. The analysis for the 22.5% condition is based on the potential of utilizing enough waste heat from the engine cooling system especially since 45% of the total waste heat generated is absorbed the engine coolant (LaGrandeur, 2005).

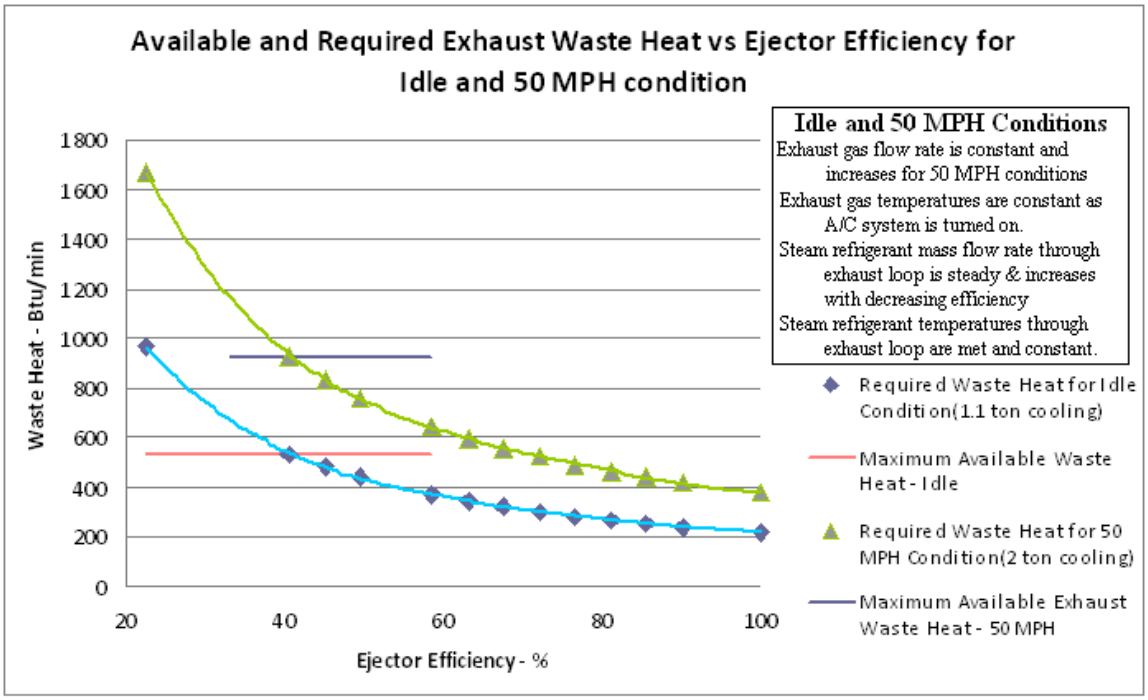

Figure 6.2.1 Plot of the required exhaust waste heat to run steam ejector A/C system at different efficiencies and corresponding maximum exhaust waste heat available during idle and 50 mph conditions for the 2005 BMW 530i sedan.

6.2.1.1 Coefficients of Performance

The coefficient of performance comparisons were conducted between the three A/C systems to determine whether an ejector A/C system can perform competitively with the one loop compressor driven A/C cycle. The conditions under review are:

- The pressure exchange ejector A/C system at various efficiencies using the turbomachinery Analog.
- A conventional steam ejector A/C unit at the Eames' theoretical average efficiency of 22.5% using turbomachinery analog
- Bhatti's conventional R134a vapor compression A/C system

The cycle COP analysis below in Equation 6.2.1 and 6.2.2, is a calculation based on the refrigerant performance with its cooling load and work done on the fluid to provide cooling. Bhatti's analysis for work input for the cycle coefficient of

performance (COP_{cycle}) calculation excluded the estimated condenser fan input, evaporator blower input, and power loss in the accumulator. This was done likewise for the two different steam ejectors to enable direct comparison. In the case of the steam ejector, there was no work added to cycle from the ejector but the primary flow's loop of the pump and heat exchangers were considered mechanical work and heat added to the cycle. The debate of whether to include heat added by the heat exchangers as part of the work done on the refrigerant can be interpreted in two different manners. The first perspective of the situation is concluding on the fact that the heat added is from an independent source and should not be included in work input for the COP_{cycle} calculation. The verification from this view point is that the source is from the combustion of gasoline used primarily to propel the car and not the A/C system where utilizing its waste heat is an independent source and a way of recovering energy that would normally be dissipated. The second manner is based on energy input required by the refrigerant in order to provide cooling regardless of the source. The manner by which the COP_{cycle} was finally analyzed was focusing on the energy required by the refrigerant in order to provide the desired cooling. Although the added energy from waste heat was independent of the air conditioning system it was required and for that reason it is included in the COP_{cycle} analysis. For other engineers who might focus more on the cycle and not the refrigerant where an independent source of waste heat would not be included in the work input, calculation with a double asterisk $**COP_{cycle}$ were calculated using Equation 6.2.2b and included in Tables 6.2.3-6.2.5. For Bhatti's conventional A/C system, the COP_{cycle} is defined as the heat absorbed in the evaporator over the work done on the steam refrigerant by the compressor:

$$COP_{cycle} = Q_{evaporator} / W_{compressor} \quad 6.2.1$$

The cycle COP for the pressure exchange ejector and 22.5 % efficient conventional steam ejector in the two loop A/C system is defined as:

$$COP_{cycle} = \frac{Q_{evap}}{W_{cycle}} = \frac{Q_{evap}}{(Q_{SPR} + Q_{PHX} + W_{pump})} \quad 6.2.2$$

$$**COP_{cycle} = \frac{Q_{evap}}{W_{cycle}} = \frac{Q_{evap}}{(W_{pump})} \quad 6.2.2b$$

In the case of the system coefficient of performance (COP_{system}) analysis, the added heat transfer enhancement devices such as the fans and accumulators are included. In Bhatti 's A/C system conventional COP_{system} is 10-15% less in comparison to the COP_{cycle}. In Bhatti's analysis, the fan used to cool the refrigerant in the condenser is the engine cooling radiator fan and isn't included in the energy balance or coefficient of performance calculations. However, the steam ejector A/C system with its larger sized condenser for the BMW 530i required more power during idling conditions from its 22.75 Btu/min (400 Watt) radiator fan. During idling conditions, the radiator/condenser fan was kept a constant maximum power and air volumetric flow rate to maximize convective cooling. Also, this condition was due in part to the inability to retrieve the power consumption at various fan speeds and corresponding air volumetric flow rate for the specific BMW 530i radiator fan. During idling for a conventional A/C system similar to Bhatti's system with low cooling load and the engine load below 25%, the power used to run radiator fan for the condenser and radiator was assumed to be 50% power. Based on this estimation, the radiator fan in the BMW 530i and Bhatti's analysis during the idle condition was

set at 11 Btu/min. The additional power of 11 Btu/min to keep the radiator/condenser fan at full power during idling condition for the steam ejector A/C system was included in the input energy balance and COP_{system} analysis. In the case for the 50 mph condition for both the Bhatti R-134a and steam PE ejector A/C systems, the ram air created by the vehicle moving exceeds the necessary volumetric flow rate through the condenser and radiator. The radiator/condenser fan was turned off under this condition.

For the steam ejector A/C unit with the exhaust waste heat recovery loop, the definition of the COP_{system} includes all the work done by the radiator fan, blower, and pump and excluding the independent waste heat thermal input into the system. As a system, the waste heat absorbed by the primary flow through the exhaust heat exchangers is from an independent source that removes heat from the car's engine regardless of air conditioning system. From this conclusion, the recovered exhaust waste heat was excluded in the work input for the COP_{system} calculation. From the conditions mentioned above, the system COP is defined as,

$$COP_{system} = \frac{Q_{evap}}{W_{system}} = \frac{Q_{evap}}{\left(W_{pump} + W_{evapblwr} + \Delta W_{cndfan}\right)} \qquad 6.2.3$$

The previous coefficients of performance equations are based on the mechanical work done on the refrigerant and leaves out the energy source of the system. The energy source of the system is a thermal source as gasoline provides energy to the engine as it combusts and is converted to mechanical energy to drive the car and the belt driven components such as the compressor or the substituted pump for ejector A/C system which powers the air conditioning system. With the public and automotive manufacturers taking a closer look at energy efficiency and energy conversation for a more fuel efficient vehicle, an important optimization of the

automotive air conditioning system is to include the efficiency of thermal energy conversion to mechanical work for a more in depth COP system analysis for the air conditioning system. The results for the thermal system COP ($COP_{thermsys}$) results are generalized thermal efficiency calculations for a sedan's engine for powering accessories and propelling the car.

$$COP_{thermsys} = \frac{Q_{evap}}{(\frac{W_{system}}{\eta_{therm}})} = \frac{Q_{evap}}{\left(\frac{(W_{pump} + W_{evapblwr} + \Delta W_{cndfan})}{\eta_{therm}}\right)} \qquad 6.2.4$$

The thermal efficiency of the vehicle was calculated based on the combustion energy of gasoline and the energy distribution percentage of the thermal energy to different components of the midsize sedan to estimate how much thermal energy is consumed in each component. The total energy distribution study from the Partnership for New Generation of Vehicle (PNGV) on a midsize sedan during highway travel was used to calculate the energy consumption for the 530i sedan travelling 50 mph with the air conditioning system turned off. The energy distribution percentages detailed in Figure 6.2.2 are derived from PNGV study and used as an estimation to the BMW 530i sedan. The 100% estimated energy consumption of 98.8 horsepower was calculated from using the combustion energy of gasoline of 108,690 Btu per gallon and determining the gasoline consumption over a period of an hour for the 530i sedan traveling at 50 mph. With its EPA estimated fuel economy of 30 miles per gallon, the calculation of one and two-thirds of gallons consumed was determined. During that one hour, the engine had burned a total of 181,250 Btu of thermal energy and was converted into thermal energy rate consumption from Btu/ min to horsepower as shown in Figure 6.2.2. This data was then used to compare the vehicle's energy consumption when using the three different air conditioning systems under the same conditions.

The percentages from figure 6.2.2 of the highway conditions were verified to close approximation based on the calculations in Appendix B.4 for the total drag from rolling resistance and aerodynamic resistance for the 530i sedan moving 55 mph. These results were based from the 530i sedan specs provided by Car and Driver and BMW detailed in Appendix B.3. As noted in figure 6.2.2, the total drag calculated for the 530i and the midsize vehicle from the PNGV analysis fall within 8% of each other under the average highway speed of 55 mph condition (Yang, 2008). Figure 6.2.2 is an average midsize vehicle under highway conditions where idling and standby does occur with traffic jam and traffic lights approaching the highway. The idling results shown in the figure of 3.6% do not apply to a vehicle that is travelling 50 mph at the moment and not knowing where the 3.6% can be redistributed, it is assumed as a percentage error to the 50 mph analysis.

Energy Distribution of the BMW 530i sedan under highway conditions

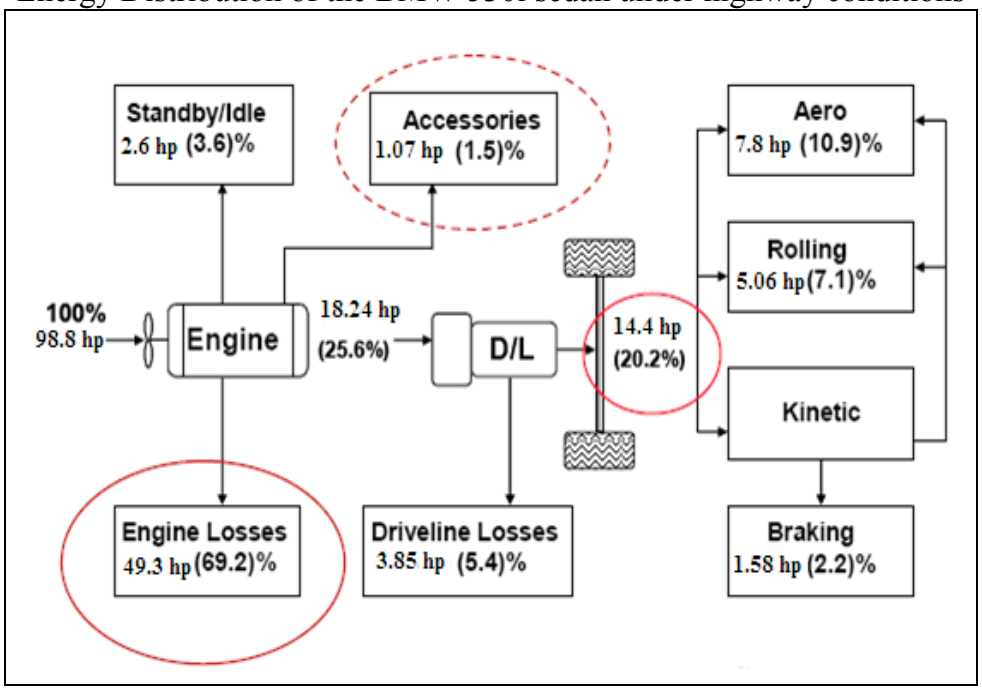

Figure 6.2.2 Energy Distribution percentage of a midsize vehicle during a Federal Test Procedure under highway conditions (Yang, 2008) and calculated power use for 530i sedan during one hour highway commute at 50 mph without air conditioning

In terms of the idling condition for the vehicle's energy distribution and consumption, the sedan is not in motion and the 500-1000 rpm engine speed is solely used to run the power steering, the engine cooling pumps at low load, and the alternator which charges up the battery. The battery is then used to provide electricity to the radio or any lights or electronic appliances that may be turned on. The fuel consumption and corresponding horsepower calculation is derived from a similar six cylinder sized engine from a midsize 2005 Chevy Malibu sedan done by Ahmad Pesaran from the National Renewable Energy Laboratory in Golden, Colorado (Pesaran, 2005). The report detailed that the vehicle consumes on average 4 grams of gasoline per second which equates to 0.35 gallons per hour. This data was used to determine the thermal energy rate of combusting gasoline where the total engine input of 15 hp was calculated and detailed in Figure 6.2.3. The energy distribution detailed in Figure 6.2.3 is derived from Pesaran's results for the Chevy Malibu of consuming 700 Watts (0.938 hp) when the air conditioning was turned off. The next step in the idling analysis is finding the specific increase in engine rpm and the added fuel consumption when the air conditioning is turned on. With limited information from BMW, technical information from Toyota mid size vehicle were used to estimate a similar engine electric control unit used in the 2005 BMW 530i sedan. The engine electric control unit (ECU) is a microprocessor device that controls the internal combustion engine based on a variety inputs such as the demands of the driver for acceleration while also monitoring and adjusting to the energy load for engine cooling, auxiliary power, air conditioning, and power steering.

Energy Distribution for midsize 6 cylinder sedan under Idling Conditions

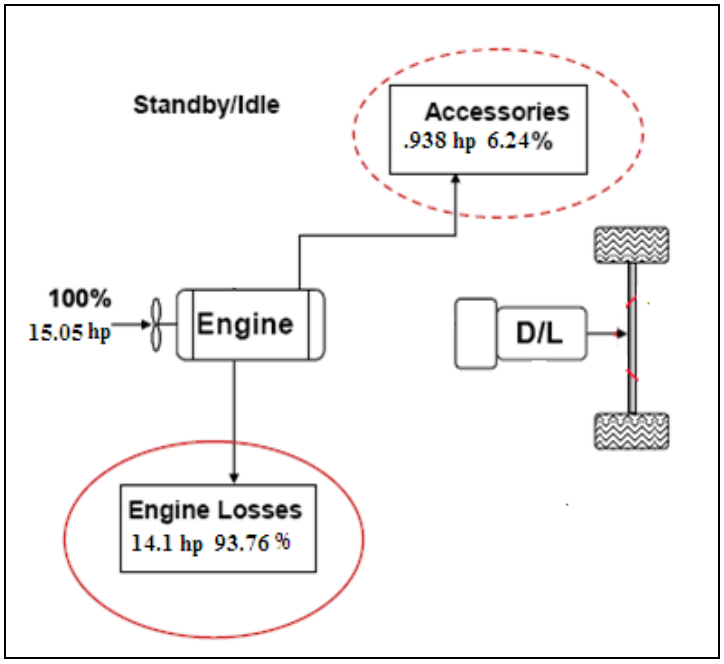

Figure 6.2.3 Idling condition percentages (Yang, 2008) and estimation calculations (700 rpm, 0.4 g/s of gasoline consumed) similar to the six cylinder BMW 530i sedan without the A/C turned on for the 6 cylinder engine of the 2005 Chevy Malibu sedan.

Further research and implementation based on the inefficient fuel consumption and harmful environment emissions during idling has created more sophisticated electric control units as the passengers and drivers are idling their car for a duration of time at the light, in traffic, or having the car turned on beforehand to cool or heat the car. From the 1980s and on, the automotive internal combustion engine have been fully monitored and controlled electronically through electric controls unit (ECU). The electronic controls unit is basically a microprocessor that can interpret and process input information at a hundred times a second and conduct output functions that control the engine to meet those input signals and demands. The output functions incorporated are

- Fuel Injection Control

- Spark Advance Control
- Idle Speed Control (ISC)
- Self Diagnosis
- Related Engine and Emissions Control
- Failure Management (fail-safe and back-up)

The newer ECU units contain memory capabilities for real time sensor processing in order to adjust with the degradation of the engine and engine wear. Previous ECU units processed data and converted outputs based on data charts stored from parameters of a brand new engine. This upgrade processes data based on monitoring the engine and other belt driven components through sensors on a more realistic engine performance. This upgrade enhances the control of the ignition timing, variable valve timing, and quantity of fuel. Within the ECU unit, the vehicle contains an idle speed control program to control idling operations which handles one or more of the following controlled condition parameters (Toyota Motors, 2005):

Table 6.2.1. Typical Idle speed control program application within the engine electronic control unit for an internal combustion engine vehicle under idling conditions.

Idle Speed Control (ISC) System Applications		
ISC Type	**Relevant Inputs**	**Controlled Condition Parameters**
Step Motor	Engine Speed	• Fast Idle
	Engine Coolant Temperature	• Warm Idle
	Air Conditioning Clutch	
Rotary Solenoid Type	Electric Load	• Automatic Transmission Idle-Up
	Throttle Signal	
Duty Control Air Control Valve type	Vehicle Speed	• Air Conditioning Idle
	Neutral Switch	
On-off control vacuum Switching Valve type		• Electric Load Idle-up

There are four different types of Idle Speed Control units listed in Table 6.2.1 that can be used for the idle speed application. Each provides a specific dynamic approach to monitor and adjust the engine rpm and fuel intake to match the relevant input demands. The controlled condition parameters listed in the table are in order by which the idle speed control (ISC) handles the relevant inputs. Once the engine is turned on, the idle speed control sets a high rpm speed to raise the engine coolant temperature to normal operating temperatures of 176°F (Toyota Motors, 2005). Once that temperature is reached, the control unit switches over to warm idle mode at lower engine rpm. Most vehicles require the engine rpm of at least 200 rpm to provide enough crankshaft rotation for fuel injection (Toyota Motors, 2005). The electric load and air conditioning clutch input signals trigger the ISC to increase the engine rpm to

meet the added energy demand. The signals are calibrated with the ISC unit in memory to raise the engine rpm a specific amount for the precise electronic trigger signal. The automatic transmission idle conditions are based on the throttle and neutral switch signals for the engine load and speed change strategy in preparation for when the vehicle starts moving and kills the ISC program.

Table 6.2.2 Target idle speeds for a typical Toyota sedan under idling conditions with various air conditioning input signals along with neutral switch.

Idle Speed Control (ISC) Target Idle Speeds		
A/C Switch Position	Neutral/Start Switch Position	Target Idle Speed
ON	ON	900 rpm
ON	OFF	750 rpm
ON	Manual Transmission	900 rpm
OFF	ON	700 rpm
OFF	OFF	600 rpm
OFF	Manual Transmission	700 rpm

The data shown in Table 6.2.2 of the target idle speeds of the ISC for a typical sedan reveal that increasing the engine load by turning on the air conditioning in fact increases the engine rpm during idling. Further in depth analysis for more precise results would require an experimental analysis to correlate the actual A/C system load with the corresponding increased engine rpm at idling condition. For the scope of this estimated analysis, the data from Table 6.2.2 of the target idle speed from 600 rpm to 900 rpm was applied when the A/C was turn on. This additional engine rpm is combined with the assumption that the fuel to air injection ratio is kept constant for the minimal increase in engine rpm and engine load. As a result, the engine rpm / fuel consumption idling ratio of 1 to 1 was used to calculate an increase of gasoline consumption from 0.35 gallons per hour to 0.62 gallons per hour for the gasoline

combustion exhaust mass flow rate when the A/C was turned on at low cooling load of 1 ton. The Bhatti's R134a A/C system analysis of the added 3.35 horsepower (142 Btu/min) power consumption rate in Table 6.2.6 during its 1 ton cooling load during idling condition was used with the 0.62 grams per second gasoline consumption. Figure 6.2.4 details the energy distribution and consumption when the A/C is turned on. This information reveal that the added 3.35 horsepower load from turning on Bhatti's conventional A/C, with an idling engine will in fact burn more gasoline as the engine rpm increases. Reducing the energy consumption from the air conditioning system during idling condition would lower the engine rpm speed and fuel consumption.

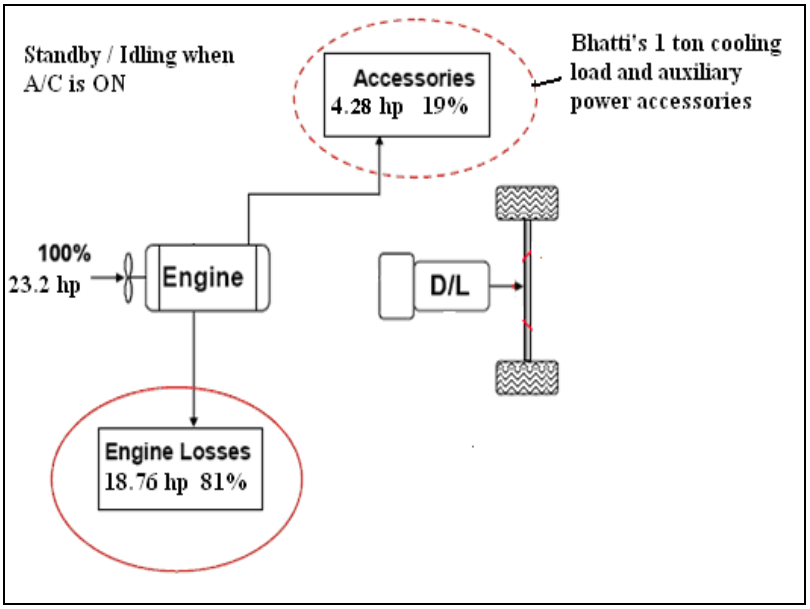

Figure 6.2.4 Idling condition percentages (Yang, 2008) and estimation calculations (900 rpm, 0.62 g/s of gasoline consumed) similar to the six cylinder BMW 530i sedan when Bhatti's A/C's 1 ton cooling load is turned on for the 6 cylinder engine of the 2005 Chevy Malibu sedan.

The calculations from figure 6.2.4 reveal that the thermal efficiency of running Bhatti's A/C system under 1 ton cooling load is around 19% when applying the chemical energy to mechanical conversion for the compressor and chemical to

electrical energy conversion for the evaporator blower, radiator fan, and accumulator. As a result, the thermal system coefficient of performance ($COP_{thermsys}$) decreases to 81% lower than the system coefficient of performance (COP_{system}).

The results from Table 6.2.3 reveal that the COP_{cycle} for Bhatti's R-134a conventional system is substantially larger than the steam PE ejector A/C system at 40.5% and 22.5% efficiency. The same drastic comparison in the COP_{cycle} between Bhatti and steam PE ejector A/C system was showcased in Table 6.2.4 for the 50 mph condition at 2 ton cooling. The addition of the exhaust waste heat recovered from the superheater and primary heat exchanger characterized as work done in the steam PE ejector COP_{cycle} calculation is the reason for the low value.

Table 6.2.3. Coefficient of performance of the conventional R-134a A/C system simulation tests (Bhatti 1999) and steam ejector A/C systems during idling condition with a 1.13 ton cooling load. *Results provided that required waste heat recovery would be attainable. (**)COP_{cycle} for steam ejector A/C system excluding waste heat as added work.

Idle Condition (Low Cooling Load – 1.13 ton)

Coefficient Of Performance	Bhatti R-134a A/C System (η_{comp} -68%)	Minimum Pressure Exchange Ejector A/C – 40.5 % Efficient	*Theoretical Conventional Ejector A/C – 22.5 % Efficient
COP_{cycle}	1.87	0.41 (**8.73)	0.23 (**5.97)
COP_{system}	1.59	5.03	3.98
$COP_{thermsys}$	0.302	1	0.79

The addition of waste heat in the COP_{cycle} analysis was based on the perspective that the added energy absorbed is required by the refrigerant in order to provide cooling even though the exhaust heat is from an independent source and required by the engine to be removed. The drastic difference in COP_{cycle} values

shown for both conditions reveal that Bhatti's system is close to five times as large as the COP_{cycle} value for steam PE ejector system at 40.5% efficient. Table 6.2.3 and 6.2.4 also contains the cycle COP value (**COP_{cycle}) which is the calculation of COP_{cycle} with the omission of the waste heat recovery as work input. This analysis is used for reference to compare with the Bhatti's result based on a different work input analysis. The comparison between ideal cases in Table 6.2.5 show an even larger comparison with Bhatti's COP_{cycle} value of 15 to 20 times larger than the COP_{cycle} for the steam PE ejector. The **COP_{cycle} value falls in competitively with Bhatti's COP_{cycle} with close to matching values for the 50 mph condition. The difference between COP_{cycle} and **COP_{cycle} for the steam PE ejector A/C system show the magnitude of including and not including the waste heat as a work input.

Table 6.2.4. coefficient of performance of the conventional R-134a A/C system simulation tests (Bhatti 1999) and steam ejector A/C systems during vehicle moving at 50 mph with a 2 ton cooling load. *Results provided that required waste heat recovery is attainable. (**)COP_{cycle} for steam ejector A/C system excluding waste heat as added work.

50 MPH Condition (High Cooling Load – 2 ton)

Coefficient Of Performance	Bhatti R-134a A/C System (η_{comp} -68%)	Minimum Pressure Exchange Ejector A/C – 40.5 % Efficient	*Theoretical Conventional Ejector A/C – 22.5 % Efficient
COP_{cycle}	2.01	0.41 (**15.16)	0.23 (**8.42)
COP_{system}	1.81	8.73	5.97
$COP_{thermsys}$	0.54	2.62	1.79

Table 6.2.5. Coefficient of performance of the conventional R-134a A/C system simulation tests (Bhatti 1999) and steam ejector A/C systems for ideal conditions during idle and vehicle moving at 50 mph conditions. (**)COP_{cycle} for steam ejector A/C system excluding waste heat as added work.

	Idle Condition (1.1 ton Cooling)		**50 MPH Condition (2 ton Cooling)**	
Coefficient Of Performance	Bhatti R-134a A/C System Ideal Conditions	Steam Pressure Exchange Ejector A/C - 100 % Efficient	Bhatti R-134a A/C System Ideal Conditions	Steam Pressure Exchange Ejector A/C - 100 % Efficient
COP_{cycle}	20.55	0.96 (**13.26)	14.05	1.01 (**37.4)
COP_{system}	11.08	6.27	10.51	13.3
$COP_{thermsys}$	2.63	1.25	2.63	3.98

The steam ejector system excels with the system and thermal system coefficient of performance results for both the idling and 50 mph condition in comparison to Bhatti's 68% compressor efficiency A/C system. The difference between the two system's COP_{system} values is a factor of 3 for idle condition and a factor of 4 for the 50 mph condition with the 40.5% efficient steam PE ejector A/C system. The 22.5 % conventional ejector system produces a COP_{cycle} 2.5 times Bhatti's system for the idling condition and 3 1/3 times for the 50 mph condition.

The various system coefficients of performance of Bhatti's R134a A/C system at different isentropic compressor efficiencies were also calculated in the report and detailed in Figure 6.2.5. A variety of different types of compressors can be used in the conventional vapor compression automotive air conditioning systems such as centrifugal, reciprocating, and scroll compressors. Bhatti's A/C system uses a reciprocating compressor with an isentropic efficiency of 68%. The reciprocating compressor can range from 60 to 70 % depending on the operating condition (Daly,

2006). The figure reveals the COP_{system} values for all ejector efficiencies above 20.5% for both the idle and 50 mph conditions contain a higher COP_{system} value than the Bhatti A/C system's value with a 90% efficient compressor. Under the 50 mph condition, the steam PE ejector system's COP_{system} from 22.5% to 100% efficient system ranges from three fold to six fold in value compared to the Bhatti's A/C system at 68% efficient. This data reveals how drastically the COP_{system} increases for a system that utilizes available waste heat to aid in driving its air conditioning system.

The ideal conditions for Bhatti's R-134a system mentioned in Table 6.2.5 were included as separate points in Figure 6.2.5 representing the perfect ideal case where the belt driven compressor runs independent of the engine and at an rpm speed matching the desired cooling load along with no losses from the evaporator blower and accumulator. Even with the ideal condition for Bhatti's R-134a system is 21% less than the ideal case for the steam PE ejector system under the 50 mph condition. The idle condition where the radiator/condenser fan work input is including in the steam PE ejector system lowers to 44% below Bhatti's ideal COP_{system} value under the same condition. The Bhatti system under this condition does not require extra fan power from the radiator fan that would increase its energy consumption and lower COP_{system}.

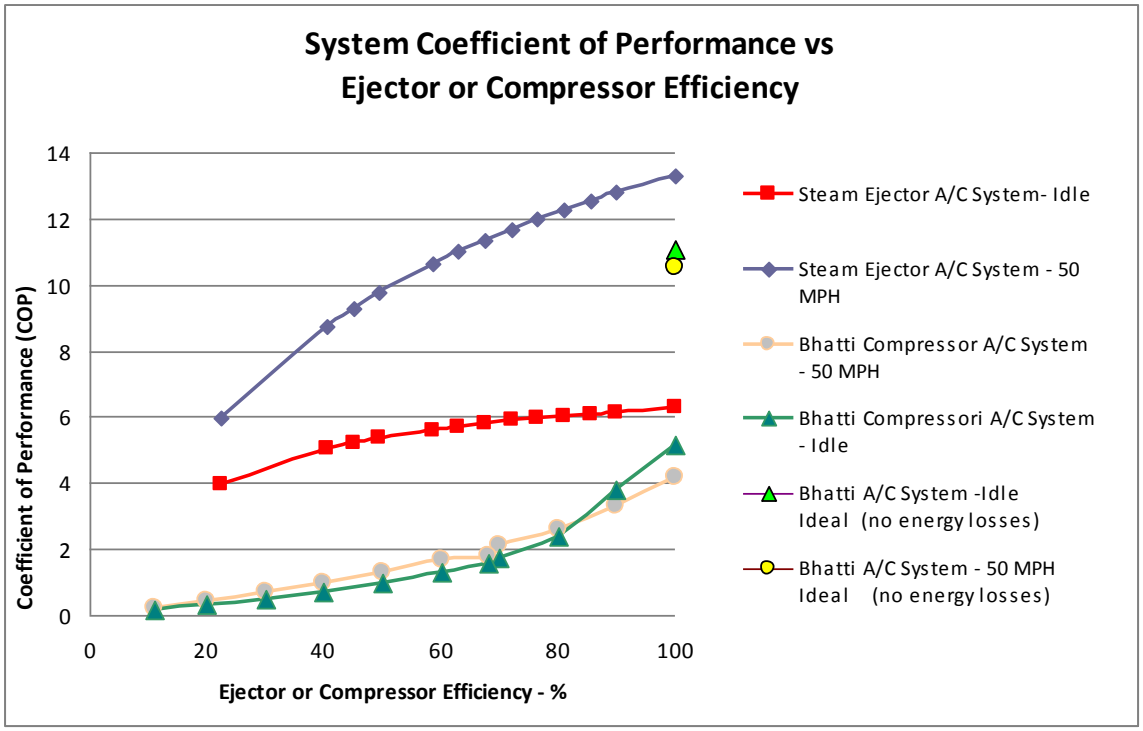

Figure 6.2.5 System coefficient of performance (COP_{system}) of automotive air conditioning system for high cooling load (50 mph) and low cooling load (idle condition).

The thermal system coefficient of performance, $COP_{thermsys}$, in Figures 6.2.6 display a larger gap in value between the 50 mile per hour condition and idling condition due primarily to the difference in thermal efficiency of the car of 27.1% when the car is traveling 50 mph and 19% when the car is idling which are detailed in Figures 6.2.2 and 6.2.4. The trends in Figure 6.2.6 are quite similar to the trends shown in Figure 6.2.5 where the $COP_{thermsys}$ values for both systems at each efficiency trial are about one fifth to one quarter of its COP_{system} value.

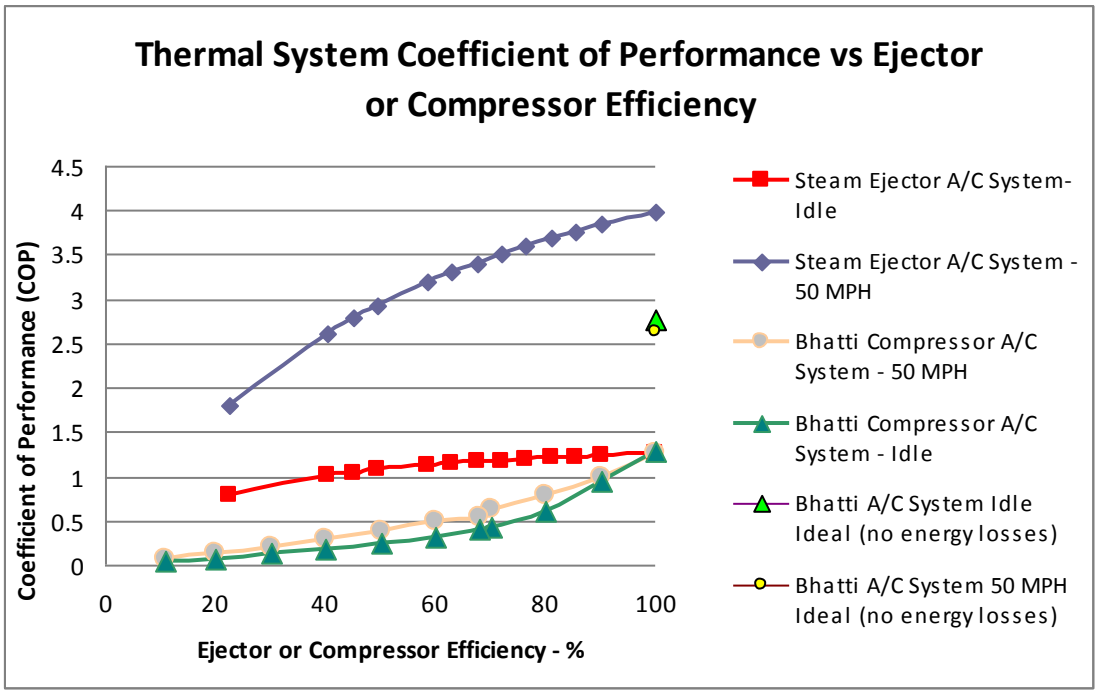

Figure 6.2.6 Thermal system coefficient of performance ($COP_{thermsys}$) of automotive air conditioning system for high cooling load (50 mph) and low cooling load (idle condition) for both the steam ejector and Bhatti R134a conventional system.

6.2.1.2 Energy Efficiency and Fuel Economy

The mechanical and electrical energy consumption of the A/C system for both the steam ejector and R-134a conventional systems are both driven by the engine and contribute to decreasing the fuel economy of the vehicle. During idling conditions, the amount of energy needed to run the A/C system for Bhatti's A/C system is simply the compressor and evaporator blower energy input along with energy losses in the accumulator and the transmission losses during the compression process. The energy consumption for all ejector efficiency trials in the steam pressure ejector A/C system detailed in Table 6.2.6 show the added condenser fan power when the fan was kept at full power during the idle conditions. The primary flow pump's power consumption was also included in the total energy consumption. The table reveals the ideal 100% efficient steam PE ejector A/C system along with the system at 40.5% ejector

efficiency of when the system reaches the maximum available waste heat recovery limit and the 22.5% ejector efficient representing the conventional ejector if hypothetically there was enough available exhaust waste heat. Ejector efficiencies below 40.5% would require the system to recover the rest of the 45% of wasted heat from the engine coolant system. The 40.5 % efficient system under the idle condition shows that it uses one third of the energy that Bhatti's system requires which equates to 97 Btu/min (2.3 hp) energy consumption savings

Figure 6.2.7 details the percent energy savings between the two systems with decreasing ejector efficiency trials at the two different operating conditions. The percent energy savings equation is simply the difference in total energy consumption rate between the steam PE ejector A/C system and Bhatti's A/C system over the Bhatti's energy consumption:

$$\% \text{ Energy Savings Percentage} = 100 * \frac{\left(W_{\text{Bhatti A/C}} - W_{\text{EjectorA/C}}\right)}{W_{\text{BhattiA/C}}} \qquad 6.2.5$$

The 50 mph condition in Table 6.2.7 reveals more energy savings when using the 40.5% ejector efficiency compared to its idling condition energy savings. This is due mainly in part of being able to turn the condenser fan off and use the ram air from the car's motion to provide cooling for the condenser. The total energy savings of 173 Btu/min (4 hp) at high cooling load is 80% increase in energy savings. Figure 6.2.7 details the comparison between Bhatti's system and the energy savings percentage for the 50 mph condition as the ejector efficiency decreases in the system. The figure also reveals an energy savings of 68 to 75% during idling conditions from the ejector efficiency ranging from 40.5% to 100% when compared to Bhatti's R-134a system.

Table 6.2.6. Energy consumption of the conventional R-134a A/C system simulation tests (Bhatti 1999) and steam ejector A/C systems during vehicle moving at 50 mph with a 2 ton cooling load. *Results provided if the required waste heat recovery was attainable

Idle Condition (Low Cooling Load – 1.13 ton)

Energy Use	Bhatti R-134a A/C System (η_{comp} -68%)	Steam Pressure Exchange Ejector A/C - 100 % Efficient	Minimum Pressure Exchange Ejector A/C – 40.5 % Efficient	*Theoretical Conventional Ejector A/C – 22.5 % Efficient
Compressor Power (Btu/min)	121	-----	-----	-----
Power loss in accumulator (Btu/min)	3	-----	-----	-----
Compressor Transmission loss (Btu/min)	4	-----	-----	-----
A/C Blower Power (Btu/min)	14	19	19	19
Pump Power (Btu/min)	-----	6.04	14.9	26.84
Added Condenser Fan Power	-----	11	11	11
Total System Power Use (Btu/min)	**142**	**36.04**	**44.9**	**56.84**

Table 6.2.7. Energy consumption of the conventional R-134a A/C system simulation tests (Bhatti 1999) and steam ejector A/C systems during vehicle moving at 50 mph with a 2 ton cooling load. *Results provided if the required waste heat recovery needed for the low efficient system was attainable

50 MPH Condition (High Cooling Load – 2 ton)

Energy Use	Bhatti R-134a A/C System (η_{comp} -68%)	Steam Pressure Exchange Ejector A/C - 100 % Efficient	Minimum Pressure Exchange Ejector A/C – 40.5 % Efficient	*Theoretical Conventional Ejector A/C – 22.5 % Efficient
Compressor Power (Btu/min)	195	-----	-----	-----
Power loss in accumulator (Btu/min)	3	-----	-----	-----
Compressor Transmission loss (Btu/min)	6	-----	-----	-----
A/C Blower Power (Btu/min)	14	19	19	19
Pump Power (Btu/min)	-----	10.47	25.86	46.54
Condenser Fan (Btu/min)	-----	-----	-----	-----
Total System Power Use (Btu/min)	**218**	**29.47**	**44.86**	**65.54**

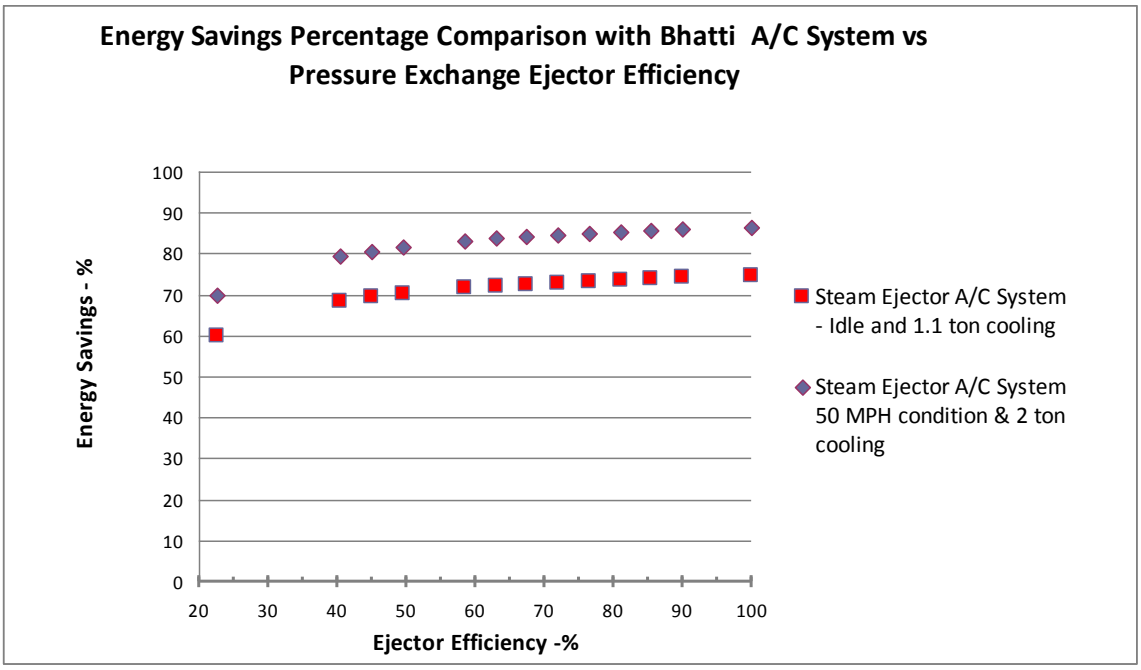

Figure 6.2.7 Plot of the energy efficient percentage savings in steam ejector A/C system's mechanical and electrical work at various ejector efficiencies in comparison to Bhatti's A/C System with its calculated 68% compressor efficiency.

The manner by which energy savings are quantified for the automobile is through the vehicle's fuel economy. The analysis for the BMW 530i sedan's fuel economy is based on the energy distribution in Figure 6.2.2 that matches to within 8% of the estimated fuel consumption calculations in Appendix B.3 using the BMW 530i specifications mentioned in section 4.2.2. The calculation for the fuel economy decrease when the A/C systems are turned on is from taking the total energy that is engine driven that produces a fuel economy of 30 mpg and then adding the A/C accessory load to that total energy. The percentage increase in the total engine driven load is the approximation of the decrease of the fuel economy for the vehicle. Table 6.2.8 reveals the decrease in fuel economy when the vehicle is traveling 50 mph and the A/C system is turned on. Bhatti's higher energy consumption rate to run the 2 ton cooling condition reveals a significant decrease in fuel economy of 26.6% which

equates to 30 mpg midsize sedan vehicle decreased to a 22 mpg fuel economy vehicle. The ejector A/C system lower energy consumption produces only a decrease of 1 to 2.4 mpg in fuel economy.

Table 6.2.8 Fuel economy estimation based on energy distribution percentages from PNGV source in figure 6.2.2. *Results provided if the required waste heat recovery needed for the low efficient system was attainable

Fuel Economy with A/C System 50 MPH Condition (High Cooling – 2 ton)

Fuel Economy	Bhatti R-134a A/C System (η_{comp} -68%)	Steam Pressure Exchange Ejector A/C - 100 % Efficient	Minimum Pressure Exchange Ejector A/C – 40.5 % Efficient	*Theoretical Conventional Ejector A/C – 22.5 % Efficient
Increased Engine Load	5.14 hp	0.7 hp	1.05 hp	1.55 hp
Percent decrease in fuel economy	26.6%	3.6%	5.5%	8.0%
Decrease in mpg	7.98	1.08	1.65	2.40

The onset on hybrid internal combustion engine and electric vehicles in the market will have a greater impact on fuel consumption and emissions. These vehicles contain additional batteries to power the electric motor during cruising speeds and the larger energy consuming A/C systems would take energy away from charging up the battery for the electric motor. The additional batteries during idling state aid in powering the same auxiliary systems that have been modified to be electrically driven as oppose to mechanically belt driven by the engine. This additional energy storage allows for the vehicle to implement into its ECU to turn on and off the combustion engine during idling if there is enough energy storage in the batteries to power the auxiliary systems. Lowering the A/C system energy consumption would keep the engine turned off for a longer duration during idling. As for the typical internal combustion engine, lowering the A/C energy consumption would decrease the engine rpm and corresponding fuel intake.

6.2.1.3 Pump & Ejector vs. Conventional Compressor Weight

One of the key important aspects when adding an accessory such as the air conditioning unit is the effect of its weight to the vehicle. Reducing the weight of the vehicle is critical in lowering the vehicle's rolling resistance and maintaining a high fuel economy. Hybrid vehicles aluminum and lighter plastics are now replacing existing steel parts in order to lower its weight (Daly, 2006). The additional weight from the waste recovery loop in the steam ejector A/C unit is a concern to vehicle's fuel economy. The substitution of using a low powered liquid pump to drive the system as oppose to a compressor shown in Figure 6.2.8 is a reduction of 13 pounds to the weight of the system. The SURflo positive displacement diaphragm pump mentioned in the figure are typically found in large RVs for running plumbing and providing drinking and service water for the kitchen and bathroom compartments. The specifications of the diaphragm pump is capable of providing the desired 60 psi and liquid water gallon per minute required by the A/C system at low ejector efficiencies where the system design requires the most liquid mass flow rate through the exhaust loop.

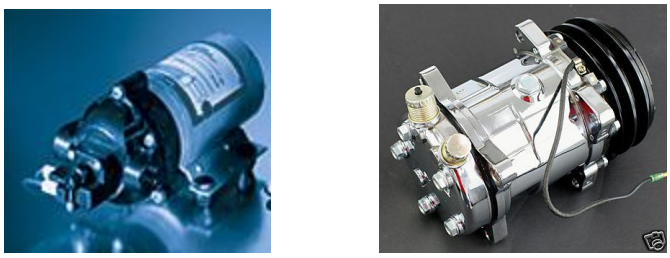

a) b)

Figure 6.2.8 a) Picture of SURflo Positive Displacement 3 Chamber Diaphragm Pump that would be applicable for steam PE ejector A/C system (4 lbs 8"x4"x4"). b) Picture a typical magnetic clutch compressor found in an R-134a conventional A/C system (17 lbs 5" dia. 10" length).

The weight of the ejector needs also to be considered but similar to the pump, the highest pressure of 60-70 psi entering the ejector leaves the opportunity to design

the pressure exchange ejector with lighter materials and keep the weight below 4 pounds. Further technical design of the PE ejector and its bearing and rotor is required to better approximation of the weight of the ejector.

6.2.2 A/C Heat Exchanger Sizing Comparison

6.2.2.1 Evaporator and Condenser Comparison to Original Size

The final volume sizing of the evaporator and condenser is based on the setting the cooling capacity range similar to Bhatti's analysis of 1 to 2 tons of cooling while attaining minimal pressure drop across the heat exchangers for optimization of the blower and fan performance. The volume of the condenser as seen in Table 6.2.9 is doubled in comparison to an original condenser used in the R-134a A/C system. The additional thickness of the ejector A/C condenser is the only dimension that is increased from the original. An additional row of aluminum tubes are designed to handle the increased mass flow rate and required heat rejection. The reason for the larger increase is due to the additional primary mass flow rate from the ejector that is mixed with the secondary flow from the air conditioning loop. The primary mass flow is dependent on the entrainment ratio of the ejector and contributes to additional heat rejection required by the condenser for the steam to condense into liquid water.

Table 6.2.9. Sizing of Heat Exchangers for the conventional and modified A/C system.

Heat Exchanger	**Original Average Sedan Size - in. (L X H X Depth)**	**49.5% Efficient Steam PE Ejector A/C & Conventional Steam Ejector A/C Systems**	**Percent Increase from Original**
Condenser	26 x 17.5 x 0.875 (398 in^3)	27 x 15 x 1.98 (802 in^3)	102%
Evaporator	12 X 9 X 1.125 (121.5 in^3)	10 x 12 x 1.425 (171 in^3)	29.2%

It should be noted that the condenser and evaporator sizing was limited to the constraints from the design template used in both heat exchangers. In addition to this constraint, the length and height dimensions were limited to within 25% of the original heat exchanger dimensions. These dimensions are critical in verifying that the heat exchanger can physically fit in the same area as the original. The thickness increase of the heat exchanger was modified with little constraint since it has little impact in determining whether the heat exchanger can fit in the designated area. The sizing of the tubing, fin arrays, and thickness were constrained to the original drawing in order to sustain the same dimensionless parameters of its fin to total surface area ratio, free-flow area to frontal area ratio and compact ratio. The compact ratio is the total heat transfer surface area divided by its volume. The condenser design in the model C in Figure 4.1.5 consists of a compact ratio of 61.9 ft^2/ft^3 (5.16 in^2/in^3) and was kept constant. The ejector A/C evaporator's compact ratio of 179 ft^2/ft^3 (14.9 in^2/in^3) likewise was kept constant. In order to keep the compact ratio constant, the height adjustments were limited to intervals of one half tube diameters to implement an additional back tube which is offset at half tube diameters below the front row of tubes. An increase in height of a full tube diameter would add a front and back tube to the heat exchanger core. The length however was independent of these parameters but as mentioned before, it was only modified to within 25% of the original. The length and height control the frontal area of the heat exchanger where free flow to frontal area ratio was also kept constant. The ejector A/C evaporator required minimal modifications to the original design in Figure 4.1.8 and required only a 30% increase in volume as a result of steam's higher specific volume.

A key factor in determining the sizing of these heat exchangers is balancing the pressure drop of air passing through and the air convection heat transfer

coefficient. During constant air mass flow rate produced by the blower and fan for both heat exchangers, increasing the air mass flux by decreasing the length or width of the heat exchanger creates a larger convection heat transfer coefficient in equation 6.2.7. At the same time, this results in a heat exchanger with less total surface area for heat transfer and a larger pressure drop as seen in Equation 6.2.8. The design of the frontal area is critical to balance the air convective heat transfer coefficient with the total surface area and efficiency of the fan. The convective heat transfer coefficient based on a constant mass flow rate has an inverse relationship with total surface area and was monitored through the design and simulation process along with the increasing air flow pressure drop as the frontal area was modified. Equations B.1.31 and B.1.33 from Appendix B.1 detail the relationship between the mass flux with air's convection heat transfer coefficient and pressure drop:

$$G_{aircond} = \frac{m_{airfan}}{\sigma_{cnd} L_{cnd} H_{cnd}} \qquad 6.2.6$$

$$h_{air} = G_{air}\, cp_{humair}\, St \qquad 6.2.7$$

$$\Delta P_{air} = \frac{G_{airevap}^{\ 2}}{2\rho_i}\left[\left(k_c + 1 - \sigma^2\right) + 2\left(\frac{\rho_i}{\rho_o} - 1\right) + f_{air}\frac{A\,\rho_i}{A_{min}\,\rho_o} - \left(1 - k_e - \sigma^2\right)\frac{\rho_i}{\rho_o}\right] \qquad 6.2.8$$

where k_c and k_e are the airflow contraction and enlargement loss coefficients and f_{air} is the friction factor of air.

An important concern in the condenser and evaporator sizes was to meet the fan and blower specifications of its performance under a specific pressure drop. As a result, the condenser and evaporator were overdesigned in volume and surface area and less compact to prevent large pressure drop across it. This provided more surface area than required for the idle and 50 mph condition and should be noted that there is

room for improvement to reduce the percent increase of the condenser sizing from the original conventional condenser shown in the last column in Table 6.2.8.

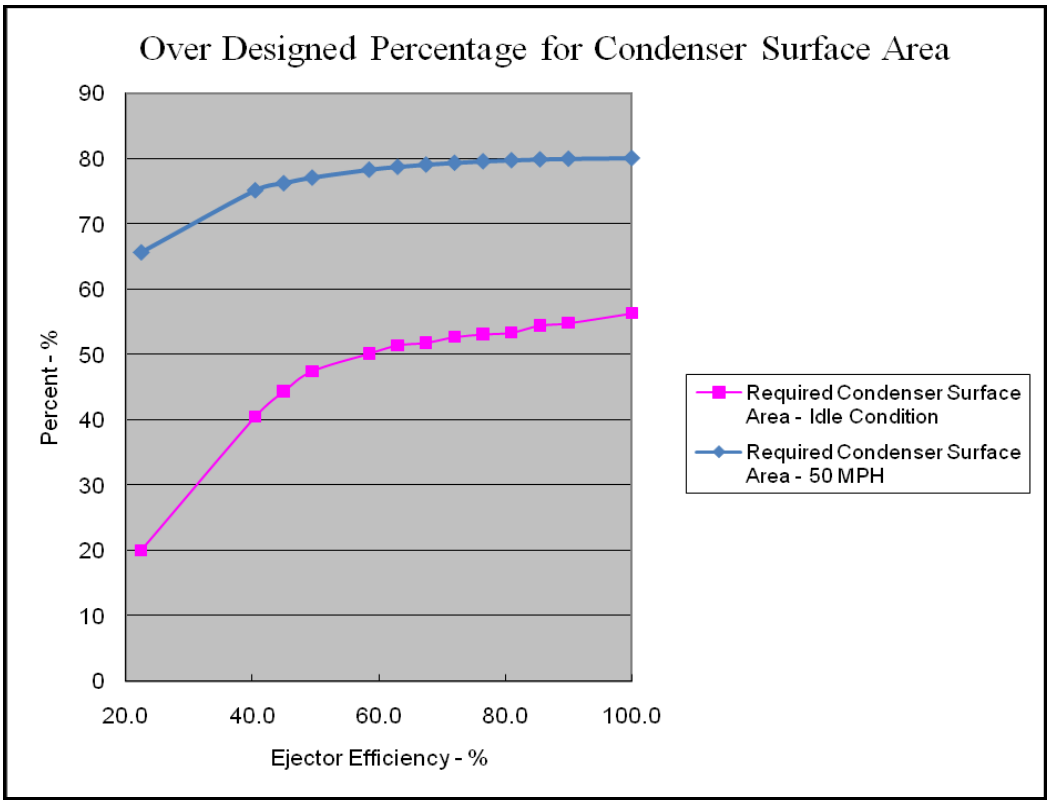

Figure 6.2.9 Diagram of overdesigned surface area percentage for condenser based on required surface area for heat transfer at various ejector efficiencies.

The condenser receiving additional flow from the primary flow mixing with the secondary flow was designed with 4,138 in^2 in total heat transfer surface area that was purposely overdesigned to assure adequate heat transfer area for condensation. Figures 6.2.9 details the overdesign percentage based on the total surface area designed and the required surface area calculated at various ejector efficiencies. Figure 6.2.10 showcases the increase in condenser surface area as the ejector efficiency decreases. The decrease in ejector efficiency creates more mixed steam mass flow rate and heat rejection through the condenser. The largest strain on the condenser size between the two conditions is condensing the steam refrigerant during idling condition due to the condenser fan's lower air convection cooling capabilities

compared to the 50 mph condition's ram air. In terms of the evaporator sizing with constant air mass flow from the blower, constant refrigerant mass flow at various ejector efficiencies, and constant inlet and outlet temperatures, the largest constraint on the evaporator to finalize the design was the high cooling load where the 2.1 ton cooling at the 50 mph condition was calculated with 10.9 % overdesigned surface area for the steam PE ejector A/C system at 40.5 % ejector efficiency. For the same ejector efficiency at idle condition, the lower cooling at 1.1 ton cooling was 47.4% overdesigned. As a result, the evaporator final design was set to the 2.1 ton cooling condition with 10.9% overdesign. The changes in ejector efficiencies in the system had no effect in the required evaporator surface area for each 1 ton and 2.1 cooling conditions since the mass flow rate through the evaporator was solely dependent on the cooling load and constant temperatures and pressures of steam entering and exiting the evaporator.

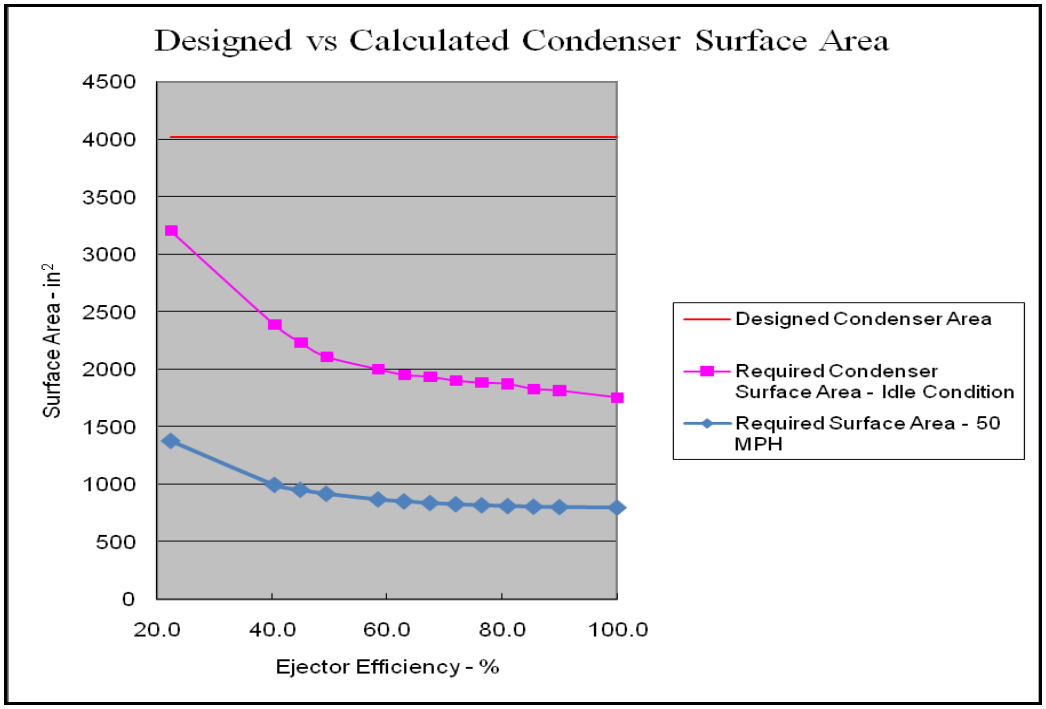

Figure 6.2.10 Plot of calculated condenser surface area with designed surface area for steam ejector A/C system at various theoretical ejector efficiencies using the turbomachinery analog

The design of the evaporator and condenser are based from heat transfer coefficient equations of steam, air, and heat exchanger material based on design specifications, fluid properties, and fan performance. This procedure provides a good final estimation of the heat exchangers' sizes but there is room for improvement. Depending on what pressure exchanger ejector efficiency is actually reached in the system, future work with an in-depth analysis of the heat exchangers using a software program that conducts a 3-D computational fluid dynamics and heat transfer finite element analysis would be suitable for controlling and modifying the dimensionless geometric design parameters and producing a more precise heat exchanger size for both the evaporator and condenser.

6.2.2.2 Exhaust Waste Heat Recovery Heat Exchangers

The waste heat shell and tube heat exchangers in the automotive category contain constraints with its length in order to fit between the existing exhaust equipment such as the muffler and catalytic converter as explained earlier in this report. The catalytic converter has forced the waste heat recovery loop for the steam ejector A/C system to be split into two heat exchangers. Likewise the maximum shell diameter for both primary heat exchanger (PHX) and superheater (SPR) was limited to 9 inches to prevent it from scraping the road on speed bumps or uneven terrain.

The PHX shell diameter comparison between the idle and the 50 mph condition consisting of a higher cooling load for the 50 mph condition This creates an increased amount of work for the ejector with a higher steam mass flow rate to compress as it exits the evaporator. An assumption for the design would be a larger heat exchanger to recover more thermal energy. However, the two operating conditions vary with the 50 mph producing more heat through the exhaust system.

Table 6.2.11 at the end of this section displays the increased exhaust gas temperature, exhaust gas mass flow rate, and a larger ΔT_{LMTD} for the 50 mph condition.

Table 6.2.10. Sizing of Heat Exchangers and weight of steam PE ejector exhaust loop

Heat Exchanger	100% Efficient Steam Ejector A/C System	49.5% Efficient Steam Ejector A/C System	22.5% Efficient Conventional Steam Ejector A/C System
PHX Heat Exchanger	3.19 in. dia. 16 in. length N_T = 8 tubes	4.77 in. dia. 16 in. length N_T = 20 tubes	6.72 in. dia. 16 in. length N_T = 35 tubes
Super Heater	4.28 in. dia. 30 in. length N_T = 11 tubes	6.38 in. dia. 30 in. length N_T = 23 tubes	9 in. dia. 30 in. length N_T = 39 tubes
Total Weight of Exhaust Loop (including piping)	52.77 lbs (23.95 kg)	70.1 lbs (31.8 kg)	95.2 lbs (43.2 kg)

The combination of these increasing variables created a larger overall heat transfer coefficient for the 50 mph condition to reduce the required total surface area. As a result shown in Figures 6.2.11 and 6.2.12, the shell diameters for both heat exchangers are similar in size for the low cooling load at idle condition and high cooling load during the 50 mph condition.

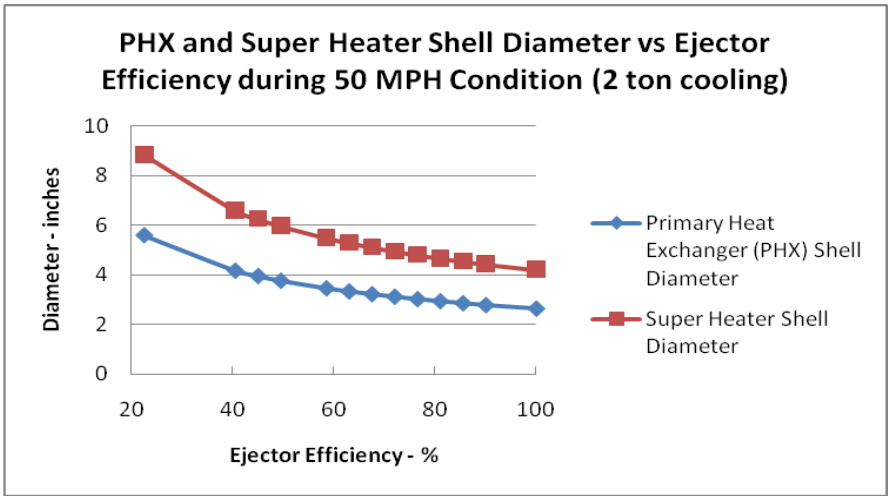

Figure 6.2.11 Shell diameter sizing for both primary heat exchanger and superheater during 50 MPH condition under 2 ton cooling load using Kern and LMTD Method

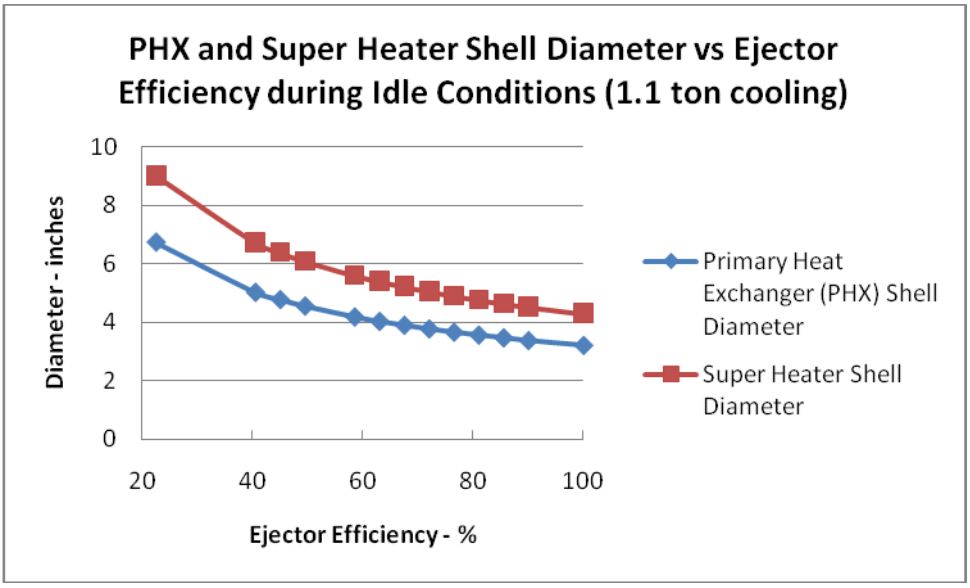

Figure 6.2.12 Shell diameter sizing for both Primary Heat Exchanger and Superheater during idle condition under 1.1 ton cooling load using Kern and LMTD Method

The idle condition actually requires a slightly larger primary heat exchanger and superheater due to the exhaust gas's low flow rate and convection properties. The LMTD analysis in equation 6.2.9 is used with calculated overall heat transfer coefficient and heat transfer rate to determine the required total surface area in equations 6.2.10. Following the calculation of total surface area, the heat exchanger's shell diameter and number of tubes can be determined using equations 6.2.11 and 6.2.12. Appendix B.4 and B.5 detail the process by which the Kern Method and the LMTD method are used for determine the dimension of the exhaust heat exchangers. The increased exhaust gas and steam mass flow rates creates an higher convection coefficient to raise higher overall heat transfer coefficients, U_{phx} , from 0.463 Btu/min-ft^2-°F in the idling condition to 0.616 Btu/min-ft^2-°F for the 50 mph condition. The result is a smaller required total surface area and diameter for the 50 mph condition. The final design for both heat exchangers based on the two conditions

is the larger PHX and SPR from the idle condition and used in the PE ejector system showcased in Table 6.2.9.

$$\Delta T_{LMTD} = \frac{\left(T_{refphxo} - T_{refphxi}\right) - \left(T_{exhphxi} - T_{exhphxo}\right)}{\ln\left[\left(T_{refphxo} - T_{refphxi}\right) / \left(T_{exhphxi} - T_{exhphxo}\right)\right]} \qquad 6.2.9$$

$$Q_{phx} = U_{phx} A_{phx} \Delta T_{LMTD} \qquad 6.2.10$$

$$D_{shell} = 0.637 \sqrt{\frac{CL}{CTP}} \left(\frac{A_{phx} \left(P_{RT}\right)^2 d_{tout}}{L_{phx}} \right)^{1/2} \qquad 6.2.11$$

$$N_T = \frac{A_{phx}}{\pi \, d_{tout} \, L_{phx}} \qquad 6.2.12$$

Table 6.2.11 Temperature readings for both the Super Heater and Primary Heat Exchanger during idling and 50 mph conditions. Temperature gradients for both steam refrigerant and exhaust gas along with the LMTD gradient for each condition (Based off data from LaGrandeur, 2006)

Exhaust Gas Temperatures							
Idle condition				**50 MPH condition**			
Exhaust Gas Flow Rate = .033 lb/sec				Exhaust Gas Flow Rate = 0.077 lb/sec			
Steam Flow Rate varied with Ejector Efficiency (max 100% -min 22.5%) = (0.0073 – 0.019 lb/sec)				Steam Flow Rate varied with Ejector Efficiency (max 100% - min 22.5% = (0.0127 – 0.0335 lb/sec)			
Primary Heat Exchanger		**Superheater**		**Primary Heat Exchanger**		**Superheater**	
Texhphxi	Texhphxo	Texhspri	Texhspro	Texhphxi	Texhphxo	Texhspri	Texhspro
°F	°F	°F	°F	°F	°F	°F	°F
628.25	350	898.25	698.25	890.5	415.5	1260.5	960.5
ΔT_{exh} = 278.25°F		ΔT_{exh} = 200°F		ΔT_{exh} = 475°F		ΔT_{exh} = 300°F	
ΔT_{ref} = 2°F		ΔT_{ref} = 238°F		ΔT_{ref} = 2°F		ΔT_{ref} = 238°F	
ΔT_{LMTD} =159.4°F		ΔT_{LMTD} = 218.1°F		ΔT_{LMTD} = 302°F		ΔT_{LMTD} = 267.4°F	

6.2.3 Pump Performance

The purpose of implementing the secondary exhaust loop with a pump is to provide energy savings in mechanical work compared to using the compressor in the typical vapor compression cycle.

As seen in Figure 6.2.12, the decreasing pressure exchange ejector efficiency in the steam A/C system requires more power from the pump in response to the added thermal input demand. With the steam refrigerant temperatures and pressures and corresponding enthalpies remaining constant across the heat exchangers in the exhaust waste heat recovery loop, the response to the increased thermal input demand is through increasing the steam mass flow rate through the loop and adding more work to the pump. The reason for this is that as the ejector efficiency decreases, the amount of thermal energy from the exhaust loop increases, as seen in figure 6.2.12, in order to compress the steam leaving the evaporator. With the exhaust gas mass flow rate, temperatures and specific heat kept constant for both idling and 50 mph condition, the only method of providing added thermal energy is to modify the steam refrigerant side and add more steam mass flow rate. With the inlet enthalpy determined by the saturated liquid steam temperature and pressures entering the pump and the pump outlet enthalpy set by the pressurized liquid water temperature and pressure set constant for each decreasing ejector efficiency case, the increasing thermal energy must come from increasing the mass flow rate passing through the pump and exhaust loop.

$$I_{refpmpi} = I_{refcndo}(2.7 \text{ psi}, 137°\text{F})$$

$$I_{refpmpo} = I(60 \text{ psi}, 150°\text{F})$$

$$W_{refpmp} = m_{ref}(I_{refpmpi} - I_{refpmpo}) \qquad 6.2.12$$

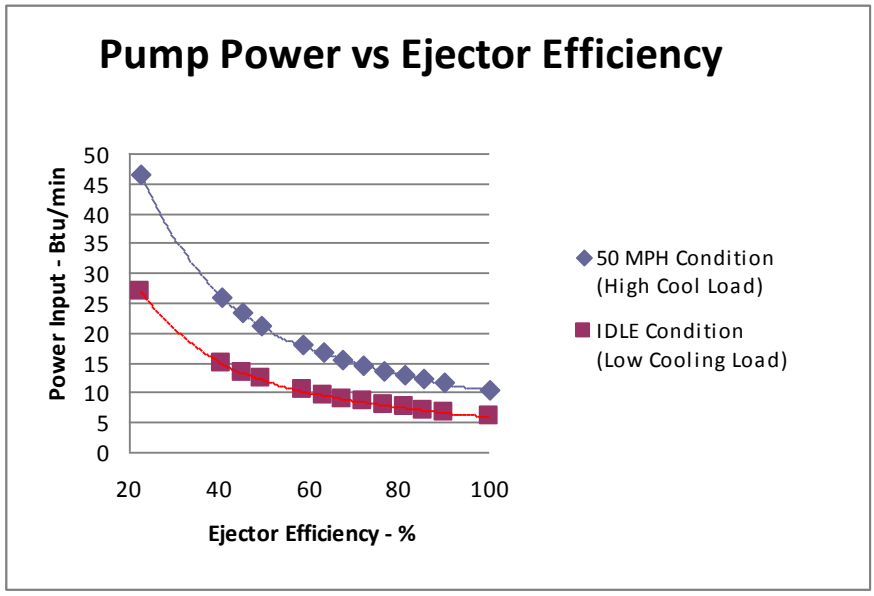

Figure 6.2.13 Analysis of the work done by pump through thermodynamic equations with various pressure exchange ejector efficiencies using the turbomachinery analog.

The goal of providing mechanical energy savings by substituting the compressor with a pump in the steam ejector A/C system is revealed in the previous Figure 6.2.7 where zero energy savings is met in comparison to Bhatti's system at around 30% ejector efficiency for both the idle and 50 mph condition.

6.2.4 Global Warming Impact

The major benefit of using steam as a refrigerant is that it contains zero ozone depletion and global warming potentials. Figure A.5 in Appendix A details the global warming potential of alternative refrigerants used in air conditioning systems. Water vapor does contain a temporary global warming effect but due its transient and short life span in the atmosphere due to precipitation, the EPA considers it negligible. The additional influences from the steam pressure exchange ejector A/C system on its global warming impact are an indirect influence based on its COP_{system} and the additional weight from the exhaust waste heat recovery loop heat exchangers that add to the vehicle's total weight. Environmentally, the impact of global warming directly

and indirectly from fuel burning vehicles and mechanical systems are determined through calculations of its total equivalent warming impact (TEWI). Information from Table 6.2.11 can be examined to get a better sense of the overall fuel usage of a typical automotive air conditioning system similar to Bhatti's system. As noted in the table, 23.5 of the 707 gallons of gasoline or 3.3% of the total yearly fuel vehicle usage is a result of the automotive air conditioning system (Bhatti, 1999).

Table 6.2.12 Average Fuel usage for a typical A/C system in comparison to total vehicle fuel usage. (Bhatti 1999)

Fuel Usage and Vehicle Number Data		
	US Fleet	World Fleet
Annual Fuel Usage, gals	140×10^6	277×10^6
Number of vehicles	198×10^6	647×10^6
Number of A/C Vehicles	168×10^6	303×10^6
Fuel per Vehicle, gal/yr	707	428
Fuel per A/C System, gal/yr	23.5	23.5

The information in Table 6.2.12 reveals an even smaller influence to global warming for a typical automotive air conditioning system. The average TEWI percentage of 2.3 % of the total vehicle TEWI shows that the global warming impact is marginal from running the automotive air conditioning system. Already knowing its small influence on the vehicle's TEWI impact, the study on the TEWI from the A/C system is primarily focused on lowering its value and appraising results based on different conditions.

Table 6.2.13 Total Equivalent Warming Impact emissions for a typical vehicular A/C system

A/C TEWI in Context of Vehicle TEWI (million metric tons of CO_2/year)		
	US Fleet	**World Fleet**
Vehicle TEWI	1,237	2451
A/C TEWI	28	51
% of Vehicle TEWI for A/C	2.3	2.1

The method by which the automotive air conditioning system TEWI is calculated in equivalent mass of CO_2 emitted per year and a combination of the indirect and direct components. The direct equivalent warming impact (DEWI) is due to emissions from the refrigerant leaking a certain percent over time. With steam having no global warming potential (GWP) in comparison to R-134a's 1300 global warming potential, there is a drastic DEWI difference between the two refrigerants. The second component is the indirect equivalent warming impact ($IEWI_m$) due to the air conditioning system's weight added to the vehicle and the extra fuel and emissions to carry it year round. As detailed in Table 6.2.13, the exhaust waste heat recovery loop adds around 58 pounds to the ejector A/C system due to the primary and superheater shell and tube heat exchangers. The smaller and lighter pump used in the system is balanced out with the additional weight of the slightly larger condenser and evaporator in comparison to the conventional A/C system used in Bhatti's analysis. Altogether the steam pressure exchange ejector A/C system at 40.5% ejector efficiency with its exhaust waste heat recovery loop would weigh a total of around 88 pounds for the two loop system while a conventional A/C system is a third of its weight at roughly 30 pounds (Bhatti, 1999). This has resulted in an $IEWI_m$ three times as high for the steam pressure exchange ejector A/C system.

Table 6.2.14 Approximate calculations for the additional weight of the steam pressure exchange ejector A/C system for DEWI calculations at 40.5% ejector efficiency due to the exhaust waste heat recovery loop.

Additional Weight from Exhaust Loop in Ejector A/C System @ 40.5 % Ejector Efficiency							
Primary Heat Exchanger (PHX)	Cross Sectional Area (in^2)	Number of Tubes	Passes	Length (in^2)	Density (lb/in^3)	Total Volume (in^3)	Weight (lbs)
Shell side - Aluminum	3.83	1	1	30	0.098	61.26	6.00
Tube side - Aluminum	0.16	14	2	30	0.098	100.63	9.86
Super Heater (SPR)							
Shell side - Aluminum	5.40	1	1	16	0.098	161.99	15.87
Tube side - Aluminum	0.16	20	2	16	0.098	188.68	18.49
Copper Piping							
Exhaust Waste Heat Loop	0.436	1		54	0.323	23.54	7.60
Total							**57.83 lb (26.23 kg)**

The last component to the TEWI calculation is the indirect equivalent warming potential ($IEWI_o$) that factors the fuel consumption and emissions to operate the mechanical and electrical components of the air conditioning system. The TEWI can be simplified to an equation:

$$TEWI = DEWI + IEWI_m + IEWI_o \qquad 6.2.12$$

Each TEWI component is an independent calculation of various factors retrieved from Bhatti's analysis:

$$DEWI = GWP\ (0.34 + 0.46л)\ ć_m / \tau$$

where

л = refrigerant charges during the life span of the A/C system

$ć_m$ = refrigerant charge in the A/C system (lb_m)

τ = life span of the A/C system (years)

$IEWI_m = \check{R}\ e_c\ \hat{W}$

$\check{R}$ = Volumetric fuel consumption rate to carry A/C unit (gal/kg)

e_c = equivalent warming impact of unit capacity (kg/gal)

$\hat{W}$ = weight of the total A/C system unit (lb)

$IEWI_o = K\ q_{max} / \eta\ COP_{vent}\ (1 - ¾\ \psi)$

where

K = Indirect equivalent warming impact of a unit cooling capacity system (kg CO_2 / yr)(Btu/min)

q_{max} = maximum cooling capacity of automotive air conditioning system in ventilation mode (Btu/min)

η = dimensionless energy conversion efficiency of system based from the conversion of a fuel burning heat engine

ψ = mass fraction of recirculated air

The calculation for the COP_{vent} is used in Bhatti's report as the averaging the use of the A/C system and is based on the combination of the COP_{system} calculations for idling and the 50 mph condition (Bhatti, 1999). These values were weighted by the percentage by which these two conditions and their cooling loads are used in the common yearly application. Matching Bhatti's assumptions, the idling condition was assumed to occur 15% of the total A/C use and 85% for the 50 mph condition under 2 ton cooling load (Bhatti, 1999). With the PE ejector A/C system producing a COP_{system} 2 to 3 times higher than Bhatti's system, the resultant COP_{vent} for the steam PE ejector A/C system, as shown in Table 6.2.14, will greatly reduce its $IEWI_o$ value.

$COP_{vent} = (0.15 * (COP_{system} @ \text{idling})) + (0.75 * (COP_{system} @ 50 \text{ mph}))$

The results shown in Table 6.2.14 are based on an additional variable that incorporates the potential ventilation and recirculation adjustments during air conditioning. The calculations were based on varying the mass fraction of recirculated air, ψ , where $\psi = 0$ is no recirculation of the inside air and all cooled air is cooled from outside air vented and blown across the evaporator blower. The mass fraction recirculated air of 1 is the opposite where all cabin air is recirculated and no outside air is vented. The steam pressure exchange ejector A/C system ranges in 63 to 70% reduction in TEWI emissions for the three different recirculation parameters. Also included in Table A.8 are the TEWI results from a steam ejector A/C system at 22.5% pressure exchange ejector efficiency which theoretically correspond to a high performing conventional ejector. The results show a TEWI reduction of 4 to 28% for the ejector system at low efficiency. A comparison between Bhatti's A/C system at ideal conditions and an ideal steam PE A/C system in Table A.7 reveals a 35 to 70% TEWI reduction in emissions. As noted in the tables mentioned above, the steam PE ejector A/C system exceeds in reducing the system's total equivalent warming impact (TEWI) in all recirculated air categories and at low and high efficiencies when compared to Bhatti's R-134a A/C system.

Table 6.2.15 Comparison of TEWI calculation between Bhatti and steam ejector A/C system for three levels of air circulation (ψ = 0.0 equates to 0% recirculation of inside air and ψ = 1 is 100% recirculation with no outside air).

Total Equivalent Warming Impact (TEWI) of Bhatti R-134a & Steam PE Ejector A/C System						
	Bhatti R-134a System			Steam PE Ejector System @ 40.5 ejector efficiency		
	ψ = 0.0	**ψ = 0.5**	**ψ = 1**	**ψ = 0.0**	**ψ = 0.5**	**ψ = 1.0**
GWP	1300	1300	1300	0	0	0
Л	1	1	1	1	1	1
m (kg)	0.91	0.91	0.91	~	~	~
τ (years)	12	12	12	~ 1 week	~ 1 week	~ 1 week
DEWI (kg CO_2 / yr)	***124***	***64***	***64***	***0***	***0***	***0***
Ř (gal/yr)	0.22	0.22	0.22	0.22	0.22	0.22
e, (kg CO_2 / gal)	8.89	8.89	8.89	8.89	8.89	8.89
Weight , Ŵ,(kg)	13.6	13.6	13.6	31.8	31.8	31.8
$IEWI_m$ (kg CO_2 / yr)	***27***	***27***	***27***	***62.2***	***62.2***	***62.2***
К (kg/yr)/(Btu/min)	0.46	0.46	0.46	0.46	0.46	0.46
Й	0.27	0.27	0.27	0.27	0.27	0.27
Q_{max} (Btu/min)	200	200	200	200	200	200
COP_{vent}	1.8	1.8	1.8	8.2	8.2	8.2
$IEWI_o$ (kg CO_2 / yr)	***189***	***118***	***47***	***41.6***	***26.0***	***10.4***
TEWI (kg CO_2 / yr)	**340**	**269**	**198**	**103.8**	**88.2**	**72.6**
% TEWI Reduction using Steam Pressure Ejector A/C System @ 40.5 % Ejector Efficiency				**69.5 %**	**67.2%**	**63.34%**
% TEWI Reduction using Steam Pressure Ejector A/C System @ 100 % Ejector Efficiency				**78 %**	**76.1%**	**72.8%**
% TEWI using Steam Pressure Ejector A/C System @ 22.5 % Ejector Efficiency				**57.6 %**	**54.7%**	**49.8%**

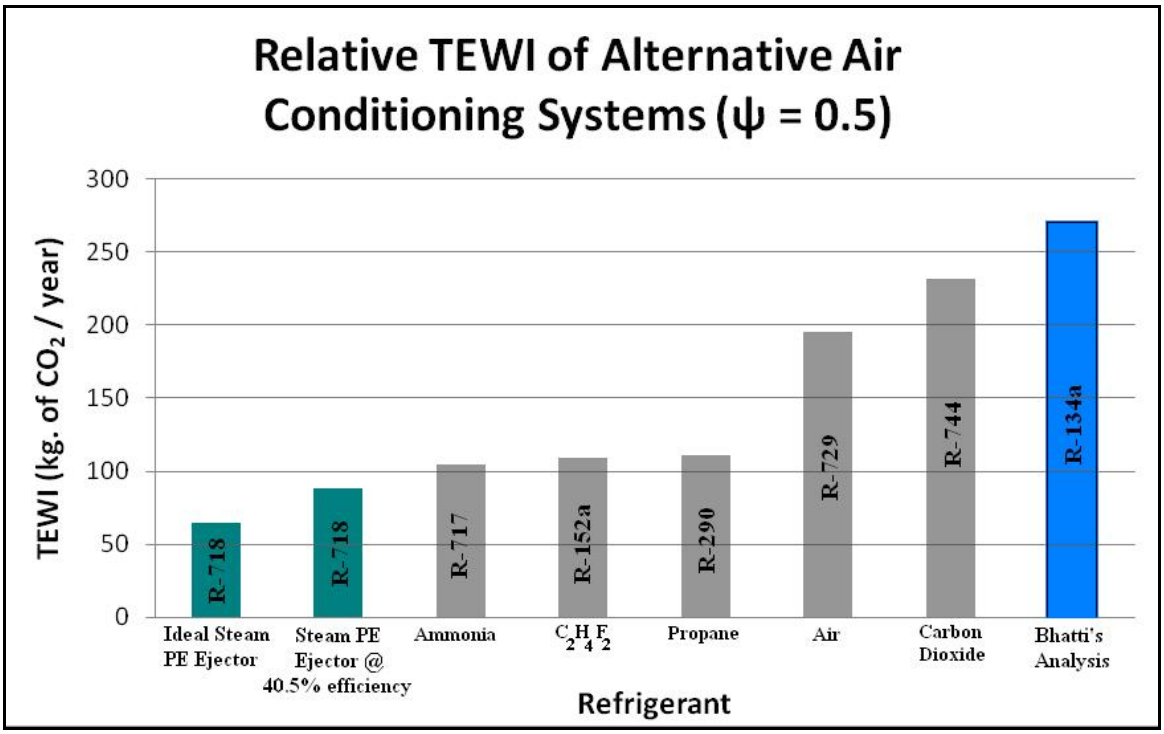

Figure 6.2.14 Relative TEWI emissions analysis under same working A/C conditions and 50% air recirculation for a variety of refrigerants along with Bhatti's system and steam PE ejector A/C system @ ideal conditions and 40.5% ejector efficiency using Turbomachinery analog.

The TEWI of the alternative air conditioning system in Figure 6.2.13 was calculated under the same lines of Bhatti and the steam ejector A/C analysis. The results mentioned in Bhatti's paper were calculated from previous conducted tests at a mass air recirculation fraction of 0.5 (Bhatti, 1999).

6.3 Error Analysis

The calculations involved in attaining results from experimental heat transfer and thermodynamic equations based on similar fluid properties and boundary condition are to be looked at a close approximation and are susceptible to variance in data. The system is an algorithm of equations where neither experimentation nor finite element analysis were used to verify the precision of these theoretical results. It can be concluded from the equations used in system and described in the sections

below that the variance in results ranges from 5 to 25% based on error analysis mention from the sources in which equations were found. This analysis is accumulation of heat transfer, fluid dynamics, internal combustion engine and vehicle energy distribution calculations that have been either conducted through experimental correlation equations, generalized equations, or from outside sources. Although this analysis covers the steam PE ejector A/C system for a generalized midsize sedan, it should be noted that certain number of these calculations are a major sources of error while others are considered negligible. The major sources of error are primarily a result of accumulation of multiple equations of 0 to 5% that could potential add up to total error of +- 20%. The list of potential major sources of error, but not necessarily, exceeding 20% are:

- Exhaust Gas Temperatures and Exhaust Gas Flow Rate
- Exhaust Shell and Tube Heat Exchangers Sizing
- Condenser Sizing
- Air Flow Rate through Condenser via Ram Air or Radiator Fan

The minor sources of error that fall below 20% error are:

- Steam and Air convective heat transfer coefficients
- Midsize sedan Energy Distribution off gasoline combustion
- Correlation between speed of vehicle and engine rpm
- Midsize Sedan Energy Distribution Survey from PNGV Source vs. Actual BMW 530i Sedan Energy Distribution

6.3.1 LMTD vs. Kern Method Convergence

The method of pre-designing the exhaust shell and tube heat exchangers through unknown geometric estimates using the Kern method and validating answers with a calculated LMTD Method made for a respectable approximation for final

geometric parameter such as shell diameter, steam velocity and number of tubes. The primary concern and use of the custom MATLAB Kern vs. LMTD method algorithm was to match the initial shell diameter using the Kern method design estimate with LMTD calculated result to within 2% of each other. As shown in Figure 6.3.1 for the primary heat exchanger results, this convergence was better through intensive iteration of the initial shell diameter guess. The comparison between the methods' steam velocities and number of tubes contained high variance between LMTD and Kern methods as the shell diameter variables converge. Figure 6.3.1 showcases the larger percent difference variance of 5.8 to 6.8% for the number of tubes calculation for both primary heat exchanger at the idling condition and the 50 mph condition.

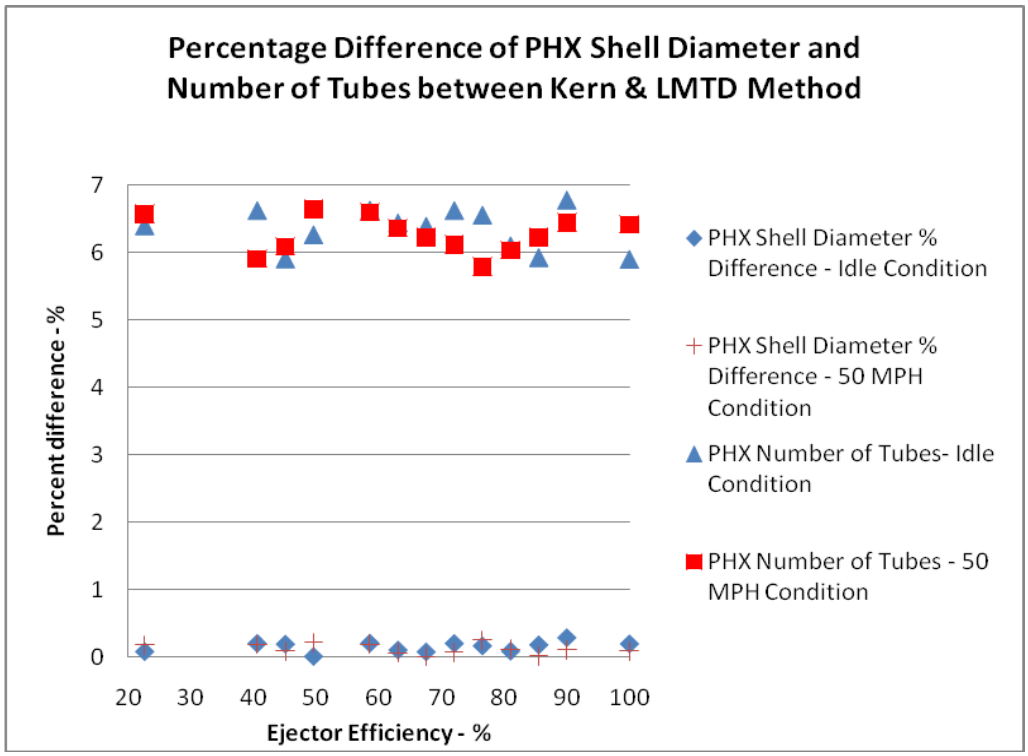

Figure 6.3.1 Convergence percentage of primary heat exchanger (PHX) shell diameter and number of tubes designed using Kern Method and calculated result from LMTD method for both idle and 50 mph condition.

The steam velocity within the PHX contained a large variance but kept its consistency as the number of tubes and shell diameter increased with decreasing ejector efficiency. The 20.8 to 22.2% variance for all 26 trials shown in Figure 6.3.2 show the consistency and limitation to an iteration driven by the shell diameter.

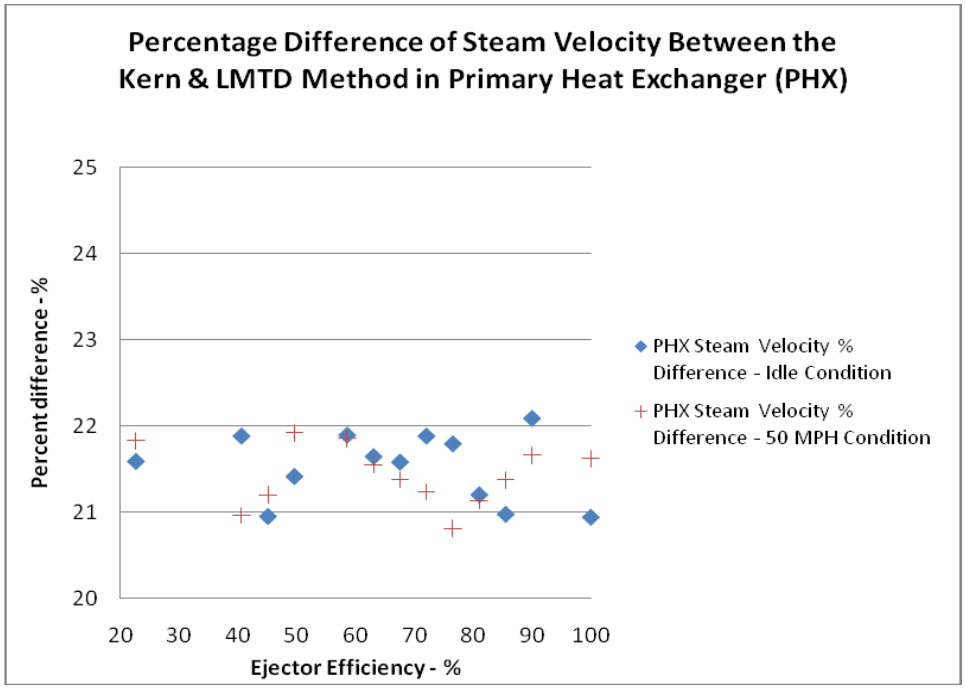

Figure 6.3.2 Convergence percentage of the PHX's steam velocity designed using Kern method and calculated result from LMTD method for both idle and 50 mph condition.

The superheater, similar in design to the PHX, contains an error analysis closely matching to the primary heat exchanger. This variance shows consistency in the algorithm method but does show room for improvement in modifying all three variables conversely to provide an lower overall error analysis. This modification may increase the shell diameter variance between the two methods in order to decrease the variance in the number of tubes and steam velocity results. Figures 6.3.3 and 6.3.4 details the error analysis of the superheater between the Kern and LMTD method and contains similar convergence results. These results are not unusual due to fact that the superheater is an upstream extension of the primary heat exchanger.

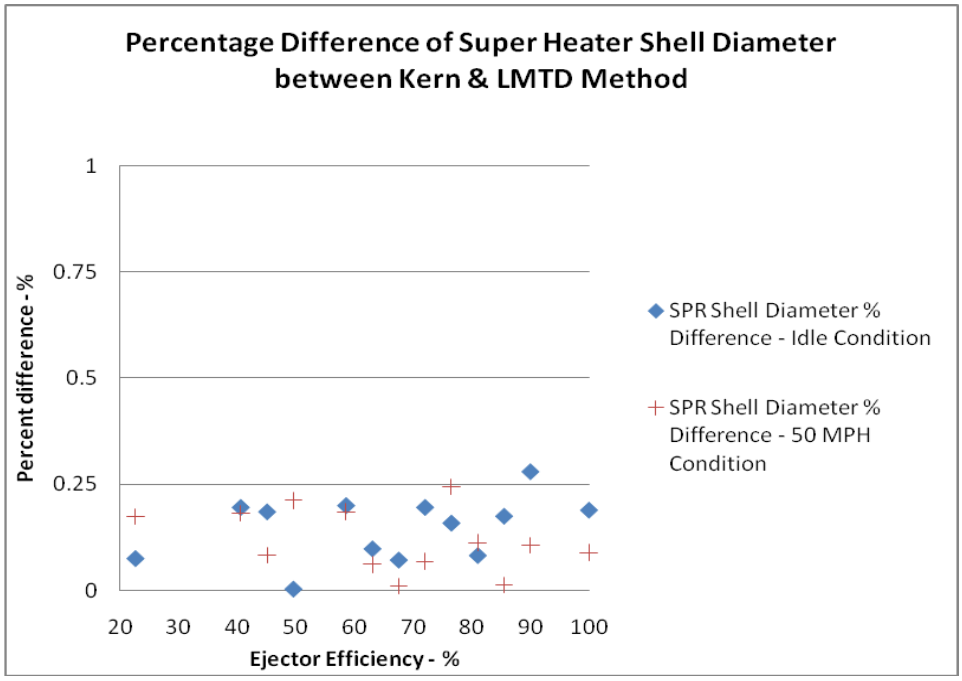

Figure 6.3.3 Convergence percentage of superheater's (SPR) shell diameter that was predesigned using Kern method and compared with calculated result from LMTD method for both idle and 50 mph condition.

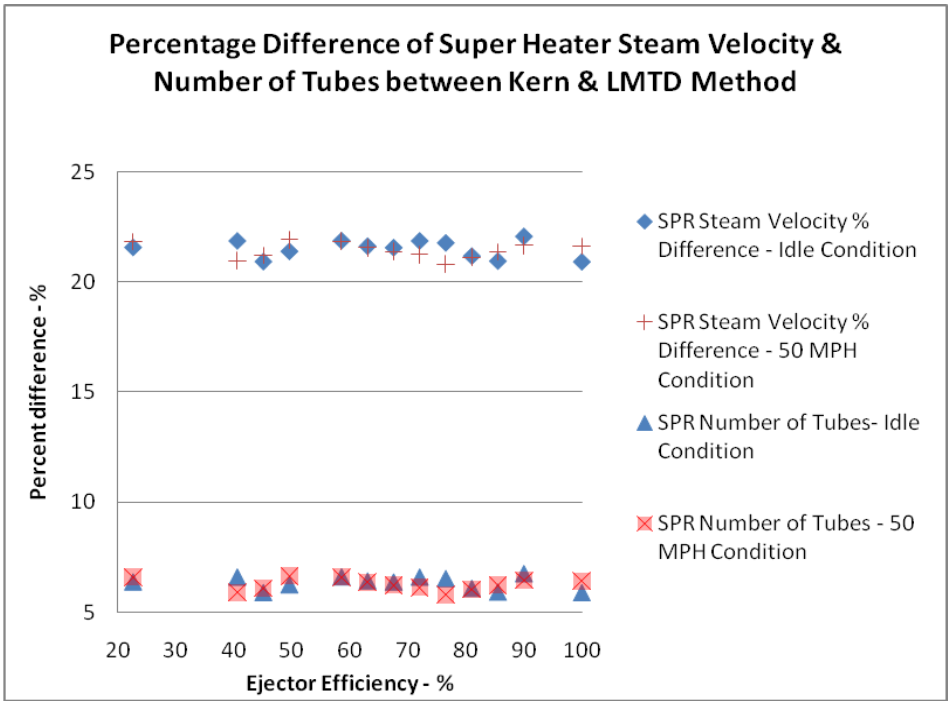

Figure 6.3.4 Convergence percentage of superheater's (SPR) steam velocity and number of tubes predesigned using Kern Method and compared with calculated result from LMTD method for both idle and 50 mph conditions.

6.3.2 Heat Transfer Coefficient Correlations

The majority of convective heat transfer coefficients derived from fluid dynamic properties are located in Kakac's heat transfer book (Kakac, 2002). The book contains a collection of equations verified through experiments and based on fluid's parameters such as single phase and two phase state, turbulent and laminar flow, and dimensionless parameters such as Prandtl and Nusselt Number. The equations with specific boundary conditions and parameters from experiments tend to develop correlations to provide a more precise result. The steam ejector A/C system with its two phase refrigerant evaporation and condensation in its heat exchangers contain certain correlation equations as a result of similar boundary conditions and parameters.

In the case of applying Shah's correlation for two phase condensation flow, experimental results show that the correlation and experiment are within 20% agreement (Kakac, 2002). As for the two phase refrigerant evaporation in the primary exhaust heat exchanger and evaporator, the combination of Shah and Gnielinski correlations to approximate the nucleate boiling and liquid heat transfer properties contain a mean deviation of 14% from experimental results conducted. The single phase heat transfer coefficient for air, exhaust gas, and superheated steam are conducted through Stanton and Prandtl numbers based on the fluid's Reynolds Number. The Stanton and Prandtl experimental values for air extrapolated from the trends graphed out for both the evaporator and condenser (Figures 4.3.2 and 4.4.1) are a direct and precise value based on the specific design of the two heat exchangers. The single phase heat transfer coefficient for laminar and turbulent flow for both the exhaust gas and superheated steam in the exhaust heat exchangers are based solely on the fluid properties without consideration of its specific interaction with the specific

heat exchanger. These results are considered more or less a close approximation of the actual heat transfer coefficient.

6.3.3 Automotive Waste Heat Recovery Data

The use of the BSST experimental results of the BMW 530i exhaust gas temperature and mass flow rate throughout the exhaust system at various engine loads and rpm aided in conducting an approximation of the conditions of these variables during the steam ejector A/C system analysis. The engine rpm vs. engine load and corresponding exhaust temperatures graph in Figure 4.6.3 was interpolated to approximate exhaust temperatures from calculated engine rpm and loads for the idling and 50 mph condition. The data collected was a combination of experimental sensors measurements on the BMW 530i exhaust along with computer simulations from Advisor software and according BSST report, the Advisor model demonstrated within 2% agreement to BMW tested fuel economy performance for the drive cycles and a 5% agreement to exhaust gas temperatures. Since the testing the vehicle under the A/C conditions of idling and 50 mph was never conducted experimental or through software from the BSST team, the exhaust waste heat recovery data used in this analysis is considered a close approximation from means of interpolation, general vehicle calculations in Appendix B.3, and trends from a combination of BSST experimental and software simulations.

6.4 Future Work

The continuation of further research on this theoretical topic for more convincing dialogue would require more specific software modeling of the interaction between A/C system and the exhaust system for precise results. The results mentioned in the earlier sections of Chapter 6 are limited in precision due to approximated and

generalized conditions that attempt to match BMW 530i midsize sedan with data from a typical sedan or a sedan of similar design and engine size. This also holds true for not containing all the pertinent information on certain conditions of the sedan itself to precisely calculate certain results. The primary overall census for future work is providing better means to simulate the variety of engine and environmental conditions involved in automotive air conditioning analysis.

Future work to fully validate and market this modified steam ejector A/C system is to design and test the pressure exchange ejector to achieve consistent ejector efficiency with the same pressure ratios of the inlet and exit pressures. Since the vehicle is under constant transient conditions, further tests under a variety of different conditions would aid in determining its reliability and performance characteristics Also, a consideration in the experimental testing is the noise creation from the primary flow's supersonic velocity through the nozzle and whether ejector noise silencers can reduce the noise to a reasonable level without damaging its overall ejector efficiency.

6.4.1 Transient Analysis

Under idle and 50 mph cruising speeds, the vehicle and environmental conditions are fairly constant and steady state. Future analysis with the steam ejector A/C system should be applied when the vehicle is accelerating, decelerating, and urban style driving with many stops and goes that create a transient exhaust waste heat recovery condition and variable pump performance being that its belt driven from the car's engine. An analysis of this magnitude was beyond the realm of this project due limited computer simulation software. A transient analysis would answer many questions about how responsive and versatile this steam pressure exchange

ejector especially with the conventional ejector's history of poor performance with varying inlet pressures and temperatures.

6.4.2 Environmental and other Conditions

This report on the steam pressure exchange ejector automotive A/C system has covered two important vehicle conditions for analysis but there are a variety of vehicle and the outside conditions to be tested and analyzed. The conditions used are of a high and low extremity to the system but temperature and humidity of the outside air are a couple of variables that can be modified and tested to monitor any performance changes from the system. The vehicle speed variations especially near the critical point of various cooling loads and corresponding required condenser air flow that may require turning on the radiator/condenser fan when the vehicle is moving a certain speed. Solar radiation and humidity factors inside the cabin would be additional variables to consider in computing the cooling rate required for passenger's desired cabin temperature.

The system also has only covered the analysis of the six cylinder midsize sedan where further analysis on versatility of the system could be conducted on larger size trucks, SUVs, and vans using a six cylinder engine. The cooling load would be slightly larger due to its larger cabin size. Since the ejector system utilizes the exhaust waste heat, an analysis with a smaller sized engine such as the standard four cylinder engine and any electric hybrid engine that produces less waste heat may be informative to find the required higher ejector efficiency that suitable for the car. Large deliver trucks and vans with eight cylinder engines would be a realistic application to this system due to its larger exhaust waste heat which would allow for a lower ejector efficiency for the A/C system.

6.4.3 Automotive Waste Heat Recovery Data

Further analyses for validity of the theoretical analysis are to experimentally test the 2005 BMW 530i or any six cylinder midsize sedan and see if the computer simulated results and actual exhaust gas recovery using temperature and flow meter through the vehicle's exhaust system match. The use of the Advisor software from BSST's analysis would create a more precise and accurate result with smaller percent error and applicable data to go along with the experimental data. If there is too much heat loss to the ambient surroundings, an insulated exhaust pipe could be considered or implementing the exhaust loop refrigerant piping inside the vehicle exhaust system as it travels to and from the exhaust heat exchangers would help in recovering additional heat.

Chapter 7 Conclusions

7.1 Conventional and Pressure Exchange Ejector Design and A/C System

The patented pressure exchange ejector was designed to enhance the performance and compression ratio of the conventional ejector. The assumption of the fluid interactions of both fluids inside the ejector acting similar to the turbomachinery analog aids in producing an ejector thermodynamic efficiency. It also provides a method of direct comparison of thermodynamic efficiencies between the conventional and pressure exchange ejector. The pressure exchange ejector was designed with a high compression ratio to produce a high exit pressure and corresponding condensation temperature entering the condenser to allow the steam refrigerant to be air cooled by the ambient air. Lower compression ratios seen in conventional ejectors produce low steam condensation temperatures and require liquid cooled condenser. The additional work and weight from a liquid pump, and extra weight from piping for the water cooled condenser would lose its competitive edge with the automotive R-134a air conditioning system.

The theoretical analysis of the pressure exchange ejector application for the automotive air conditioning industry is to determine the ejector's potential in the industry and set goals to be tested experimentally in the future. With limited available waste heat in the engine exhaust system, the steam PE ejector system under the design requires an ejector efficiency of greater than 40.5% to avoid the implementation of a more complex and heavier design to recover additional heat from the engine cooling system. The pressure exchange ejector in the A/C system requires a compression ratio of 15 for steam as a refrigerant in order to contain a high enough steam condensation temperature for an air cooled condenser. Steam conventional ejectors have reach a

maximum 20% efficiency and a compression ratio of 7 using the turbomachinery analog based from experimental data. The comparison shows that the pressure exchange ejector is required to double its predecessor thermodynamic efficiency to 40.5% and compression ratio to 15 in order to operate under the design constraints of the automotive steam PE ejector A/C system. This information is critical for benchmarking experimental goals for the pressure exchange ejector testing. Further tests experimentally along with simulations from computer fluid dynamic software will aid in determining whether the pressure exchange ejector can handle the increased performance measures and maintain consistency with transient environmental and vehicle conditions.

7.2 Conclusions on Bhatti R-134a vs. Steam Pressure Exchange Ejector

The automotive steam pressure exchange ejector A/C system that utilizes the waste heat created by vehicle's internal combustion engine has been analyzed based on vehicle data from BMW, Chevy, and Toyota for a midsize vehicle. The validation and performance of the system is based on comparing the system with the results from the existing conventional R-134a A/C system conducted by M.S. Bhatti of Delphi Thermal Systems. There are seven major topics of the automotive air conditioning system that are addressed in the comparison between the two systems:

- Coefficients of Performances
- Energy Savings Comparison
- Fuel Economy
- Air Conditioning System Weight
- Heat Exchangers' Sizing
- Pump vs. Compressor Comparison
- Total Equivalent Warming Impact

These topics under the various system parameters and vehicle, engine, and environmental conditions are included in the concluding remarks.

7.2.1 R-134a vs. Steam Ejector A/C Coefficients of Performance

The concept of the existing vapor compression cycles strictly considers the mechanical work to the run the system along with its beneficial cooling load. The conclusions from analyzing the three A/C systems of the typical vapor compression cycles and the two loop steam conventional and pressure exchange ejector A/C system is to include the source of energy and its thermal efficiency of producing the mechanical work. The typical R-134a conventional A/C system with a 68% compressor efficiency produces a COP_{cycle} 2 to 3 times better than the steam PE ejector system at ideal conditions. However, the result is based on the energy added to the refrigerant whether it is recovered or produced by the system. The reason for the low COP_{cycle} for the steam PE ejector system is the inclusion of the exhaust waste heat recovered because it is required by the cycle and refrigerant. In the COP_{system} analysis, a closer look was needed to assess the sources of the energy that run the system. The heat from the exhaust gas is generated from an independent source and is required by engine to be removed regardless of whether the A/C system was on or off. It was concluded in the COP_{system} analysis that the exhaust heat recovery is not considered as work input but as an independent heat source. The concluding COP_{system} results of the steam PE ejector system reveal the small amount of work required to run the ejector A/C system. The steam PE ejector A/C system from 100% to 22.5% ejector efficiency under idling conditions contains a higher COP_{system} of at least 2.5 times the COP_{system} value of the Bhatti's R-134a A/C system. The 50 mph condition also produces factor of 5.5 to 3.75 in larger COP_{system} values in comparison to the R-134a A/C system. The ideal COP_{system} comparison adds to the conclusion that the steam PE ejector A/C

system at low efficiencies exceeds the performance of the conventional R-134a A/C system when using recovered wasted heat in the system.

The combustion of gasoline for mechanical work provides a low mechanical efficiency for the automobile and the thermal system analysis exposes this deficiency. The steam ejector A/C system however captures the wasted heat from gasoline combustion and uses it to thermally energize the system. Similar to the COP_{system} analysis, the PE ejector A/C system produces better $COP_{thermsys}$ results for idle and 50 mph conditions in comparison to Bhatti's R-134a A/C system results. Analyzing the system based on thermal efficiencies and under the consideration that the exhaust waste heat recovery is an independent source of energy is key to understanding how the steam pressure exchange ejector A/C system under certain efficiencies can match and succeed the system COP and thermal system COP results of the conventional R-134a A/C system.

7.2.2 Energy Savings and Fuel Economy Potential

The results from the steam pressure exchange A/C system analysis reveal that the efficiency of the ejector is the main factor in determining whether the system is beneficial in comparison to the R-134a system. The comparison between Bhatti's R-134a system and the two loop ejector A/C system at idling and 50 mph condition shows significant energy savings. The trend shows that the steam PE ejector system design beginning at 40.5% consumes at least 68% less energy than Bhatti's R-134a system

Any additional energy usage to run the A/C system in an automobile is a direct relationship to the decreasing of the vehicle's fuel economy. The PE ejector A/C system uses a less amount of energy than Bhatti's A/C system and shows a better fuel economy along with a less amount of harmful environmental gas emissions. In the

40.5% to 100% ejector efficiency range, the energy savings approximates to a range of 6.3 to 6.9 mpg better fuel economy than Bhatti's system for the BMW 530i sedan traveling at 50 mph. For the BMW 530i sedan with 30 mpg fuel economy, the steam pressure exchange ejector A/C system when running on high load and 50 mph only decreases the sedan's fuel economy by no more than 6 % for systems with ejector efficiencies above 40.5%. The conventional ejector if supplied enough heat from the engine coolant and exhaust system would only decrease the fuel economy by 8%. This system at low ejector efficiency condition even exceeds Bhatti's A/C system which decreases BMW 530i sedan's fuel economy by 26.6% when traveling 50 mph. The conclusive evidence of energy savings and better fuel economy with the ejector A/C system for high and low cooling loads shows promise for implementation into the midsize sedans that are aiming to become more fuel efficient.

7.2.3 Original vs. Steam Ejector A/C Equipment Weight & Sizing

The added complexity of the second exhaust waste heat loop can give the notion that the system is adding bulk and weight and would cancel any signs of fuel economy improvement. However, the lower ejector efficiency A/C systems at 40.5% ejector efficiency would only add 40 pounds to system when factoring the extra piping and exhaust heat exchangers. Any efficiency above 40.5% would require less waste heat from the exhaust system resulting in smaller exhaust heat exchangers and weight where the weight under ideal conditions would only be 22 pounds heavier than the conventional R-134a system. That additional 2 to 3% weight to the 1780 pound 530i BMW sedan has negligible effect on additional rolling resistance or weight to propel the vehicle. This analysis on the additional weight shows that it has little or no effect on the degrading of the vehicle's fuel economy. The weight of system while using steam as a refrigerant also has little effect on indirect and direct emission for the

total equivalent warming impact (TEWI) analysis. The steam PE ejector A/C system's TEWI remains lower than other refrigerants due to its zero global warming potential (GWP). The zero GWP aids in balancing out the slight increase in indirect equivalent warming impact ($IEWI_m$) from the added CO_2 emissions based on the weight of the A/C system.

The sizing comparison between the existing evaporators and condensers show that the frontal areas for both the new ejector A/C condenser and evaporator are a close proximity to the size of the original heat exchangers. Limited modifications on the thickness of the two heat exchangers made for an oversized heat exchanger. The conclusion based on the comparison between the R-134a and steam thermal properties show that although steam require a slight increase in surface area, the final design of the new evaporator and condenser adds nominal weight or price to the system. Furthermore, the slightly larger sized evaporators and condensers are small enough to fit inside the BMW 530i's undercarriage without any modification to the existing system.

The ability to modify certain design parameters in the condenser and evaporator would aid in reducing the over design size of the heat exchangers. Adequate computational heat transfer software using computation fluid dynamics and finite element analysis on the specific evaporator and condenser at various cooling loads and environmental conditions would aid verifying this numerical heat transfer analysis along with potentially reducing the size of the heat exchangers.

7.2.4 Waste Heat Recovery Pump vs. Compressor Comparison

The main contributor to the steam ejector A/C system's high COP_{system} , better fuel economy, and low additional weight of A/C system is through replacing the high powered compressor with a low powered pump. The weight of the pump contains an

advantage over the compressor used in the conventional vapor compression A/C cycle. The specifications show that the pump weighs 4 pounds which is 13 pounds less than the weight of the typical R-134a A/C compressor. This aids in reducing the overall weight of the two loop steam PE ejector A/C system. Both components are driven by the vehicle's engine with its total work input calculated thermodynamically based on the assigned isentropic efficiency. The key discovery is that as the ejector efficiency decreases, the ejector requires more heat from the waste heat recovery loop. As a result of this demand, the steam mass flow rate increases through the exhaust system and requires more work from the pump. However that added work from the low powered pump in ejector A/C system is less than 1 hp for both idle and 50 mph conditions. The low power demand enables the pump of potentially being driven electrically through the alternator or battery. This would allow for better control of the pump as oppose to the belt driven option like in the compressor which is controlled by the engine rpm as opposed to the response of the cooling load. Another advantage of the electrically driven pump is the freedom of placing the pump away from the space stricken engine compartment. The most important discovery is that depending on the ejector efficiency in the A/C system, the pump requires one twentieth to one quarter of the energy required by the compressor in the conventional R-134a system under the same conditions. This result is the source of the all the energy savings, better fuel economy, and less harmful greenhouse gas emissions found in using the steam PE ejector A/C system as oppose to the conventional R-134a A/C system.

7.2.5 Environmental Impacts

The use of a steam refrigerant with that is naturally occurring in the atmosphere would help elevate the buildup of refrigerant gas emissions in the

atmosphere due leaks and during servicing and maintenance. A/C systems using carbon dioxide, hydrocarbons and hydrofluorocarbons as refrigerants contain a higher GWP and longer atmospheric lifespan that is contributing to the global warming and climate change phenomenon. Previous studies and analysis show that running the A/C system over the span of a year has marginal emissions effects in comparison the vehicle exhaust emissions. Incremental improvements from all aspects of the vehicle need to be improved especially if there are roughly 303 billion air conditioned cars worldwide where each car uses an average of 24 gallons of gasoline per year to run their air conditioning system. That is roughly 7.3 trillion gallons of gasoline per year in the world used up for air conditioning use (Bhatti, 1999). With the calculated 40.5% efficient steam ejector A/C system results, midsize sedans using the ejector system in comparison to Bhatti's system would have a seven percent decrease in fuel consumption and 65% decrease in TEWI while using their air conditioning system. If all vehicles were equipped with the steam PE ejector A/C system, it would equate to roughly 511 million gallons saved and a reduction of 5.9 million metric tons CO_2 emitted.

The comparison of the alternative air conditioning systems , such as R-152a's secondary loop and CO_2 system under the same conditions, reveal that the steam PE ejector A/C system with 40% ejector efficiency contain the lowest TEWI calculation. This aids in proving that as long as the steam pressure exchange ejector system can produce this efficiency and perform under various cooling loads and environmental conditions, the system has environmental benefit over the new alternative A/C systems aiming replace the conventional R-134a system that is soon to become extinct in Europe and facing an undetermined future in the United States.

References

ASHRAE. Steam-jet Ejector Refrigeration. Equipment Handbook, Chapter 13.1-13.6. 1979.

Fox, Robert, Alan T. McDonald, and Philip J Pritchard. Introduction to Fluid Mechanics 6th Edition John Wiley & Sons, Inc. Hoboken, NJ. 2003.

Hartnett, James, Thomas Irvine, Young Cho, & George Greene. Advances in Heat Transfer, "Microchannel Heat Exchange Design for Evaporator and Condenser Applications" Man-Hoe Kim, Sang Yong Lee, Sunil Mehendale, & Ralph Webb. Elsevier Inc. New York, NY. 2003. Volume 37

Daly, Steven. Automotive Air Conditioning and Climate Control. Butterworth-Heinemann. New York, NY. September 2006.

Dwiggins, Boyce. Automotive Air Conditioning 4th Edition. Litton Educational Publishing, Inc. New York, NY. 1978.

Kakac, Sadik and Hongtan Liu. Heat Exchangers. Selection, Rating, and Thermal Design. CRC Press. Washington, D.C. 2002.

Kaniaru, Daniel. The Montreal Protocol : Celebrating 20 years of Environmental Progress; ozone and climate protection. Cameron. London, England. 2007

Kays, W.M. and A.L. London. Compact Heat Exchangers Third Edition. Krieger Publishing Company. Malabar, Florida. 1984.

Moran, Michael and Howard Shapiro. Fundamentals of Engineering Thermodynamics Fourth Edition. John Wiley and Sons, Inc. 2000.

Pratap, Rudra. Getting Started with MATLAB. A Quick Introduction for Scientists and Engineers Version 6 Oxford University Press. New York, NY. 2002.

Stubblefield, Mike and John Haynes. Haynes Techbook Automotive Heating and Air Conditioning. Haynes Publications, Inc. Newbury Park, CA. 2000

White, Frank. Heat and Mass Transfer. Addison-Wesley Publishing Company. New York, NY. 1988.

Articles and Dissertations

Bhatti, M.S. "Enhancement of R-134a Automotive Air Conditioning System." SAE Paper No. 1999-010870. SAE International. International Congress and Exposition. Detroit, Michigan. March 1st – 4th, 1999.

Balasubramaniam, M. "Combined Engine Cooling System and Waste-Heat-Driven Jet Vapor Compression Automotive Air-Conditioning System," Doctoral Dissertation in Energy Management and Policy presented to the Faculty of the Graduate School of Arts and Sciences of the University of Pennsylvania, 1975.

Bulusu, K. ,et al. "Evaluation of Efficiency in Compressible Flow Ejectors." ASME Paper Number IMECE2008-67622. ASME International Mechanical Engineering Conference and Exposition. Boston, MA. 2008.

Eames, I.W. et al. "A Theoretical and Experimental Study of Small Scale Steam Jet Refrigerator." Elsevier Ltd. Journal of Refrigeration. Volume 18 No. 6 pg 378-386. Great Britain. April 1995.

Everitt, P and S.B. Riffat. "Steam Jet Ejector System for Vehicle Air Conditioning" International Journal of Ambient Energy. Volume 20 No. 1. January 1999.

El-Dessouky, Hisham, et al. "Evaluation of Steam Jet Ejectors" Chemical Engineering and Processing Journal Vol.41.Safat, Kuwait. September 2001.

Ewing. "Traffic Calming: State of the Practice." Institute of Transportation Engineers, Publication No. FHWA-RD-99-135, August 1999

Garris, Charles Ph.D., et al. "An Environmentally Friendly Pressure Exchange Ejector Refrigeration System." ASME Paper Number FEDSM98-4812. Fluids Engineering Division Summer Meeting. Washington, DC. June 1998.

Garris Jr., Charles Ph.D., "Pressure Exchange Ejector" U.S. Patent 7,497,666. Washington D.C. 2009

Garris Jr., Charles Ph.D., "Pressure Exchanging Ejector and Refrigeration Apparatus and Method" U.S. Patent 5,647,221. Washington, DC. 1997.

Ghodbane, Mahmoud. "An Investigation of R152a and Hydrocarbon Refrigerants in Mobile Air Conditioning." SAE Paper No. 1999-01-0874. SAE International. 1999.

Gifford N.L. "Experimental Study of Low Pressure Automotive Cooling Fan Aerodynamics Under Blocked Conditions." Canada Society of Mechanical Engineers(CSME) Forum 2006.

Hammer, R.M. "An Investigation of An Ejector-Compression Refrigeration Cycle and Its Application to Heating, Cooling, and Energy Conservation." Doctoral Dissertation for Doctor of Philosophy in Mechanical Engineering in the Graduate School of the University of Alabama, 1978.

Harman, Thomas. "Waste Heat Recovery in Data Centers: Ejector Heat Pump Analysis." Masters Thesis. School of Mechanical Engineering at the Georgia Institute of Technology. 2008.

Heisler, H. Advanced Engine Technology. SAE International. 1995. Warrenton, PA. pp. 345.

Heinz, Martin and F. Porsche. "The Posip System – Improving Occupant Protection in Convertibles and Coupes during Side Impacts," National Highway Traffic

Safety Administration. 1998. http://www-nrd.nhtsa.dot.gov/pdf/nrd-01/Esv/esv16/98S8W27.PDF

Hendricks, T. "Multi-Variable Optimization of Electrically- Driven Vehicle Air Conditioning Systems Using Transient Performance Analysis." C599-061. 2001 NREL. Golden, CO.

Koban, Mary and David Wilson. "HFO-1234yf A Low GDP Refrigerant for Mobile Air Conditioning. 2nd International Workshop for Mobile Air Conditioning and Auxiliary Systems." Torino, Italy 2007

LaGrandeur, J., et al., "Automotive Waste Heat Conversion to Electric Power Using Skutterudite, TAGS, PbTe, and BiTe," Proceedings of the 25th International Conference on Thermoelectrics, Vienna, Austria, August 2006.

LaGrandeur, J., et al., "Vehicle Fuel Economy Improvement through Thermoelectric Waste Heat Recovery," Proceedings of the 11th Diesel Engine Emissions Reduction (DEER) Conference, Chicago, Illinois, August 2005.

Kamara, Martin. An Investigation of the Effect of Variable Ejector Efficiency on the Performance Characteristics of a Steam Condenser in an Ejector Refrigeration System. M.S. Thesis at The George Washington University. Washington, D.C. 2005.

Matsuura, Moritaka, et al. "Fuel Consumption Improvement of Vehicles by Idling Stop." Society of Automotive Engineers International. Paper No. 2004-01-1896. Fuels and Lubricants Meeting and Exhibition. Toulouse, France. June 2004.

Pesaran, Ahmad, et al. "Ultracapacitors and Batteries for a Hybrid Vehicle." National Renewable Energy Laboratory (NREL). Proceeding of the Advanced Capacitor Summit. San Diego, CA. July 2005.

Office of Atmospheric Programs. "Greenhouse Gases and Global Warming Potential Values. Excerpt from the Inventory of U.S. Greenhouse Emissions and Sinks: 1999-2000." Environmental Protection Agency. Washington, D.C. April 2002

Yang, Jihui. "Thermoelectric Energy Conversion" American Physical Society March Meeting Energy Workshop. New Orleans, LA March 9th, 2008.

Zhang, Hongfang. "Flow Induction by Supersonic Pressure Exchange," Doctoral Dissertation in Mechanical Engineering presented to the Faculty of the Mechanical and Aerospace Engineering of The George Washington University, 2007.

Software and Websites

Holmgren, Magnus. "X Steam for MATLAB" Excel Engineering. January 2006. www.x-eng.com.

Department of Energy Information Administration. 2005. http://www.eia.doe.gov/pub/oil_gas/petroleum/analysis_publications/oil_market_basics/demand_text.htm. "September 25th 2008"

Appendix A Steam PE and Conventional Ejector A/C System Figures

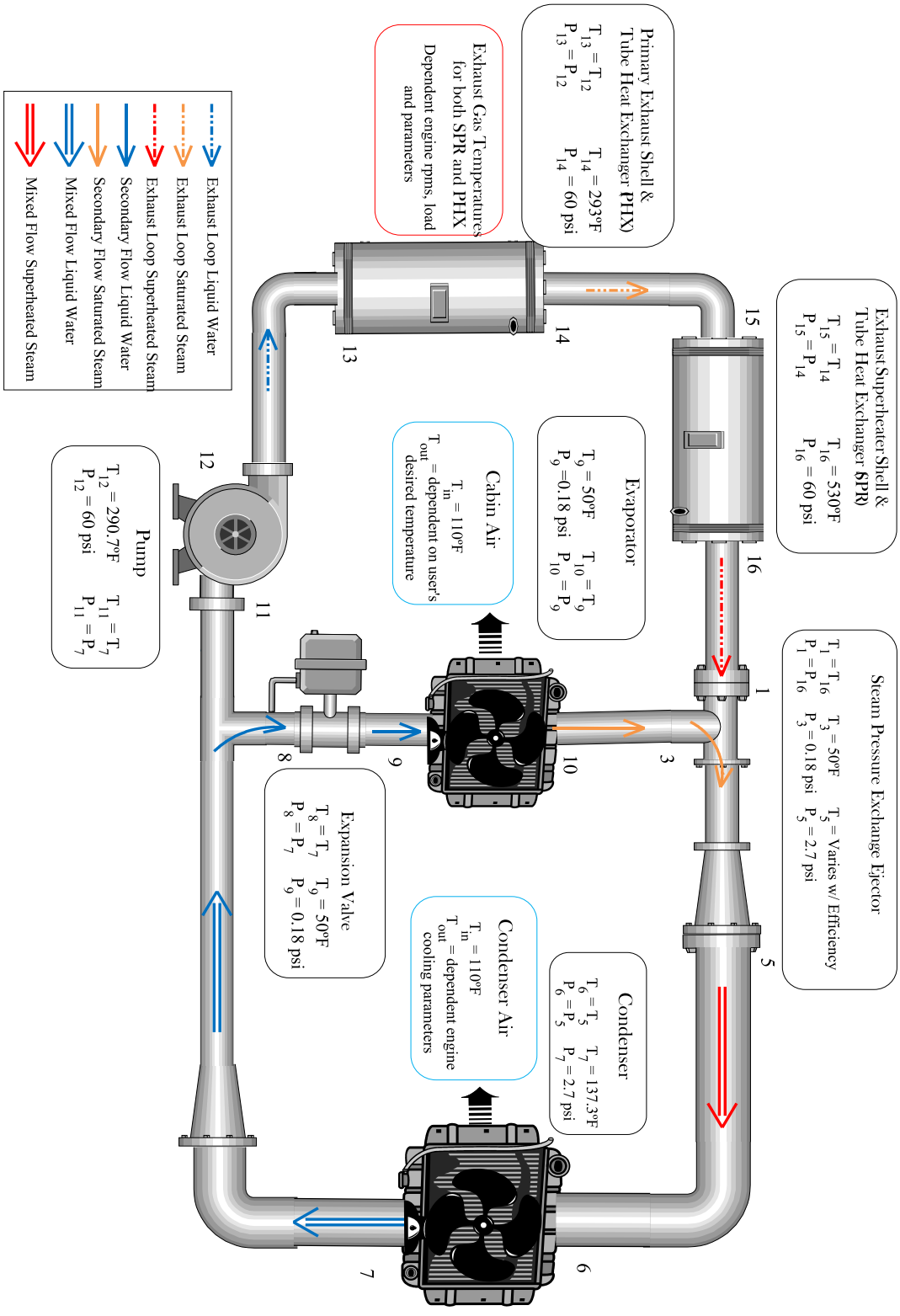

Figure A.1 Graphical Schematic of Modified Steam Pressure Exchange Ejector Air Conditioning System for the Automotive Applic

Table A.1. Experimental data of Everitt auto steam ejector A/C System with ejector efficiency based on the turbomachinery analog (Everitt 1999)

Everitt Steam Ejector Auto A/C System using Turbomachinery Analog w/ 77F Condensation Temperature								
Evaporator		Condenser		Primary Inlet		Entrainment Ratio	Ejector Efficiency	COPcycle
Temp	Psat	Temp	Psat	Temp	Psat	M_{sec}/M_{prim}		
F	PSI	F	PSI	F	PSI		%	
44.6	0.145	77	0.46	185	8.39	0.52	21.99	0.3
44.6	0.145	77	0.46	176	6.87	0.5	22.74	0.27
w/ 68F Condensation Temperature								
Evaporator		Condenser		Primary Inlet		Entrainment Ratio	Ejector Efficiency	COPcycle
Temp	Psat	Temp	Psat	Temp	Psat	M_{sec}/M_{prim}		
F	PSI	F	PSI	F	PSI		%	
44.6	0.145	68	0.34	185	8.39	0.57	15.68	0.34
44.6	0.145	68	0.34	176	6.87	0.56	16.45	0.3
44.6	0.145	68	0.34	167	5.60	0.57	18.00	0.26
44.6	0.145	68	0.34	158	4.52	0.54	18.49	0.22

Table A.2 Summary of Experimental Data on Conventional Steam Ejectors

$\frac{A_{diff}}{A_{thr}}$	P_{prim} (kPa)	P_{sec} (kPa)	P_{exit} (kPa)	$\frac{P_{prim}}{P_{sec}}$	$\frac{P_{exit}}{P_{sec}}$	Entrnmnt	Reference
90	198.7	1.23	3.8	161.8	3.09	0.59	Eames
	232.3	1.23	4.2	189.1	3.42	0.54	
	270.3	1.23	4.7	220.1	3.83	0.47	
	313.3	1.23	5.3	255.1	4.31	0.39	
	361.6	1.23	6	294.4	4.89	0.31	
90	198.7	1.04	3.6	191.6	3.47	0.5	Eames
	232.3	1.04	4.1	223.9	3.95	0.42	
	270.3	1.04	4.6	260.7	4.44	0.36	
	313.3	1.04	5.1	302.1	4.91	0.29	
	361.6	1.04	5.7	348.7	5.49	0.23	
90	198.7	0.87	3.4	227.7	3.89	0.4	Eames
	232.3	0.87	3.7	266.2	4.24	0.34	
	270.3	0.87	4.4	309.8	5.04	0.28	
	313.3	0.87	5.1	359	5.85	0.25	
	361.6	0.87	5.4	414.4	6.19	0.18	
200	834	1.59	3.2	521.7	2.0	0.58	Munday
	400	1.59	3.07	250.2	1.92	1.13	
	669	1.71	3.67	392.3	2.15	0.58	
	841	1.59	3.51	526.1	2.19	0.51	
	690	1.94	3.38	356	1.74	0.86	
	690	1.94	3.51	356	1.81	0.91	
81	270	0.87	4.1	309.5	4.7	0.22	Munday
	270	0.87	4.2	309.5	4.8	0.19	
	270	0.87	4.4	309.5	5.04	0.16	
	270	0.87	4.5	309.5	5.16	0.14	
	270	0.87	4.7	309.5	5.39	0.11	
145	660	1.55	5.3	426.5	3.42	0.27	Bagster
	578	1.55	5.3	373.5	3.42	0.31	
	516	1.58	5.3	326.9	3.36	0.35	
	440	1.57	5.03	280.6	3.21	0.38	
	381	1.59	4.77	239.9	3	0.42	
	312	1.62	4.23	192.6	2.61	0.46	
	278	1.68	4.1	165.1	2.44	0.42	
81	143.4	1.23	2.53	116.8	2.06	0.59	Sun
	169.2	1.23	2.67	137.8	2.17	0.51	
	198.7	1.23	3.15	161.8	2.56	0.43	
	232.3	1.23	4	189.1	3.26	0.35	
	270.3	1.23	4.75	220.1	3.87	0.29	
81	1720	57.7	143	29.7	2.47	0.5	Arnold
	1720	51.4	143	33.5	2.78	0.4	
	1720	45.5	143	37.8	3.14	0.3	
	1720	37.01	143	46.5	3.86	0.27	

Table A.3 Summary of experimental data found in Table A.1.1 with corresponding ejector efficiency using the turbomachinery analog (El-Dessouky, 2001).

Conventional Ejector Literature Experimental Data with Turbomachinery Analog

Area Ratio	Tboilsat	Tevapsat	Tcondsat	Entrainment Ratio	Turbomachinery Analog Efficiency	Reference
A_{diff} / A_{thr}	°F	°F	°F	M_{sec} / M_{prim}	%	
90	248	50	82.94	0.59	17.75	Eames
	257	50	86.02	0.54	17.56	
	266	50	89.42	0.47	16.66	
	275	50	93.20	0.39	15.09	
	284	50	97.34	0.31	13.08	
90	248	45.58	80.87	0.50	16.47	Eames
	257	45.58	84.90	0.42	15.33	
	266	45.58	88.52	0.36	14.24	
	275	45.58	91.81	0.29	12.23	
	284	45.58	95.41	0.23	10.38	
90	248	40.91	80.87	0.40	15.29	Eames
	257	40.91	84.90	0.34	14.23	
	266	40.91	88.50	0.28	12.59	
	275	40.91	91.80	0.25	11.89	
	284	40.91	95.40	0.18	9.11	
200	341.87	57.04	77.29	0.58	7.40	Munday
	290.50	57.04	76.04	1.13	15.47	
	325.63	59.07	81.46	0.58	8.68	
	342.50	57.05	80.10	0.51	7.53	
	327.87	62.62	78.94	0.86	9.02	
	327.87	62.62	80.10	0.91	10.29	
81	265.94	40.92	84.90	0.22	8.87	Munday
	265.94	40.92	85.65	0.19	7.84	
	265.94	40.92	87.11	0.16	6.90	
	265.94	40.92	87.82	0.14	6.16	
	265.94	40.92	89.20	0.11	5.04	
145	56.34	93.05	324.67	0.27	7.29	Bagster
	56.34	93.05	315.28	0.31	8.60	
	56.87	93.05	307.45	0.35	9.79	
	56.69	91.37	296.75	0.38	10.43	
	57.04	89.67	287.36	0.42	11.06	
	57.56	85.88	274.76	0.46	10.67	
	58.58	84.90	267.70	0.42	9.19	
81	50.04	70.29	229.86	0.59	10.79	Sun
	50.04	71.88	238.94	0.51	9.78	
	50.04	76.81	247.81	0.43	10.15	
	50.04	84.13	256.94	0.35	10.76	
	50.04	89.54	265.94	0.29	10.40	
81	400.79	184.87	229.86	0.50	19.39	Arnold
	400.79	179.61	229.86	0.40	17.61	
	400.79	174.17	229.86	0.30	14.90	
	400.79	165.20	229.86	0.27	16.04	

Table A.4 Ideal Theoretical Summary of Eames Steam Jet Ejector Refrigeration Analysis.

Eames Conventional Ejector using Turbomachinery Analog Theoretical Analysis with Diffuser/Throat Area Ratio of 90							
Evaporator		Condenser		Primary Inlet		Performance	
						Entrainment Ratio	Ejector Efficiency
Temp	Psat	Temp	Psat	Temp	Psat		
F	PSI	F	PSI	F	PSI	msec / mprim	%
50.00	**0.18**	**82.94**	**0.56**	**248.00**	**28.81**	**0.74**	**22.59**
50.00	**0.18**	**86.02**	**0.62**	**257.00**	**33.67**	**0.66**	**21.67**
50.00	**0.18**	**89.42**	**0.69**	**266.00**	**39.19**	**0.57**	**20.53**
50.00	**0.18**	**93.20**	**0.77**	**275.00**	**45.41**	**0.49**	**19.22**
50.00	**0.18**	**97.34**	**0.88**	**284.00**	**52.42**	**0.42**	**17.74**
45.58	**0.15**	**80.87**	**0.52**	**248.00**	**28.81**	**0.64**	**21.22**
45.58	**0.15**	**84.90**	**0.59**	**257.00**	**33.67**	**0.55**	**19.98**
45.58	**0.15**	**88.52**	**0.67**	**266.00**	**39.19**	**0.47**	**18.71**
45.58	**0.15**	**91.81**	**0.74**	**275.00**	**45.41**	**0.41**	**17.39**
45.58	**0.15**	**95.41**	**0.83**	**284.00**	**52.42**	**0.36**	**16.19**
41.00	**0.13**	**79.13**	**0.49**	**248.00**	**28.81**	**0.54**	**24.42**
41.00	**0.13**	**81.72**	**0.54**	**257.00**	**33.67**	**0.49**	**23.07**
41.00	**0.13**	**87.11**	**0.64**	**266.00**	**39.19**	**0.40**	**17.06**
41.00	**0.13**	**91.81**	**0.74**	**275.00**	**45.41**	**0.35**	**16.38**
41.00	**0.13**	**93.65**	**0.78**	**284.00**	**52.42**	**0.30**	**14.58**

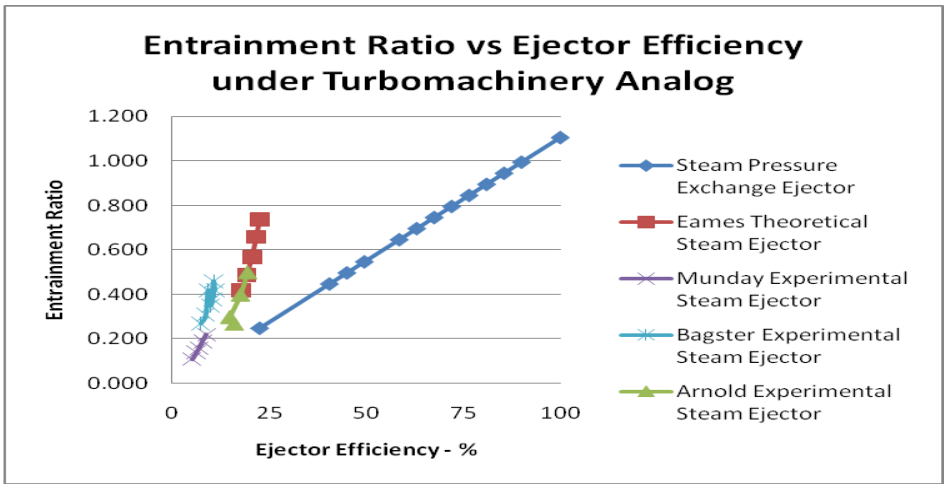

Figure A.2 Comparison plot of the experimental and theoretical entrainment ratio results of the conventional ejector along with theoretical pressure exchange ejector at various ejector efficiencies using the Turbomachinery Analog.

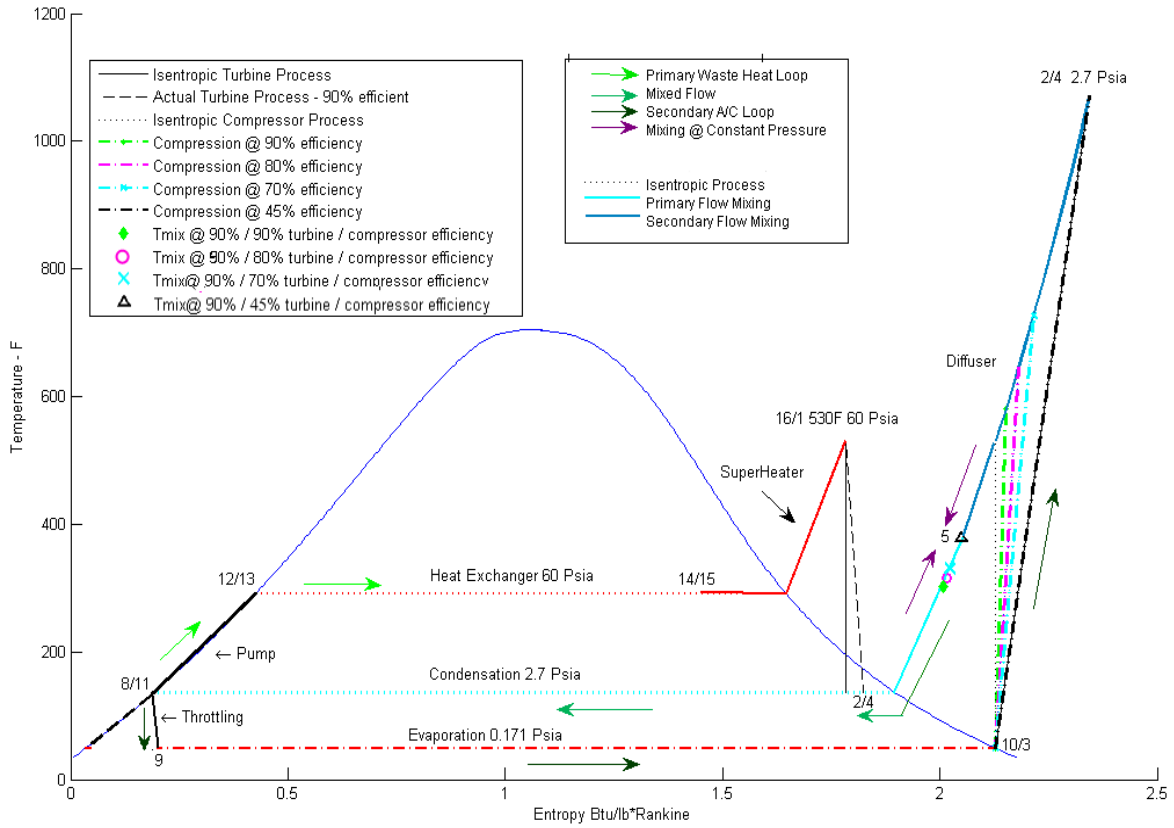

Figure A.3 TS Chart of the steam refrigerant for the pressure exchange ejector air conditioning system at various ejector efficiencies using turbomachinery analog.

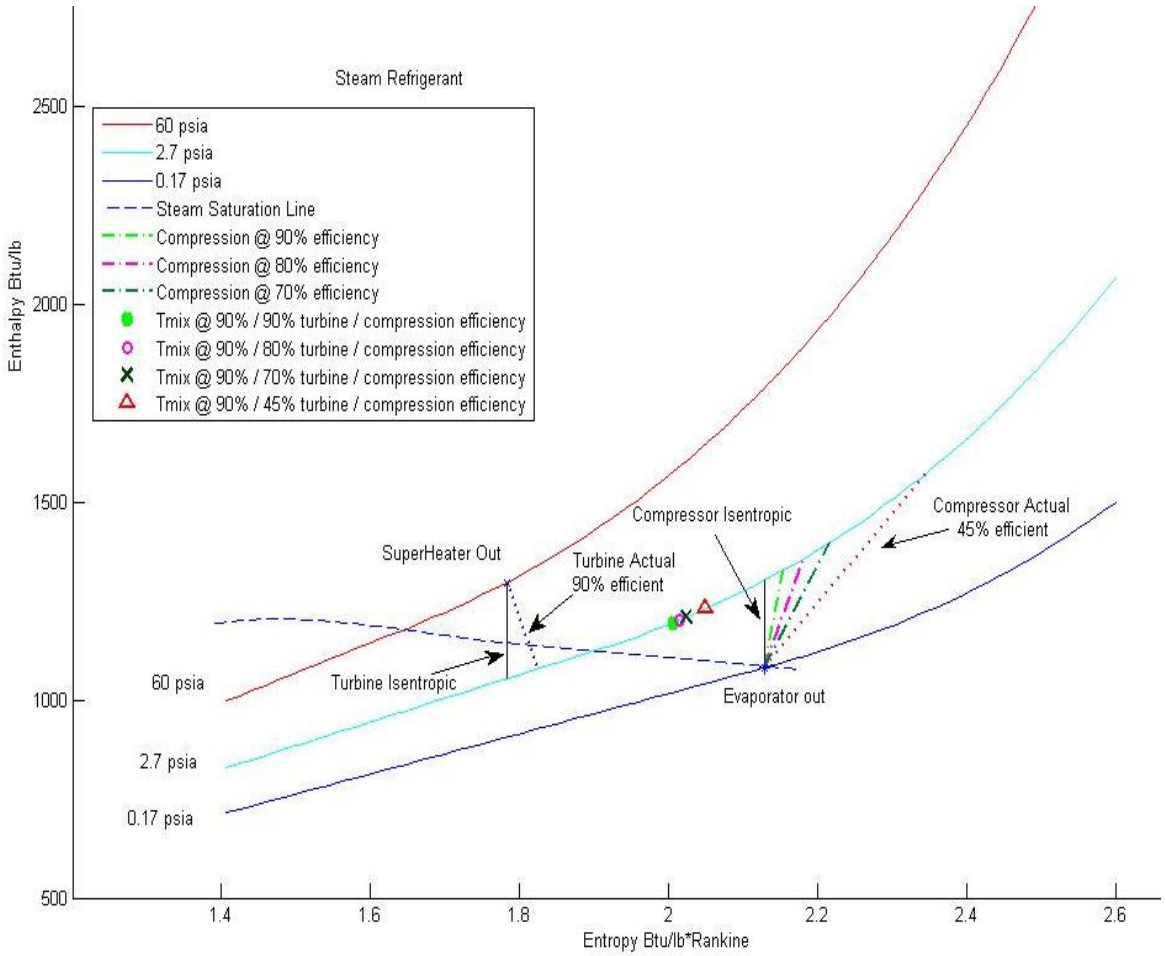

Figure A.4 Mollier Chart of the steam refrigerant for the pressure exchange ejector air conditioning system at various ejector efficiencies using turbomachinery analog.

Table A.4 Direct comparison between Bhatti's R-134a and steam ejector A/C systems during Idling and 50 mph conditions with set efficiencies

Air conditioning Performance for Delphi A/C System @ 68% compressor efficiency & Steam Ejector A/C System @ 40.5% Ejector Efficiency				
Properties	Bhatti R-134a A/C Idle	Steam PE Ejector A/C Idle	Bhatti R-134a A/C 50 MPH	Steam PE Ejector A/C 50 MPH
Outside Air Temperature, °F	20	120	100	100
Outside Air Relative humidity, %	22.4	40	22.4	40
Evaporator Air flow rate, ft3/min	250	380	250	380
Evaporator Mass flow Rate, lb/min	17.7	19.1	17.7	19.1
Conditioned Cabin Air temperature, °F	70	70	50	50
Condenser Air Flow Rate, ft3/min	600	1830	2000	6812
Condenser Mass Flow Rate, lb/min	41	127.2	142	485
Condenser Air Out Temperature, °F	135	170	117	125
7Refrigerant Mass Flow Rate thru Evaporator, lb/min	5.34	0.231	7.45	0.401
Refrigerant Mass Flow Rate thru Condenser, lb/min	5.34	0.747	7.45	1.3
Compression/Ejector Suction Pressure, psi	64	0.17	41	0.17
Compression/Ejector Suction Temp., °F	59	49	35	49
Compressor/Ejector Exit Pressure, psi	354	2.7	203	2.7
Compressor/Ejector Exit Temperature, °F	205	377.8	181	377.8
Compressor/Ejector efficiency, %	68	40.5	68	40.5
Compressor rotational speed, RPM	1000	----	2000	----
Compressor Power, hp	2.85	----	4.59	----
Exhaust Pump Power, hp	----	0.352	----	0.609
Exhaust Pump Suction Pressure, psi	----	2.7	----	2.7
Exhaust Pump Suction Temperature, °F	----	137	----	137
Exhaust Pump Exit Pressure, psi	----	60	----	60
Exhaust Pump Exit Temperature, °F	----	160	----	160
Exhaust Pump efficiency, %	----	80	----	80
Condenser Refrigerant out pressure, psi	322	2.7	193	2.7
Condenser Refrigerant out temperature, °F	157	137	103	137
Condenser temperature effectiveness	0.34	0.2	0.22	0.1
Condenser Desuperheating, Btu/min	68	83	97	143.5
Condensing in Condenser, Btu/min	216	841	373	1458
Subcooling in Condenser, Btu/min	65	0	120	0
Cooling Capacity in Condenser, Btu/min	350	924	590	1601.5
Evaporator in pressure, psi	77	0.17	50	0.17
Evaporator in Temperature, °F	64	49	41	49
Refrigerant Quality at Evaporator Inlet, %	0.47	0.07	0.38	0.07
Evaporator Temperature Effectiveness	0.9	0.98	0.85	0.98
Evaporator latent load, Btu/min	21	226	180	392
Evaporator sensible load, Btu/min	205	0	213	0
Evaporator cooling capacity, Btu/min	226	226	392	392

Table A.5 Global Warming Potential (GWP) of alternative A/C refrigerants

Greenhouse Gas	Refrigerant Name	Global Warming Potential
Air	R-729	0
Water (H_20)	R-718	0
Ammonia (NH_3)	R-717	0
Carbon Dioxide (CO_2)	R-744	1
Propane (C_2 H_6)	R-290	11
Methane (CH_4)	R-50	21
Difluoroethane ($C_2H_4F_2$)	R-152a	121
Nitrous Oxide (N_20)	R-744a	210
Tetrafluoroethane ($C_2H_2F_4$)	R-134a	1300
Dichlorodifluoromethane (CCl_2F_2)	R-12	8500

Table A.6 Approximate calculations of the additional weight for the exhaust waste heat recovery loop in the steam pressure exchange ejector A/C system at ideal conditions.

Additional Weight from Exhaust Loop in Ejector A/C System for Ideal 100% Ejector Efficiency							
Primary Heat Exchanger (PHX)	Cross Sectional Area (in^2)	Number of Tubes	Passes	Length (in^2)	Density	Total Volume (in^3)	Weight (lbs)
Shell side - Aluminum	2.41	1	1	16	0.098	38.64	3.77
Tube side - Aluminum	0.16	8	2	16	0.098	40.25	3.95
Super Heater (SPR)							
Shell side - Aluminum	2.85	1	1	30	0.098	85.41	8.37
Tube side - Aluminum	0.16	11	2	30	0.098	141.5	13.87
Copper Piping							
Exhaust Waste Heat Loop	0.436	1		54	0.323	23.54	7.60
Total							**37.57 lb (17.04 kg)**

Table A.7 Comparison of TEWI calculation between Bhatti and steam PE ejector A/C system for ideal conditions for three levels of air circulation (ψ = 0.0 to 1, 0% with all outside air to 100% recirculation with no outside air).

Total Equivalent Warming Impact (TEWI) of Ideal Bhatti R-134a & Ideal Steam PE Ejector A/C System						
	Bhatti R-134a System @ 100% compressor efficiency			Steam PE Ejector System @ 100% ejector efficiency		
	ψ = 0.0	**ψ = 0.5**	**ψ = 1**	**ψ = 0.0**	**ψ = 0.5**	**ψ = 1.0**
GWP	1300	1300	1300	0	0	0
л	1	1	1	1	1	1
m (kg)	0.91	0.91	0.91	~	~	~
τ (years)	12	12	12	12	12	12
DEWI (kg CO_2 / yr)	***124***	***64***	***64***	***0***	***0***	***0***
Ř (gal/yr)	0.22	0.22	0.22	0.22	0.22	0.22
e, (kg CO_2 / gal)	8.89	8.89	8.89	8.89	8.89	8.89
Weight , Ŵ,(kg)	13.6	13.6	13.6	23.95	23.95	23.95
$IEWI_m$ (kg CO_2 / yr)	***27***	***27***	***27***	***46.8***	***46.8***	***46.8***
К (kg/yr)/(Btu/min)	0.46	0.46	0.46	0.46	0.46	0.46
й	0.27	0.27	0.27	0.27	0.27	0.27
Q_{max} (Btu/min)	200	200	200	200	200	200
COP_{vent}	10.58	10.58	10.58	12.24	12.24	12.24
$IEWI_o$ (kg CO_2 / yr)	***32.2***	***8.1***	***20.1***	***27.8***	***17.4***	***7.0***
TEWI (kg CO_2 / yr)	**183.2**	**99.1**	**111.1**	**74.7**	**64.2**	**53.8**
% TEWI Reduction using Ideal Steam Pressure Ejector A/C				**59.2 %**	**35.1%**	**51.6%**

Table A.8 Comparison of TEWI Calculation between Bhatti and steam ejector A/C system @ 22.5 % ejector efficiency for three levels of air circulation (ψ = 0.0 to 1, 0% with all outside air to 100% recirculation with no outside air).

Total Equivalent Warming Impact (TEWI) of Bhatti R-134a & Steam PE Ejector A/C System						
	Bhatti R-134a System @ 68% compressor efficiency			Steam PE Ejector System @ 22.5 ejector efficiency		
	ψ = 0.0	**ψ = 0.5**	**ψ = 1**	**ψ = 0.0**	**ψ = 0.5**	**ψ = 1.0**
GWP	1300	1300	1300	0	0	0
л	1	1	1	1	1	1
m (kg)	0.91	0.91	0.91	~	~	~
τ (years)	12	12	12	12	12	12
DEWI (kg CO_2 / yr)	***124***	***64***	***64***	***0***	***0***	***0***
Ř (gal/yr)	0.22	0.22	0.22	0.22	0.22	0.22
e, (kg CO_2 / gal)	8.89	8.89	8.89	8.89	8.89	8.89
Weight , Ŵ,(kg)	13.6	13.6	13.6	49.9	49.9	49.9
$IEWI_m$ (kg CO_2 / yr)	***27***	***27***	***27***	***81.9***	***81.9***	***81.9***
K (kg/yr)/(Btu/min)	0.46	0.46	0.46	0.46	0.46	0.46
й	0.27	0.27	0.27	0.27	0.27	0.27
Q_{max} (Btu/min)	200	200	200	200	200	200
COP_{vent}	1.8	1.8	1.8	1.4	1.4	1.4
$IEWI_o$ (kg CO_2 / yr)	***189***	***118***	***47***	***243.4***	***152.1***	***60.8***
TEWI (kg CO_2 / yr)	**340**	**269**	**198**	**325.3**	**234**	**142.7**
% TEWI using Steam Pressure Ejector A/C @ 22.5 % Ejector Efficiency				**4.3 %**	**13.0%**	**27.9%**

MODEL: 8000-543-290

SPECIFICATIONS:

MODEL NUMBER: 8000-543-290
PUMP DESIGN: Positive Displacement 3 Chamber Diaphragm Pump
CAM: 3.0 Degree
MOTOR: Permanent Magnet, P/N 11-111-00
VOLTAGE: 12VDC Nominal
PRESSURE SWITCH: None (1/4"-18 NPT Female Front Fitting Connection)
LIQUID TEMPERATURE: 170 Degrees Fahrenheit (77 Degrees Centigrade) Max.
PRIME: Self-Priming Up To 5 Ft. Vertical,
Max. Inlet Pressure 30 PSI (2.1 Bar)
PORTS: 3/8"-18 NPT Female
MATERIAL OF CONSTRUCTION:
PLASTICS- Polypropylene
VALVES- Viton
DIAPHRAGM- Santoprene
FASTENERS- Zinc Plated Steel
NET WEIGHT: 4.0 Lbs (1.8 Kg)
DUTY CYCLE: Continuous (See Temperature Rise Chart)
TYPICAL APPLICATIONS: Agricultural Spraying

MODEL: 8000-543-290

TEMPERATURE RISE

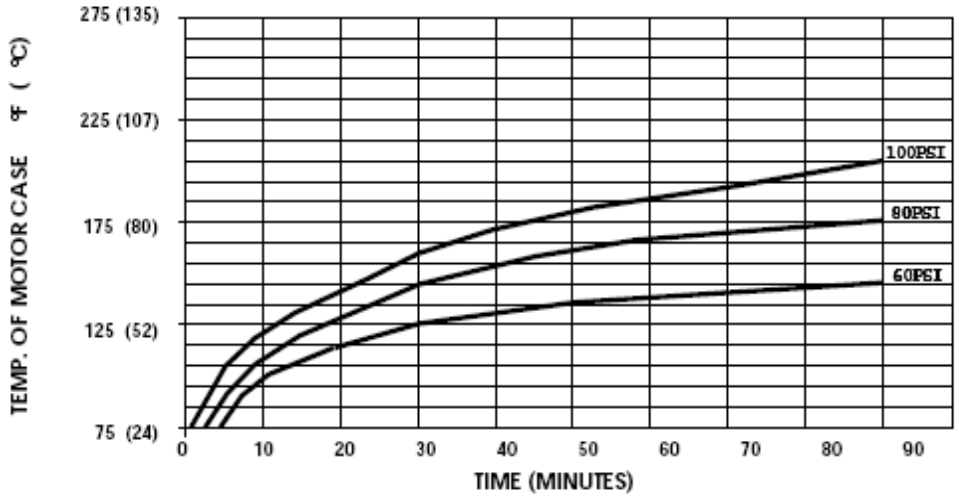

Figure A.5 Specifications of an electrically driven pump that fits the requirements of the steam PE ejector system. Courtesy of SURFlo.

PRESSURE (PSI)	FLOW (GPM/LIT)	RPM MIN/MAX	CURRENT (AMPS)	VOLTAGE (VOLTS)
OPEN	1.8/6.8	2300/2375	3.7	12VDC
10	1.31/4.9	2260/2290	4.4	"
20	1.26/4.7	2215/2240	5.0	"
30	1.20/4.5	2175/2190	5.7	"
40	1.14/4.3	2130/2145	6.2	"
50	1.08/4.1	2085/2095	6.8	"
60	1.02/3.9	2050/2065	7.3	"
70	0.97/3.7	2015/2030	7.7	"
80	0.93/3.5	1965/1995	8.0	"
90	0.89/3.4	1935/1960	8.4	"
100	0.84/3.2	1885/1920	8.8	"

Figure A.6 Mechanical performance of an electrically driven pump for the steam PE ejector system. Courtesy of SURFlo.

Appendix B Automotive Steam Ejector A/C System's Heat Exchangers

B.1 Evaporator

The first set of thermodynamic and heat exchange equations for the steam ejector automotive air conditioning system lies in the evaporator sub function. The cooling capacity required from the car is set based on what the user desires in terms of the cooling discharge air temperature and the air flow rate at which this cooling occurs. The cooling capacity range for a sedan ranges from 1 to 2 tons of refrigeration (200 to 400 Btu/min) and is used in Bhatti's analysis. For the comparison with Bhatti's R134a air conditioning analysis for a typical sedan cooling capabilities, the low and high cooling loads were set at 1.1 tons and 2 tons of refrigeration respectively. The desired cooled air temperature, outside environmental conditions, and cooling rate used in Bhatti's analysis was also matched. As noted in Chapter 2, the cool air is created from the ventilated air from the outside environment and blown into the cabin while the hot and humid cabin air is pushed out from rear of the vehicle. The two main variables that determine whether the sizing of the evaporator is adequate is the blower fan air volume flow rate performance providing enough cooling from air's low heat transfer coefficient to keep the required evaporator's total surface area lower than the designed area. The boundary conditions set for the evaporator were as followed:

- Humidity was factored in and included with the dry air portion calculation and considered an ideal gas.
- Bulk properties of specific heat, density, dynamic viscosity, kinematic viscosity, and enthalpy for air were linearly interpolated between 10°F intervals using air property charts. (Fox 2003)

- To prevent frost built up along the evaporator tubes, the steam refrigerant temperature was kept above water's freezing point temperature of 32°F.
- Refrigerant and ventilation and cabin air through the evaporator was set at incompressible flow and steady state flow.
- Refrigerant and air mass flow rates were kept constant at low cooling load during varying ejector efficiency and likewise for high cooling load.
- The refrigerant entered evaporator at 100% saturated liquid and underwent full evaporation inside the evaporator at constant pressure and temperature.
- The refrigerant was designed for complete vapor phase change with no superheat at the exit of the evaporator.

Evaporator Sub function

Predetermined Inputs

- Outside Temperature, Humidity, Efficiency of Evaporator Blower
- Cooling Rate, Desired Cabin Air Temperature
- Constant Pressure and Temperature of refrigerant through evaporator
    - Inlet and outlet steam enthalpy, entropy, thermal conductivity, density, and viscosity using MATLAB XSteam sub function (Appendix C)

The predetermined relative humidity of outside air, the thermal properties of the actual air were determined using the corresponding saturated pressures and partial vapor pressures calculations.

$$P_{satvap} = \frac{e^{(77.3450 + 0.0057T_{out} - \frac{7,235}{T_{out}})}}{T_{out}^{8.2}} \quad \text{B.1.1}$$

$$P_{vap} = Hum_{rel} P_{satvap} \quad \text{B.1.2}$$

The specific humidity then can be determined which enables the calculation of the specific heat of the humid air.

$$Hum_{spec} = \frac{\left(0.62198 * P_{vap}\right)}{\left(P_{atm} - P_{vap}\right)} \quad \text{B.1.3}$$

$$Cp_{humair} = Cp_{dryair}\left(\left(\left(\frac{0.0088}{0.01}\right) Hum_{spec}\right)+1\right) \quad \text{B.1.4}$$

$$H_{humair} = Cp_{humair}\ T_{out} \quad \text{B.1.5}$$

The density of the humid air can be calculated on the basis of the ideal gas law through equations B.1.6-8:

$$P_{air} = \frac{(\rho_{air} T_{out})}{0.0035} \quad \text{B.1.6}$$

$$P_{atm} = P_{air} + P_{vap} \quad \text{B.1.7}$$

$$\rho_{atm} = \frac{\rho_{dryair}\ (1 + Hum_{spec})}{(1 + 1.609 Hum_{spec})} \quad \text{B.1.8}$$

Evaporator Heat Exchanger Conditions

- The evaporator frontal area and volume are constant and 30% larger than the existing BMW 530i evaporator dimensions.
- The evaporator total surface area to volume ratio are set constant

Evaporator Blower and Air Mass Flow Rate

The method of determining whether the evaporator contains enough total surface area to provide cool air for the vehicle cabin and at the same time to fully

evaporate the steam refrigerant is dictated by geometric size limitations and the lowest heat transfer coefficient constraint. For an air cooled evaporator, the lowest convective heat transfer coefficient that creates the largest heat transfer resistance is air with its low specific heat. A blower fan is installed to provide a cool air to the cabin and increase the convective heat transfer to minimize the total surface area needed from the evaporator to fully evaporate the steam. The calculated total surface area is compared with the designed total surface area from the geometric parameters of the evaporator. With the designed total surface area to volume ratio set constant, the comparison between the designed and calculated total surface area is necessary for proper volume sizing of the evaporator. The final design was based on previous trials and calculations in the MATLAB evaporator algorithm.

The thermodynamic energy equation in B.1.9 is matched with the heat transfer potential of the air cooled evaporator.

$$Q_{refevp} = m_{refevp} (I_{refevpo} - I_{refevpi}) \qquad \text{B.1.9}$$

$$Q_{refevp} = Q_{airevp} = m_{airreq}\ cp_{airevp} (T_{airevpi} - T_{airevpo}) \qquad \text{B.1.10}$$

The effectiveness of the evaporator is the ratio of the actual heat transfer to the thermodynamically maximum heat transfer rate that occurs in a counterflow heat exchanger of infinite size (Bhatti, 1999). The heat capacity rate C, a product of the mass flow rate and specific heat, cp , is expressed as:

$$\varepsilon_{evp} = \frac{C_{refevp}\left(T_{refevpi} - T_{refevpo}\right)}{C_{min}\left(T_{refevpi} - T_{airevpi}\right)} = \frac{C_{airevp}\left(T_{airevpi} - T_{airevpo}\right)}{C_{min}\left(T_{airevpi} - T_{refevpo}\right)} \qquad \text{B.1.11}$$

and can be simplified during condensation and evaporation processes where $C_{max} = C_{refevp}$ and $C_{min} = C_{airevp}$ to:

$$\varepsilon_{evp} = \frac{\left(T_{airevpi} - T_{airevpo}\right)}{\left(T_{airevpi} - T_{refevpo}\right)}$$

Dividing ε_{evp} to both sides of the energy equation in B.1.10, the minimum required mass flow can be calculated in terms of the effectiveness of the condenser and the inlet temperature difference between the two fluids:

$$Q_{airevp} = Q_{evp} = m_{airreq}\ cp_{airevp}\ \varepsilon_{evp}\ (T_{airevpi} - T_{refevpi}) \qquad \text{B.1.12}$$

The MATLAB program is designed to import the evaporator blower's volumetric flow rate at high load, $V_{airblwr}$, and determine its mass flow rate and velocity based on the free flow area to frontal area ratio, σ_{evp}, air density, and frontal cross sectional area.

$$M_{airblwr} = V_{airblwr}\ \rho_{airevp} \qquad \text{B.1.13}$$

$$Vel_{airblwr} = \frac{m_{airblwr}}{\sigma_{evp}\ L_{evp} H_{evp}\ \rho_{airevp}} \qquad \text{B.1.14}$$

The two mass flow rates, $m_{airblwr}$ and m_{airreq}, are compared and if the air mass flow rate created by the evaporator blower is less than the required mass flow in equation B.1.12, the system would need to replace the blower with a larger one. In all ejector efficiency cases, the 200 Watt evaporator blower provides adequate air mass flow rate through the evaporator blower for the steam refrigerant to fully evaporate and provide cool air to the cabin under the volume and surface area constraints.

Now that the thermodynamic equations are satisfied, the heat transfer between the steam and air were calculated to verify that there is enough total surface area to accommodate for the process. In order to capture the process, the proper surface area is calculated with approximating the convection and conduction coefficients of the

two fluids along with the evaporator's wall and fouling resistances. The overall heat transfer equation, consisting of all these variables, is defined as,

$$Q_{evp} = U_{evp}\, F_{evp}\, A_{evp}\, \Delta T_M \qquad \text{B.1.15}$$

where the mean temperature $\Delta T_{M,}$ is calculated using the log mean temperature difference (LMTD), $\Delta T_{LMTD,}$ which better approximates the average temperature during heat transfer process. The LMTD process is defined as:

$$\Delta T_M \approx \Delta T_{LMTD} = \frac{\left(T_{refevpo} - T_{refevpi}\right) - \left(T_{airevpi} - T_{airevpo}\right)}{\ln\left[\left(T_{refevpo} - T_{refevpi}\right) / \left(T_{airevpi} - T_{airevpo}\right)\right]} \qquad \text{B.1.16}$$

The non-dimensional LMTD correction factor, F_{evp} , is dependent on the fluids' temperature effectiveness, heat capacity rate ratio, and flow arrangement. With known inlet and outlet temperatures for both fluids, the F_{evp} can be determined using Figure B.1.1. A correction factor that is equal to 1 represents a true counterflow heat exchanger characteristic and anything below 1 relates closer to a crossflow or multipass arrangement. One note is that if one fluid has a minimal temperature gradient such as the evaporation process undergoing a phase change, it offsets the temperature effectiveness such that F_{evp} is set to 1 (Kakac, 2002).

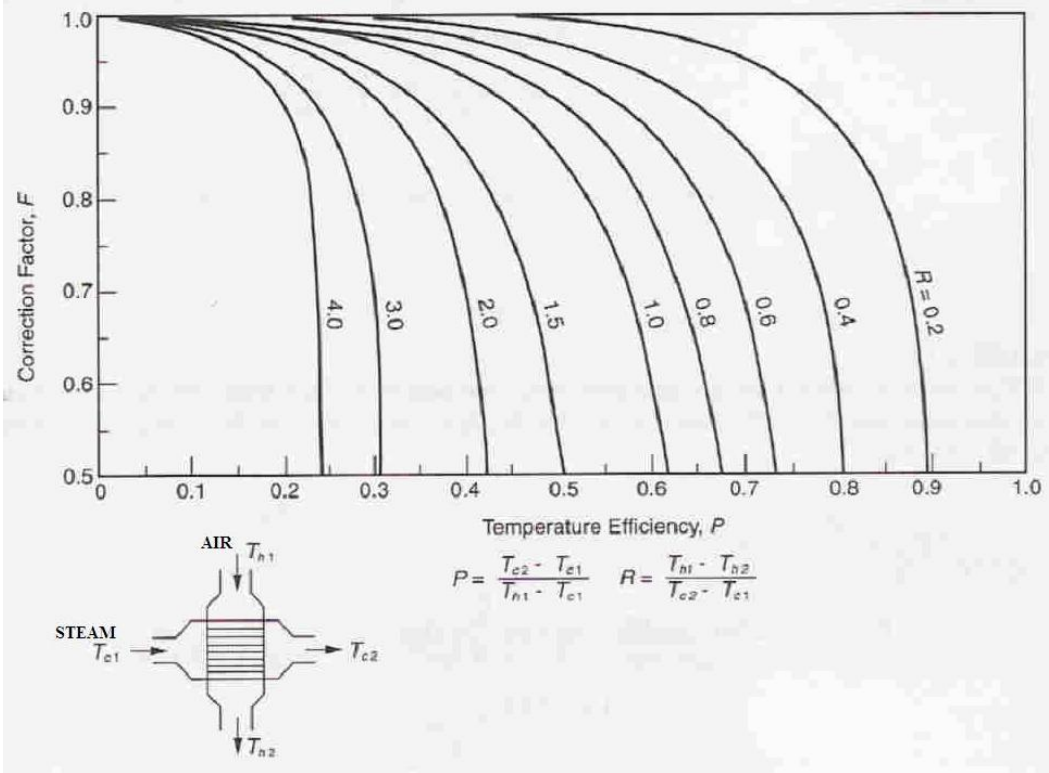

Figure B.1 Correction factor chart based on temperature difference across a crossflow with one fluid mixed (Air) and another fluid unmixed (Steam) (Kakac 2002)

The overall heat transfer coefficient can be estimated using area ratios, convection and fouling resistances between the interior and exterior surfaces (London 1984):

$$U_{evp} = \frac{A_{out}}{A_{in}\, h_{in}} + \frac{A_{out}}{A_{in}} R_{fint} + A_{in} R_{wall} + \left(\frac{R_{fout}}{n_o}\right) + \frac{1}{n_o h_o} \qquad \text{B.1.17}$$

where R_{wall} represents the wall conduction resistance:

$$R_{wall} = \frac{\ln\left(r_{evpo} \;/\; r_{evpi}\right)}{2\,\pi\, L_{evp}\, k_{wall}} \qquad \text{B.1.18}$$

The overall fin efficiency, n_o , for the external plate fins attached to refrigerant coiled tubes is calculated using the fin area ratio found in Figure 4.1.6 in Chapter 4 with a specific fin efficiency set at 95%.

$$n_o = 1 - (A_{finrat}\ (1 - n_{fin})) \qquad \text{B.1.19}$$

Refrigerant Side Heat Transfer Coefficient - h_{in}

In order to capture an accurate result for the convection heat transfer rate for the tube side steam refrigerant under full evaporation phase, Gnielinski and Shah's correlations for a two phase flow are applied. The calculation of the Reynolds number in the liquid phase will determine whether the refrigerant is turbulent ($2300 < Re_{tliq} > 100{,}000$) or laminar ($Re_{tliq} < 2300$). The calculation for the Reynolds number:

$$Re_{tliq} = \frac{\left(G_{evptube}\ d_{tins} \right)}{\mu_{tliq}} \qquad \text{B.1.20}$$

where $G_{evptube}$ equals the mass flux of steam refrigerant (lb/min-ft^2):

$$G_{evptube} = \frac{M_{ref}}{A_{tcrss}} \qquad \text{B.1.21}$$

and the cross-sectional area is calculated:

$$A_{tcrss} = \frac{\pi\left(d_{tin}^{\ 2}\right)}{4}$$

If the Reynolds number reveals that the flow is turbulent, the boiling factor, Prandtl and Nusselt number are calculated under Gnielinski correlation:

$$f_{boil} = ((1.58 * \ln(Re_{tliq})) - 3.28)^{-2} \qquad \text{B.1.22}$$

$$Pr_{tliq} = \frac{\left(\mu_{tliq} cp_{tliq} \right)}{k_{tliq}} \qquad \text{B.1.23}$$

$$Nu_{tliq} = \frac{\left(\left(f_{boil} / 2\right)\left(Re_{tliq} - 1000\right) Pr_{tliq}\right)}{\left(1 + \left(12.7\left(f_{boil} / 2\right)^{1/2}\left(Pr_{tliq}^{2/3} - 1\right)\right)\right)} \quad \text{B.1.24}$$

And if the Reynolds number is below 2300 making the flow inside the tubes laminar, the Seider and Tate correlation is used as long as these conditions are satisfied:

$$\left(\frac{Re_{tliq}\, Pr_{tliq}\, d_{tin}}{L_{evp}}\right)^{1/3}\left(\frac{\mu_{tblk}}{\mu_{wall}}\right)^{0.14} > 2$$

and

$$\frac{\mu_{tblk}}{\mu_{wall}} < 9.75$$

The laminar Nusselt number can be found using equation:

$$Nu_{tliq} = 1.86\left(\frac{Re_{tliq}\, Pr_{tliq}\, d_{tin}}{L_{evp}}\right)^{1/3}\left(\frac{\mu_{tblk}}{\mu_{wall}}\right)^{0.14} \quad \text{B.1.25}$$

The dynamic viscosity, μ , for steam bulk temperature is calculated using XSteam MATLAB program at 0.5 quality in the saturation region. The air dynamic viscosity properties were taking at the median temperature between the inlet and outlet air temperatures. Once the laminar or turbulent Nusselt number is calculated, the liquid phase convection heat transfer coefficient can be determined:

$$H_{tliq} = \frac{Nu_{tliq}\, k_{tliq}}{d_{tin}} \quad \text{B.1.26}$$

Now that the liquid phase convection heat transfer coefficient is calculated using Gnielinski along with Seider and Tate correlations, the next step is to add the boiling vapor coefficient using Shah's correlation which are based on four dimensionless parameters: Froude number (Fr), convection number (Co), boiling

number (Bo), and enhancement factor (F). These four dimensionless parameters are used to characterize the flow and employed to estimate the two-phase boiling convective contribution (Kakac, 2002). The Froude number which determines whether stratification is negligible or not is defined as:

$$Fr = \frac{G_{tliq}^{\ 2}}{\rho_{tliq}^{\ 2}\, g * d_{tin}} \qquad \text{B.1.27}$$

If the Froude number, Fr, is greater than 0.04 then stratification is negligible and the inertial forces dominant over gravitational forces with the correction factor, K_{FR} set to 1. However if the Froude number is below 0.04, K_{FR} is defined as:

$$K_{FR} = (25\ Fr)^{-0.3} \qquad \text{B.1.28}$$

The convection number, Co, that's dependent on vapor quality is defined as:

$$Co = \left[\frac{(1-x)}{x}\right]^{0.8} \left(\frac{\rho_{tliq}}{\rho_{tvap}}\right)^{0.5} K_{FR} \qquad \text{B.1.29}$$

For pure convection boiling with high vapor qualities and low boiling numbers from a low convection number results in a convection boiling factor, F_{CB}, defined as:

$$F_{CB} = 1.8\ Co^{-0.8} \quad \text{when } Co < 1.0$$

and for low vapor qualities and low boiling numbers

$$F_{CB} = 1.0 + 0.8\, e^{[1-(Co^{0.5})]} \quad \text{when } Co > 1.0$$

Where $F = F_{CB}$ and the enhancement factor, F_o, can be calculated using:

$$F_o = F\ (1 - x)$$

Finally the overall convective boiling heat transfer coefficient is calculated combining the liquid convection heat transfer and the boiling enhancement factor:

$$H_{tcb} = F_o\ H_{tliq} \qquad \text{B.1.30}$$

Air Side Heat Transfer Coefficient - h_o

The air side heat transfer coefficient is determined using Kay's experimental results from the heat exchangers chosen for this analysis. The friction factor, f, and the Stanton-Prandtl Number, $StPr^{2/3}$, are measured from Figure 4.1.6 to better approximate the heat transfer coefficient based on air's Reynolds number. The mass flux of air can be determined using the evaporator's free flow to frontal area ratio and front area dimensions:

$$G_{airevp} = \frac{m_{airblwr}}{\sigma_{evp} L_{evp} H_{evp}} \quad \text{B.1.31}$$

$$Re_{air} = \frac{\left(G_{airevp} \, d_h \right)}{\mu_{air}} \quad \text{B.1.32}$$

The air heat transfer coefficient for the evaporator can be determined by the following equation:

$$h_{air} = G_{airevp} \, cp_{humair} \, St \quad \text{B.1.33}$$

Airflow Pressure Drop

The evaporator blower is designed to specifically handle certain static pressure increases while achieving the desired volumetric flow rate. The blower's efficiency is maximized based on overcoming the additional static pressure to produce the desired volumetric flow rate. The static pressure rise as air passes through the plate finned circular tube evaporator is the pressure drop created across the heat exchanger (Kakac, 2002):

$$\Delta P_{airevp} =$$

$$\frac{G_{airevp}^{\,2}}{2\rho_i}\left[\left(k_c + 1 - \sigma^2\right) + 2\left(\frac{\rho_i}{\rho_o} - 1\right) + f_{air}\frac{A\,\rho_i}{A_{min}\,\rho_o} - \left(1 - k_e - \sigma^2\right)\frac{\rho_i}{\rho_o}\right] \quad \text{B.1.34}$$

Where the evaporator contraction loss coefficient, k_c, and the enlargement loss coefficient, k_e, are determined using Figure B.1.2. The minimum free flow area, A_{min}, is the frontal evaporator surface area for the passing air. The outlet air densities are dependent on the air temperature decrease across the heat exchanger for cooling purposes.

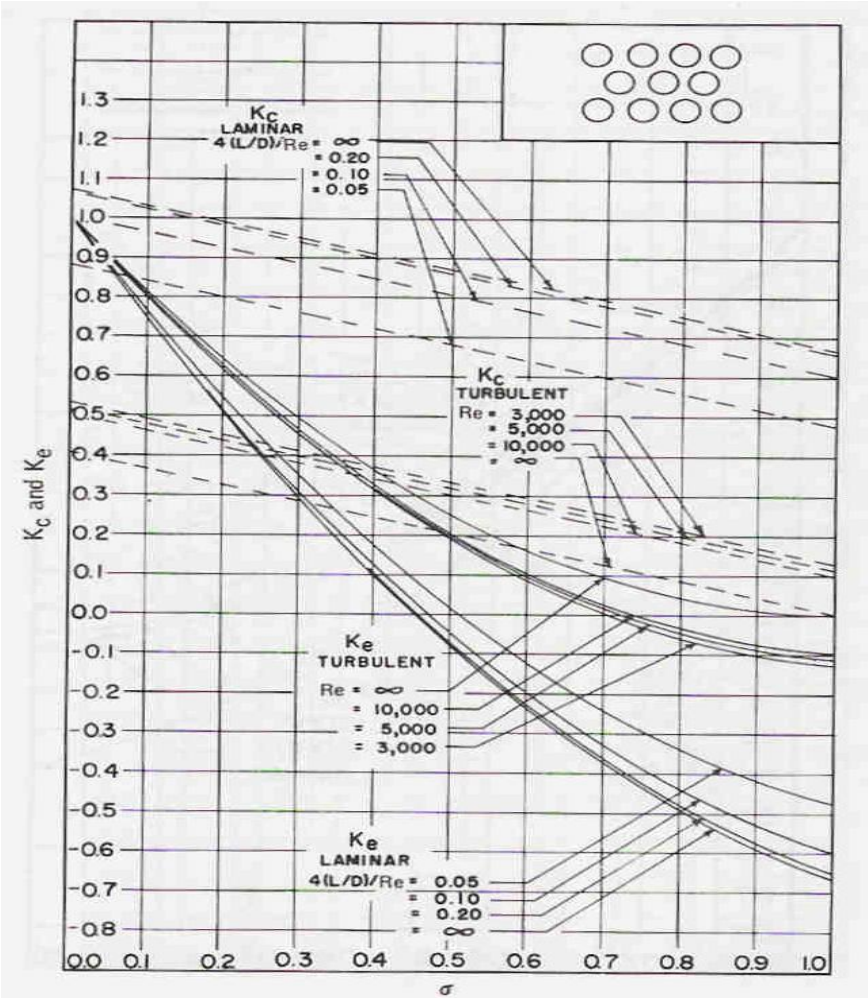

Figure B.2 Entrance and exit pressure loss coefficients for a multiple-tube heat exchanger core with abrupt contraction entrance and expansion exit (Kays 1984)

Additional Evaporator Appendix Nomenclature

B_o	Shah's Correlation Boiling number
Co	Shah's Correlation Convection Number
F	Shah's Correlation Enhancement Number
F_{CB}	Shah's Convection Boiling Factor
F_O	Shah's Enhancement Factor
Fr	Shah's Froude Number
ε	Dimensionless heat transfer effectiveness being ratio of actual heat transfer rate to thermodynamic maximum heat transfer rate
Hum	Humidity
K_{FR}	Shah's Correction Factor
k_c	Evaporator Airflow Contraction Loss Coefficient
k_e	Evaporator Airflow Enlargement Loss Coefficient
η_{fin}	Specific fin efficiency
η_o	Overall fin efficiency of the heat exchanger surface
r	Radius of tube side heat exchanger

Acronyms and Subscripts

atm	Atmospheric Conditions
blwr	Evaporator Blower
boil	Boiling Conditions
cb	Convective Boiling
crss	Cross Sectional Area
dry	Dry air conditions
fin	Evaporator Fin Parameters
hum	Humid air conditions
min	Minimum (Free flow)
rat	Ratio
rel	Relative in terms of humidity
req	Required
spec	Specific in terms of humidity
vap	Vapor State

B.2 Condenser

The boundary conditions set for the condenser are as followed:

- Humidity was factored in with the dry air calculation for the outside air and considered an ideal gas using same equations mentioned in evaporator appendix.
- Specific heat, density, dynamic viscosity, kinematic viscosity, and enthalpy for condenser air at bulk temperatures were linearly interpolated between 10°F intervals from air property charts. (Fox, 2003 and White, 1988)
- Refrigerant inside the condenser and condenser ram air or air from condenser fan was set as a incompressible flow and at steady state conditions.
- The condenser frontal area were closely matched the existing BMW 530i condenser with an additional tube row which added heat transfer surface area, condenser core depth, and volume .
- Condenser size and total surface area to volume ratio were set constant
- If there wasn't enough convection heat transfer from the ram air to fully condense the steam refrigerant, the condenser fan was turned on.
- If engine rpm are high (> 1000 rpm), exit condenser air temperature was limited to 25°F above its inlet temperature for engine cooling purposes
- If engine rpm are low (≤ 1000 rpm), exit condenser air temperature was limited to 90°F above its inlet temperature for engine cooling purposes

Condenser Sub function

Predetermined Inputs

- Outside Temperature and Humidity, Efficiency of Condenser Fan

- Outlet Ejector Refrigerant Temperature, Pressure, and Thermal properties from the Turbomachinery Analysis
- Constant Pressure and Temperature of refrigerant during full condensation through condenser
    - Inlet and outlet steam enthalpy, entropy, thermal conductivity, density, and viscosity using MATLAB XSteam sub function

The condenser sub function begins with the predetermined inputs mentioned above along with thermal properties and fluid properties of the mixed steam refrigerant leaving the ejector. The flow of the steam refrigerant through the piping from the ejector to the condenser was considered adiabatic and at constant pressures such that:

$I_{refcndi} = I_{refejro}$

$S_{refcndi} = S_{refejro}$

$T_{refcndi} = T_{refejro}$

With the full steam condensation performed within the condenser and the mass flow rate constant, the total heat rejection required is calculated using equation B.2.1. The design of the system sets the exit ejector pressure equal to the desired saturation pressure in which the refrigerant enters the condenser in the superheated region. The condenser is designed for complete condensation at the saturation temperature and pressure in which the MATLAB XSteam function calculates exit enthalpy, entropy, and thermal properties.

$I_{refcndo}$ found using (T_{refsat}, P_{refsat})

$S_{refcndo}$ found using (T_{refsat}, P_{refsat})

For equation B.2.2, the air inlet temperature is given as 110°F and the exit temperature is determined based on the engine speed conditions. Since the same air

that passes through the condenser is used to cool the engine radiator, the condenser exit air temperature is limited based on how much cooling is needed for the radiator. For the case of the idling condition, there is minimal engine cooling required and the exit air temperature leaving was limited to 90°F above inlet temperature. In the case of the 50 mph condition, the engine load is at medium range and requires typical engine cooling and similar to Bhatti's analysis the exit air temperature was limited to 25°F above the inlet temperature. At adiabatic conditions with known inlet and outlet pressures and temperatures for both fluids, the energy equation balance between the two fluids was conducted to determine the unknown air mass flow rate needed.

$$Q_{refcnd} = m_{refmix} (I_{refcndi} - I_{refcndo}) \quad \text{B.2.1}$$

$$Q_{refcnd} = Q_{aircnd} = m_{air} \; cp_{aircnd} (T_{aircndo} - T_{aircndi}) \quad \text{B.2.2}$$

The condenser geometric parameters were imported from a selection of various heat exchanger sizes and shapes (Kays, 1984). The first trials for the new condenser was an air cooled flat finned tube condenser in which the small hydraulic diameter due to its high surface area to volume ratio, α, resulted to high of a pressure drop across the condenser. As a result of the high pressure drop and limited resources of fan performance for static pressure above 0.02 psi (130 Pa), the flat finned tube condenser was replaced with a less compact coiled finned tube condenser. To compensate for the lower surface area to volume ratio, the limited condenser width and length was slightly increased and yet small enough to fit in the vehicle's front section, the thickness was increased to provide two rows of finned tubes. Tests were conducted with the models shown in Figure 4.3.2 in Chapter 4 and pressure drops were calculated with the same volume size and air volumetric rate.

Condenser Fan and Air Mass Flow Rate during Idling

The method of determining whether the condenser air will provide enough heat transfer to fully condense the steam refrigerant is dictated by geometric size limitations and the highest heat transfer resistance. For an air cooled condenser, the highest heat transfer resistance that causes high surface area is air's low convective heat transfer coefficient due to its low specific heat.

The energy equation in B.2.2 is matched with the heat transfer potential of the condenser. The effectiveness of the condenser is the ratio of the actual heat transfer to the thermodynamically maximum heat transfer rate that occurs in a counterflow heat exchanger of infinite size (Bhatti, 1999). The heat capacity rate C, a product of the mass flow rate and specific heat, cp , is expressed as:

$$\varepsilon_{cnd} = \frac{C_{refcnd}\left(T_{refcndi} - T_{refcndo}\right)}{C_{min}\left(T_{refcndi} - T_{aircndi}\right)} = \frac{C_{aircnd}\left(T_{aircndi} - T_{aircndo}\right)}{C_{min}\left(T_{aircndi} - T_{refcndo}\right)} \qquad \text{B.2.3}$$

and can be simplified during condensation and evaporation processes where $C_{max} = C_{refcnd}$ and $C_{min} = C_{aircond}$ to:

$$\varepsilon_{cnd} = \frac{\left(T_{aircndi} - T_{aircndo}\right)}{\left(T_{aircndi} - T_{refcndo}\right)}$$

Dividing ε_{cnd} to both sides of the energy equation in B.2.2, the required mass flow can be calculated in terms of the effectiveness of the condenser and the inlet temperature difference between the two fluids:

$$Q_{aircnd} = Q_{cnd} = m_{aircndreq}\ cp_{aircnd}\ \varepsilon_{cnd}\ (T_{aircndi} - T_{refcndi}) \qquad \text{B.2.4}$$

The MATLAB program is designed to import the car's speed or lack of speed, Vel_{car} , and determine its mass flow rate based on the free flow area to frontal area ratio, σ_{cnd} , air density, and frontal cross sectional area.

$$m_{aircar} = Vel_{car}\ \sigma_{cnd}\ L_{cnd}\ H_{cnd}\ \rho_{aircnd} \qquad \text{B.2.5}$$

The two mass flow rates, m_{air} and m_{aircar}, are compared and if the air mass flow rate created by the motion of the vehicle is less than the required mass flow in equation B.2.4, the difference between the two is the mass flow rate needed from the radiator/condenser fan. The 50 mph vehicle speed provided more than enough air mass flow rate through the condenser and hence the radiator/condenser fan was kept turned off. For the case of the idling condition, there was no air mass flow rate and the condenser fan needed to be turned on and operated. Once equation B.2.4 determined the required air mass flow rate, the volume flow rate and air velocity was calculated using equation B.2.6 and B.2.7 and compared with the 540 ft^3/min volume flow rate of the typical sedan 250 Watt (14.2 Btu/min) condenser/radiator fan detailed in Chapter 2. In all cases, the 250 Watt condenser/radiator fan under full power provides adequate air mass flow rate through the condenser for the steam refrigerant to condense under the volume and surface area constraints.

$$V_{aircndreq} = \frac{m_{aircndreq}}{\rho_{aircnd}} \qquad \text{B.2.6}$$

$$Vel_{aircndreq} = \frac{m_{aircndreq}}{\sigma_{cnd}\ L_{cnd} H_{cnd}\ \rho_{aircnd}} \qquad \text{B.2.7}$$

The calculated total surface area is compared with the designed surface area from the geometric parameters of the condenser. This procedure is explained in further detail in the algorithm chart and future calculations below.

Now that the thermodynamic equations are satisfied, the heat transfer between the steam and air were calculated to verify that there is enough total surface area to accommodate for the process. In order to capture the process, the proper surface area is calculated with approximating the convection and conduction coefficients of the

two fluids along with the aluminum condenser's wall and fouling resistances. The overall heat transfer equation, consisting of all these variables, is defined as,

$$Q_{cnd} = U_{cnd}\, F_{cnd}\, A_{cnd}\, \Delta T_M \qquad \text{B.2.8}$$

where the mean temperature $\Delta T_{M,}$ is calculated using the log mean temperature difference (LMTD), $\Delta T_{LMTD,}$ that better approximates the average temperature during heat transfer process. The LMTD process is defined as:

$$\Delta T_M \approx \Delta T_{LMTD} = \frac{\left(T_{refcndi} - T_{refcndo}\right) - \left(T_{aircondo} - T_{aircondi}\right)}{\ln\left[\left(T_{refcondi} - T_{refcondo}\right) / \left(T_{aircondo} - T_{aircondi}\right)\right]} \qquad \text{B.2.9}$$

The non-dimensional LMTD correction factor, F_{cnd} , is dependent on the fluids' temperature effectiveness, heat capacity rate ratio, and flow arrangement. With known inlet and outlet temperatures for both fluids, the LMTD correction factor can be determined using Figure B.2.1. A correction factor F_{cnd} that is equal to 1 represents a true counterflow heat exchanger characteristic. During the condensation or evaporation process undergoing a phase change, the steam side temperature effectiveness is negligible and F_{cnd} is set to 1.

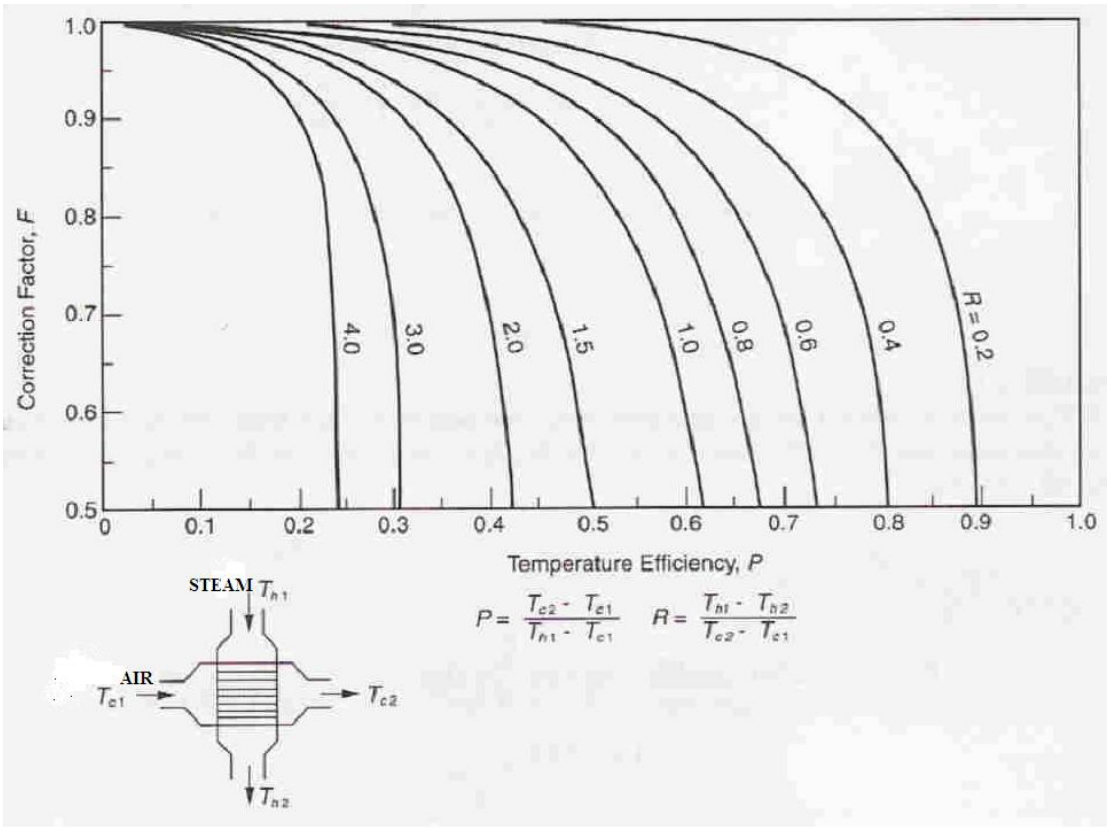

Figure B.3 Correction factor chart based on temperature difference across a crossflow with one cold fluid mixed (Air) and another hot fluid unmixed (Steam) (Kakac 2004)

The overall heat transfer coefficient can be estimated using area ratios and convection and fouling resistances between the interior and exterior surfaces (London , 1984):

$$U_{cnd} = \frac{A_{out}}{A_{in}\, h_{in}} + \frac{A_{out}}{A_{in}} R_{fint} + A_{in} R_{wall} + \left(\frac{R_{fout}}{n_o}\right) + \frac{1}{n_o h_o} \qquad \text{B.2.10}$$

Where R_{wall} represent the wall conduction resistance:

$$R_{wall} = \frac{\ln\left(r_{cndo} \,/\, r_{condi}\right)}{2\,\pi\, L_{cnd}\, k_{wall}} \qquad \text{B.2.11}$$

The overall fin efficiency, n_o , for the external coiled fins attached to refrigerant coiled tubes are similar to evaporator fins and likewise the specific fin efficiency is set at 95%.

$$n_o = 1 - (A_{finrat}\ (1 - n_{fin})) \qquad \text{B.2.12}$$

Refrigerant Tube Side Heat Transfer Coefficient - h_i

In order to closely approximate the full heat transfer process between the air and steam refrigerant, the heat transfer coefficient must include the two phase process of the steam converting from gas to liquid. Shah's correlation of condensation inside tube ducts under forced convection is applied to fully convey the process which the air cooled condenser is undergoing. Since there is full condensation of the steam refrigerant in the condenser, the bulk properties inside the condenser were set at 0.5 quality. The analysis combines the vapor heat transfer coefficient with the liquid state shown below:

$$h_{tliq} = 0.023\ \left(\frac{G_{refcnd}\ (1\ -\ x)\ d_{tin}}{\mu_{tliq}}\right)^{0.8} \frac{Pr^{0.4}\ k_{refliq}}{d_{tin}} \qquad \text{B.2.13}$$

where the mass flux, G_{refcnd} , and the Prandtl number are defined as:

$$G_{refcnd} = \frac{m_{refcnd}}{\sigma_{cnd}\ L_{cnd}\ H_{cnd}} \qquad \text{B.2.14}$$

$$Pr = \mu_{tliq}\, cp_{tliq} / k_{tliq} \qquad \text{B.2.15}$$

and with steam's total convective steam heat transfer coefficient from superheat to liquid.

$$h_i = H_{tliq}\ \left(0.55 + \frac{2.09}{Pr^{0.38}}\right) \qquad \text{B.2.16}$$

Air Side Heat Transfer Coefficient - h_o

The air side convective heat transfer coefficient is determined using Kay's experimental results from the heat exchangers chosen for this analysis. The friction factor, f, and the Stanton-Prandtl Number, $StPr^{2/3}$, are measured from Figure 4.3.2 in Chapter 4 to better approximate the heat transfer coefficient based on air's Reynolds number. The mass flux of air can be determined using the evaporator's free flow to frontal area ratio and front area dimensions:

$$G_{aircnd} = \frac{m_{airfan}}{\sigma_{cnd} L_{cnd} H_{cnd}} \qquad \text{B.2.17}$$

$$Re_{air} = \frac{\left(G_{aircnd} \, d_h \right)}{\mu_{air}} \qquad \text{B.2.18}$$

The air heat transfer coefficient for the condenser can be determined by the following equation:

$$h_{air} = G_{aircnd} \, cp_{humair} \, St \qquad \text{B.2.19}$$

Airflow Pressure Drop

The condenser/radiator fan is designed to handle certain static pressure increases while achieving the desired volumetric flow rate. The fan's efficiency is optimized based on designing the blades and shroud leading into the fan based on the additional static pressure measured or calculated across the heat exchangers being cooled. This process aids in producing the desired volumetric flow rate from the fan. The scope of the project does not involve designing or optimizing fan performance and solely attains the performance of a conventional radiator fan designed and optimized at 0.02 psi (130 Pa) static pressure. The static pressure rise for the coiled finned circular tube evaporator is the pressure drop calculated across the heat exchanger (Kakac, 2002):

$$\Delta P_{aircnd} = \frac{G_{aircnd}^{\ 2}}{2\rho_i}\left[\left(f_{air}\ \frac{A\,\rho_i}{A_{min}\,\rho} + \left(1+\sigma^2\right)\left(\frac{\rho_i}{\rho_o} - 1\right)\right)\right] \qquad \text{B.2.20}$$

where average density, ρ, is estimated:

$$\frac{1}{\rho} = \frac{1}{2}\left(\frac{1}{\rho_i} + \frac{1}{\rho_o}\right)$$

The outlet air densities are dependent on the allowable air temperature increase mentioned in boundary conditions section of this appendix.

B.3 BMW 530i Exhaust Gas Temperature Correlations

The data provided by the BSST and BMW team of the BMW 530i sedan exhaust gas system and corresponding measured temperatures are critical in the waste heat ejector air conditioning system. The challenge in the exhaust waste heat assisted air conditioning system is to collect the data of gas temperatures based on the engine rpm, engine load, and interpolate an estimate of the speed of the car at those points specifically during idling and 50 mph in the case of this air conditioning analysis.

Speed of Car and RPM Correlation

Data from the Car and Driver test and specifications from the BMW website on the BMW 530i sedan aid in calculating engine performance along with friction losses and aerodynamic drag. The theoretically speed of the car without losses was calculated based on engine's rpm and transmission and rear gear ratios. The BMW 530i contains a six speed transmission where each gear contains a different transmission ratio, R_{tran}, to apply specific torque for acceleration. For a cruising speed of 50 mph, the fifth gear was chosen along with the 3.15 rear gear ratio, R_{rear}, where the vehicle's final speed is dictated by the rear wheel drive, R_{drive}. The use of the Dunlop SP Sport 01 DSST, 245/40WR-18 tires on the BMW 530i gives the vehicle a wheel diameter of 18 inches and an outside tire diameter, D_{tire}, of 25.7 inches. The equation used for determining final speed, V_{car} based on engine rpm, E_{RPM}, is:

$$R_{drive} = E_{RPM} / (R_{tran}\, R_{rear}) \qquad \text{B.3.1}$$

where the distance traveled in inches per minute, L_{rev} , is determined through multiplying the rear drive with the tire circumference.

$$L_{rev} = \pi * D_{tire} * R_{drive} \quad \text{B.3.2}$$

Finally the resultant converted from in/min to mph:

$$Vel_{car} = L_{rev} * (60 / 63, 630) \quad \text{B.3.3}$$

The theoretically velocity based on the engine's revolutions per minute, rpm, is correlated with the indicated power output or indicated horsepower under the same engine rpm with BMW 530i's engine specs. The net power output, E_{hp} , can be determined using the design parameters below. (Heisler, 1995)

P_{engc} = mean effective pressure
D_{cyl} = diameter of cylinders
L_{str} = length of cylinder stroke
N_{str} = Number of effective strokes
N_{cyl} = Number of engine cylinders

$$E_{hp} = P_{engc}\, \pi\, D_{cyl}^{\,2}\, L_{str}\, N_{str}\, N_{cyl}\, E_{RPM} \,/\, 4 * 60 \quad \text{B.3.4}$$

The BMW 530i specifications chart state that the max engine horsepower produced at 6600 rpm was 255 horsepower and checking with equation B.3.4 above, the values are within 5 % with a calculated value at 6600 of 247 horsepower. Further calculations were made to determine what power is required to overcome aerodynamic drag and rolling resistance at 50 mph cruising speeds. The results would be the minimum energy required from the vehicle's engine to sustain the cruising speed with no acceleration of 50 mph. The total drag resistance is a combination of aerodynamic and rolling resistance (Fox, 2001):

$$F_D = c_{fr}\, m_{veh}\, g + \tfrac{1}{2}\, \rho_{air}\, A_{fveh}\, c_{fd}\, V_{veh}^{\,2} \quad \text{B.3.5}$$

$$P_D = F_D * Vel_{veh} \quad \text{B.3.6}$$

Table B.1 Calculations of the 2005 BMW 530i's speed under flat road conditions traveling in the 5th gear of a six gear transmission.

BMW 530i Sedan Engine RPM vs. Vehicle Speed under Flat Road Conditions						
Engine Speed (rpm)	Engine Power (hp)	Ideal Vehicle Speed (mph)	Vehicle Speed after 6% Transmission Loss	Vehicle Speed after Trans. & Drag Losses	Aero Drag Loss (hp)	Total Drag Loss [Aero and Rolling Resistance (hp)]
3000	110.39	72.21	67.88	**58.85**	13.643	14.683
2800	103.03	67.4	63.36	**55.89**	11.092	12.132
2600	95.67	62.58	58.83	**52.73**	8.881	9.921
2400	88.31	57.77	54.3	**49.37**	6.985	8.025
2200	80.95	52.96	49.78	**45.83**	5.380	6.420
2000	73.59	48.14	45.25	**42.13**	4.042	5.082

The final speed highlighted in bold in Table B.3.1 is based on the added inefficiency in power due to added resistance of transmission losses and aerodynamic drag force losses that are factored in a moving vehicle. The linear relationship shown in equations B.3.1 and B.3.4 between the engine rpm and engine horse power corresponds directly with the rear drive of the vehicle while all of the design parameters are kept constant. The loss power due to transmission and drag force losses are factored with the total engine power in equation B.3.4 to determine the actual engine rpm and vehicle speed in the fifth gear of the BMW 530i six gear transmission.

Courtesy of BMW:

Engine:	Gasoline inline 6 cylinder
Vehicle:	BMW 530i
Displacement:	2996 ccm
Compression ratio	10.7
Max Power	255 hp @ 6600 rpm
Max Torque	243.4 lbf-ft @ 2500 rpm

Additional Nomenclature

A_{fveh}	Frontal Area of Vehicle
c_{fd}	Coefficient of Drag created by vehicle
c_{fr}	Coefficient of Vehicle Rolling friction
E_{RPM}	Engine's Cylinder Stoke Revolution per Minute
F_D	Total Drag Force
m_{veh}	Mass of Vehicle
P_D	Total Power Loss due Drag Force
Vel_{veh}	Velocity of Vehicle

B.4 Exhaust Waste Heat Primary Shell & Tube Heat Exchanger (PHX)

The preliminary analysis for sizing and rating of the automobile's waste exhaust gas heat exchanger is managing the lower specific heat from exhaust gas and providing enough heat transfer to the higher specific heat of steam. The automotive exhaust system contains a number geometric limitations and constraints explained in Section 4.6 that force the waste heat recovery system to be comprised of two heat exchangers. Thermodynamically under adiabatic conditions with no heat loss to the outside surroundings and following the energy equation, the heat needed to evaporate and superheat the steam refrigerant for the ejector's motive fluid must equal the heat lost and transferred from the exhaust gas to the steam. The energy equation is then simplified to:

$$Q_{refphx} = m_{ref} (I_{refphxi} - I_{refphxo}) \quad \text{B.4.1}$$

$$Q_{refphx} = Q_{exhphx} = m_{exh} \; cp_{exh} (T_{exhphxi} - T_{exhphxo}) \quad \text{B.4.2}$$

The limitations existing in the exhaust system that make it difficult to thermodynamically design the system is the exhaust gas low specific heat and low mass flow rate from the automobile's engine as shown in Figure 4.6.2. The combination of low specific heat and mass flow rates forces a large exhaust gas temperature gradient in equation B.4.2 in order facilitate the heat transfer. A second limitation is the catalytic converter in the exhaust system needs to operate above 582°F (300°C) (Heisler, 1995). That temperature is the median temperature of the exhaust system and hence why the converter lies geometrically in the middle of the exhaust system. The exhaust system for the BMW 530i also contains two mufflers which limits the length of the heat exchangers. Finally as mentioned in previous chapter, the diameter of the shell and tube heat exchange is limited to 10 inches due to

the fact that the exhaust piping is low to the ground. The combination of these limitations forces the system to have two heat exchangers in front and behind the catalytic converter. As shown in Figure 4.6.6, the exhaust shell and tube heat exchanger lies behind the catalytic converter while the super heater lies in front and closer to the car's engine with the higher exhaust gas temperatures.

As shown in Figure 4.6.1, the average exhaust gas mass flow rate during the New European Drive Cycle (NEDC) is 15 grams per second in which during the idling condition it was kept as the maximum. For the 50 mph condition, the exhaust gas mass flow was kept constant at 25 grams per second. The exhaust gas temperature gradient was calculated in advance to make sure that there was enough heat generated by the engine exhaust for the steam refrigerant. Modifications were conducted to enable proper sizing and heat transfer in the two heat exchangers in order for the steam refrigerant to reach from the sub-cooled state to the superheated steam state as it passed through the exhaust system. As a result, the exhaust primary heat exchanger (PHX) was designed to only partially vaporize the steam refrigerant to 70 percent quality due to the limitations mentioned above and the large enthalpy gradient in equation B.4.1 for steam's latent heat of vaporization.

Equation B.4.2 was calculated with known inlet and outlet steam enthalpy and exhaust gas temperatures to determine thermodynamically the minimum exhaust gas mass flow rate to provide enough heat to superheat the steam refrigerant. Higher increased heat transfer coefficient can be accomplished through increased shell diameter, baffle spacing, or number of tube passes. To withhold the constant pressure boundary condition across the heat exchanger, modifications for proper heat exchanger design were made to change the variables that minimize the amount of pressure drop.

Inputs from the pump function of the steam refrigerant's exit entropy, enthalpy, pressure, and temperature were taken with no losses to the environment and set equal to the exhaust heat exchanger's inlet refrigerant properties.

$I_{refphxi} = I_{refpmpo}$

$S_{refphxi} = S_{refpmpo}$

$T_{refphxi} = T_{refpmpo}$

The temperature of the refrigerant exiting the pump was set to two degrees below the saturation temperature. Using the XSteam function in MATLAB, the exit steam refrigerant's enthalpy and entropy were calculated when assigning the exit temperature and quality of steam of 0.7 at the exit of the heat exchanger.

$I_{refphxo}$ found using ($T_{refphxo}$, x)

$S_{refphxo}$ found using ($T_{refphxo}$, $I_{refphxo}$)

Rating and Sizing of Exhaust Primary Heat Exchanger (PHX)

The transfer of heat from the exhaust gas to partially vaporize the steam refrigerant to 0.70 quality will be facilitated using a shell and tube heat exchanger. In order to capture that process, the proper surface area along with adequate convection and conduction coefficients of the two fluids along with the heat exchanger's wall and fouling resistances need to be analyzed and optimized. The overall heat transfer equation, consisting of all these variables, is defined as,

$$Q_{phx} = U_{phx} A_{phx} \Delta T_M \qquad \text{B.4.3}$$

where the mean temperature $\Delta T_{M,}$ is calculated using the log mean temperature difference (LMTD), $\Delta T_{LMTD,}$ for a more accurate average temperature approximation during heat transfer process. The LMTD process is defined as:

$$\Delta T_M \approx \Delta T_{LMTD} = \frac{\left(T_{refphxo} - T_{refphxi}\right) - \left(T_{exhphxi} - T_{exhphxo}\right)}{\ln\left[\left(T_{refphxo} - T_{refphxi}\right) / \left(T_{exhphxi} - T_{exhphxo}\right)\right]} \quad \text{B.4.4}$$

The inlet and outlet temperatures for both fluids are determined and to calculate the total surface area, A_{hex}, in equation B.4.3. The overall heat transfer coefficient can be estimated using equation:

$$U_{phx} = \frac{A_{shell}}{A_{tube}}\left(\left(\frac{1}{n_t h_t}\right) + \left(\frac{R_{ftube}}{n_t}\right)\right) + A_{shell} R_{fshell} + \left(\frac{R_{fshell}}{n_{shell}}\right) + \frac{1}{n_{shell} h_{shell}} \quad \text{B.4.5}$$

which can be simplified using Gnielinski's correlation (Kakac 314):

$$U_{phx} = \frac{d_{tout}}{d_{tins} h_t} + \frac{d_{tins} \ln\left(d_{tout} / d_{tins}\right)}{2k_t} + \frac{d_{tout} R_t}{d_{tins}} + R_{shell} + \frac{1}{h_{shell}} \quad \text{B.4.6}$$

Thermal properties of exhaust gas and steam refrigerant of specific heat, density, thermal conductivity, and kinematic and dynamic viscosities were measured at bulk temperature properties:

$$T_{exhblk} = \frac{T_{exhi} + T_{phxrefsat}}{2} \quad .$$

The steam refrigerant properties were taken at the median of the vapor quality at saturation temperature of the exhaust heat exchanger's 0 to 0.7 vapor quality

$$T_{phxrefblk} = T_{phxrefsat} \text{ @ } x = 0.35$$

The wall temperature for tube and shell side was set to median of fluids' inlet temperatures:

$$T_{wall} = \frac{T_{exhi} + T_{phxrefsat}}{2}$$

Before starting the shell sizing and design stages, the tube conditions were given existing geometric parameters to conduct preliminary analysis.

Table B.2 Shell and tube heat exchanger design for exhaust loop primary heat exchanger (PHX) with recommendations and referencing from Kakac.

Primary Heat Exchanger Design and Material Selection

Tube inside diameter	0.75 in.
Tube outside diameter	0.68 in.
Square tube pitch	1 in.
Number of Tube Passes	2
Baffle Spacing	0.45 * Shell Diameter
Baffle Cut	25%
Number of Tube Passes	2
Number of Shell Passes	1
Tube Material	Copper
Shell Material	Aluminum
Length	16 in.

Based on the two tube pass and one shell pass design shown in Figure B.4.1, the LMTD correction factor, F, will be in the 0.95 to 1 range due to the existing condition of the high temperature gradient in the hot fluid (ΔT_h) of the exhaust gas compared to a few degrees gradient in steam changing phase from sub-cooled to saturated vapor at constant temperature. The correction factor does not represent a means of determining an efficient heat exchanger but that when the correction Factor, F, equals 1 the heat exchanger resembles a counterflow behavior (Kakac, 2002). The CTP and CL are the tube count and tube layout calculation constant which accounts for the incomplete coverage of the shell diameter by the tubes due to necessary clearances between the shell and the outer tube circle and the tube omissions suitable with the tubes' pass lanes for multi-tube pass design (Kakac, 2002)

CL = 1.0 for 90 degrees and 45 degrees

CTP = 0.90 for two tube passes

The shell and tube exhaust heat exchanger contains unknown geometric parameters such as the diameter size of the cylindrical shaped heat exchanger, number of tubes inside, and velocity of the steam refrigerant inside the tubes where an initial estimate of one of variables is necessary to solve for the rest. Since there are no typical references to sizing a heat exchange for this application, two types of methods of calculating for these geometric parameters were used for convergence to determine the best overall parameter. The two types of methods are the Kern method and LMTD method where Kern method uses pre process of initial design and fluid properties parameters to calculate unknown geometric parameters.

The Kern method (2 equations 3 unknowns – N_T , $D_{shellprim}$, u_m)

$$M_{ref} = \rho_{ref}\, u_m \;\; A_{tcrss}\, N_T \qquad \text{B.4.7}$$

$$D_{shellprim} = \sqrt{\frac{\left(N_T\,(CL)\left(P_{RT}\right)^2\, d_{tout}{}^2\right)}{\left(0.785\left(CTP\right)\right)}} \qquad \text{B.4.8}$$

The initial design estimate of the shell diameter was used to solve for heat exchanger's number of tubes and steam refrigerant velocity in equation B.4.7 and B.4.8.

In order to capture an accurate result for the convection heat transfer rate for the tube side steam refrigerant under partial evaporation phase, Gnielinski correlation is applied. The calculation of the Reynolds number in the liquid phase will determine whether the refrigerant is turbulent ($2300 < Re_{tliq} > 100{,}000$) or laminar ($Re_{tliq} < 2300$). The calculation for the Reynolds number:

$$Re_{tliq} = \frac{\left(G_{phxtube}\ d_{tins} \right)}{\mu_{tliq}} \qquad \text{B.4.9}$$

where $G_{phxtube}$ equals the mass flux of steam refrigerant (lb/min-ft^2):

$$G_{phxtube} = \frac{M_{ref}}{A_R} \qquad \text{B.4.10}$$

with the equivalent area based on number of tubes and passes expressed:

$$A_R = \frac{A_{tcrss}\ N_T}{N_P} \qquad \text{B.4.11}$$

and the cross-sectional area:

$$A_{tcrss} = \frac{\pi\left(d_{tin}^{\ 2}\right)}{4}$$

If the Reynolds number reveals that the flow is turbulent, the boiling factor, Prandtl and Nusselt number are calculated under Gnielinski correlation:

$$f_{boil} = ((1.58 * \ln(Re_{tliq})) - 3.28)^{-2} \qquad \text{B.4.12}$$

$$Pr_{tliq} = \frac{\left(\mu_{tliq} cp_{tliq} \right)}{k_{tliq}} \qquad \text{B.4.13}$$

$$Nu_{tliq} = \frac{\left(\left(f_{boil} / 2 \right) \left(Re_{tliq} - 1000 \right) Pr_{tliq} \right)}{\left(1 + \left(12.7 \left(f_{boil} / 2 \right)^{1/2} \left(Pr_{tliq}^{\ 2/3} - 1 \right) \right) \right)} \qquad \text{B.4.14}$$

If the Reynolds number is below 2300 making the flow inside the tubes laminar, the Seider and Tate correlation is used as long as these conditions are satisfied:

$$\left(\frac{Re_{tliq}\ Pr_{tliq}\ d_{tin}}{L_{phx}} \right)^{1/3} \left(\frac{\mu_{tblk}}{\mu_{wall}} \right)^{0.14} > 2$$

and

$$\frac{\mu_{tblk}}{\mu_{wall}} < 9.75$$

The laminar Nusselt number can be found using equation:

$$Nu_{tliq} = 1.86 \left(\frac{Re_{tliq} \; Pr_{tliq} \; d_{tin}}{L_{phx}} \right)^{1/3} \left(\frac{\mu_{tblk}}{\mu_{wall}} \right)^{0.14} \qquad \text{B.4.15}$$

Once the laminar or turbulent Nusselt number is calculate the liquid phase convection heat transfer coefficient can be determined:

$$H_{tliq} = \frac{Nu_{tliq} \; k_{tliq}}{d_{tin}} \qquad \text{B.4.16}$$

The next step after calculating the liquid phase convection heat transfer coefficient is to include the boiling vapor coefficient using Shah's correlation which are based on four dimensionless parameters, Froude number (Fr), convection number (Co), boiling number (Bo), and enhancement factor F. These four dimensionless parameters are used to characterize the flow and employed to estimate the two-phase boiling convective contribution (Kakac, 2002). The Froude number which determine whether stratification is negligible or not is defined as:

$$Fr = \frac{G_{tliq}^{\;2}}{\rho_{tliq}^{\;2} \; g * d_{tin}} \qquad \text{B.4.17}$$

If the Froude number, Fr, is greater than 0.04 then stratification is negligible and inertial forces dominant over gravitational forces and the correction factor, K_{FR} is set to 1. However if the Froude number is below 0.04, K_{FR} is defined as:

$$K_{FR} = (25 \; Fr)^{-0.3} \qquad \text{B.4.18}$$

The convection number, Co, is defined as:

$$Co = \left[\frac{(1-x)}{x}\right]^{0.8} \left(\frac{\rho_{tliq}}{\rho_{tvap}}\right)^{0.5} K_{FR} \qquad \text{B.4.19}$$

For pure convection boiling with high vapor qualities and low boiling numbers, the convection boiling factor is determined using:

$$F_{CB} = 1.8\ Co^{-0.8} \quad \text{when } Co < 1.0$$

and for low vapor qualities and low boiling numbers

$$F_{CB} = 1.0 + 0.8\, e^{[1-(Co^{0.5})]} \quad \text{when } Co > 1.0$$

Where $F = F_{CB}$ and the enhancement factor, F_o , can be calculated using:

$$F_o = F\ (1 - x)$$

Finally the overall convective boiling heat transfer coefficient is calculated combining the liquid convection heat transfer and the boiling enhancement factor:

$$H_{tcb} = F_o\ H_{tliq} \qquad \text{B.4.20}$$

Shell side Heat Transfer Coefficient

The shell side exhaust gas convection heat transfer coefficient under single phase condition uses shell diameter equivalent, D_{eq}, to determine flow's Reynolds number. The shell diameter is calculated is using tube diameter in relation to tube pitch (Kakac, 2002):

$$D_{eq} = \frac{4\,(Tb_{ptch}^2 - \frac{\pi\,(d_{tout})^2}{4})}{\pi d_{tout}} \qquad \text{B.4.21}$$

$$Re_{shell} = \frac{D_{eq}\left(\frac{m_{exh}}{A_{shell}}\right)}{\mu} \qquad \text{B.4.22}$$

where the inside area of the shell is determined through the Kern method's primary calculation on the shell diameter, clearance between tubes (C), baffle spacing (B), and tube pitch :

$$A_{shell} = D_{shellprim} * C * B / Tb_{ptch} \qquad \text{B.4.23}$$

Where the heat transfer coefficient is calculated using

$$H_{shell} = (0.36\, k_{exh} / D_{eq})\, Re_{shell}^{0.55} Pr_{shell}^{1/3}$$

And plugged back into equation B.4.6:

$$U_{phx} = \frac{d_{tout}}{d_{tins} h_t} + \frac{d_{tins} \ln\left(d_{tout} / d_{tins}\right)}{2k_t} + \frac{d_{tout} R_t}{dt_{ins}} + R_{shell} + \frac{1}{h_{shell}}$$

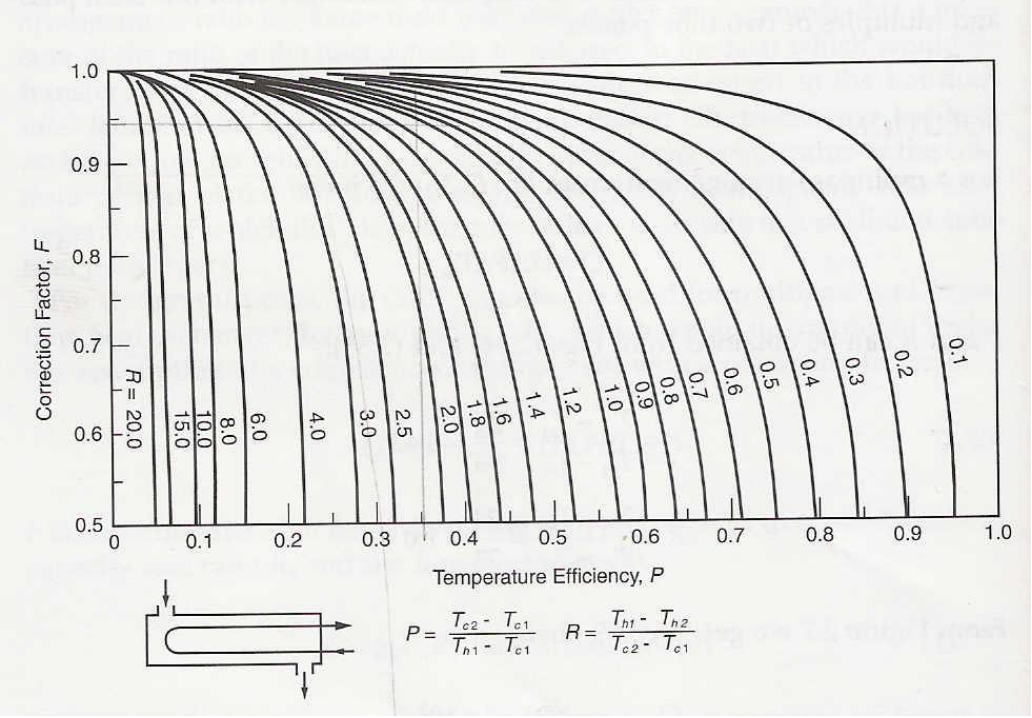

Figure B.4 LMTD correction factor F_{hex} for a shell and tube heat exchanger with one shell pass and two or multiple of two tube pass. © Tubular Exchanger Manufacturers Association.

The original heat equation as mentioned before in equation B.4.3 has been modified to better approximate the heat transfer based on log based method of finding the mean temperature and accounting for the temperature efficiency and heat capacity rate between the fluids with the LMTD correction factor. Once F_{hex} is determined, the total heat transfer area can be determined using equation B.4.24.

$$Q_{ref} = U_{phx} A_{phx} F_{phx} \Delta T_{LMTD} \qquad \text{B.4.24}$$

The length of heat exchanger is kept constant at 16 inches allowing for the unknown shell diameter and number of tubes to be determined by using LMTD method equations:

$$D_{shell} = 0.637 \sqrt{\frac{CL}{CTP}} \left(\frac{A_{phx} \left(P_{RT}\right)^2 d_{tout}}{L_{phx}} \right)^{1/2} \qquad \text{B.4.25}$$

$$N_T = \frac{A_{phx}}{\pi \, d_{tout} \, L_{phx}} \qquad \text{B.4.26}$$

The Kern method preliminary design dimensions that determined the shell-side and tube-side heat transfer coefficients used in the LMTD analysis were compared with the calculated LMTD's shell diameter, refrigerant velocity and number of tubes dimensions. This aided to verify if the initial design dimensions matched the calculated LMTD results. If the Kern and LMTD dimensions were within 7% variance from each other or below, the results are final and the LMTD results are taken. If the shell diameter dimensions didn't fall in the percent difference range, the Kern method's initial dimensions were modified and heat transfer coefficients were recalculated until the 5-7% percentage difference was reached. Error analysis was conducted on the variance between the LMTD and Kern method for sizing and rating of the primary heat exchanger.

Tube-side Pressure Drop

The tube side pressure drop across the shell and tube heat exchanger can be calculated using the number of passes, length of heat exchanger, and velocity of refrigerant. The total pressure drop is a calculation of the refrigerant moving through the tubes along with the sudden expansions and contractions during the bends of the tube return (Kakac, 2002).

$$\Delta P_{tubetotal} = \Delta P_t + \Delta P_{return} \qquad \text{B.4.27}$$

Where pressure through the tubes, ΔP_t , is expressed:

$$\Delta P_t = 4\, f_t \frac{L_{phx} N_p G_{refphx}^{\ 2}}{\left(d_{tins}\ 2\, \rho_{ref}\right)} \qquad \text{B.4.28}$$

And the return pressure drop:

$$\Delta P_{return} = 4\, N_p \frac{\rho_{ref} Vel_{ref}^{\ 2}}{2} \qquad \text{B.4.29}$$

The results from the tube side pressure drop revealed a 0.15 psi maximum pressure drop and were considered negligible in the pumping power analysis.

B.5 Exhaust Waste Heat Superheater Shell and Tube Heat Exchanger

The superheater (SPR) is a continuation of the primary heat exchanger (PHX) on the upstream side of the catalytic converter and closer to the engine exhaust manifold. This allows the higher temperature exhaust gas to super heat the steam refrigerant. The heat from the exhaust gas is used to fully evaporate the steam from 0.7 quality to superheated steam at 530°F. This super heated steam will be the ejector's motive fluid through the supersonic nozzle. With known exhaust temperatures from the BMW 530i sedan at the location of the superheater, known

superheater inlet and outlet steam enthalpy, and calculated required heat gain for steam refrigerant, Q_{refspr} , to thermally power the pressure exchanger ejector, the minimal exhaust gas mass flow rate is calculated. The energy equation under adiabatic conditions is then simplified to:

$$Q_{refspr} = m_{ref}(I_{refspri} - I_{refspro}) \quad \text{B.5.1}$$

$$Q_{refspr} = Q_{exhspr} = m_{exh}\ cp_{exh}\ (T_{exhspri} - T_{exhspro}) \quad \text{B.5.2}$$

Similar to the PHX, the diameter of the shell and tube heat exchange is limited to 10 inches due to the fact that the exhaust piping is low to the ground With exhaust gas mass flow rate kept constant through the exhaust system, the average mass flow rate during the New European Drive Cycle (NEDC) is 15 grams per second and kept as the maximum for the idling condition. Likewise the exhaust gas mass flow rate during the 50 mph condition was kept constant through the Superheater at 25 grams per second.

.Inputs from the exhaust PHX function were imported and consisted of the steam refrigerant's exit entropy, enthalpy, pressure, and temperature were taken with no losses to the environment and set equal to the exhaust Superheater's inlet refrigerant properties.

$$I_{refspri} = I_{refphxo}$$

$$S_{refspri} = S_{refphxo}$$

$$T_{refspri} = T_{refphxo}$$

Rating and Sizing of Super Heater Heat Exchanger (SPR)

The same procedure for the rating and sizing of the primary heat exchanger (PHX) was used for the superheater. The only difference is the length of heat exchanger due to lower heat transfer rate when superheating steam with sensible heat.

The log mean temperature difference along with its counterflow correction factor is applied. The only difference is steam's tube side heat transfer coefficient that is treated as a single phase heat transfer due to the fact that the steam is already close to being completely evaporated in the vapor state when entering at 0.7 quality. The exhaust gas thermal properties of specific heat, density, thermal conductivity, and kinematic and dynamic viscosities were measured at bulk temperature properties:

$$T_{exhblk} = \frac{T_{exhi} + T_{exho}}{2} \quad .$$

The steam refrigerant bulk properties were taken at the median of the superheated region

$$T_{refsprblk} = \frac{T_{refspri} + T_{refspro}}{2}$$

The wall temperature for tube and shell side was set to median of fluids' inlet temperatures:

$$T_{wall} = \frac{T_{exhspri} + T_{refspri}}{2}$$

Tube Side Heat Transfer Coefficient

The MATLAB program determines the Reynolds number of the steam vapor using its bulk properties and checks whether the flow is turbulent or laminar. A Reynolds number between 2300 and 10^4 in the transition region or above is considered turbulent forced flow and Gnielinski correlation through circular ducts with constant properties is recommended (Kakac, 2002).

$$Re_{tblk} = \frac{\left(G_{tspr} \; d_{tins} \right)}{\mu_{tblk}} \qquad \text{B.5.3}$$

Where G_{tspr} equals the mass flux of steam refrigerant

$$G_{tspr} = \frac{M_{ref}}{A_R} \qquad \text{B.5.4}$$

with the equivalent area based on number of tubes and passes expressed:

$$A_R = \frac{A_{tcrss}\ N_T}{N_P} \qquad \text{B.5.5}$$

and the cross-sectional area:

$$A_{tcrss} = \frac{\pi\left(d_{tin}{}^2\right)}{4}$$

The Nusselt number used in Gnielinski correlation for turbulent flow through circular ducts is expressed as:

$$Nu_{tblk} = \frac{(f/2)\left(Re_{tblk} - 1000\right) Pr_{tblk}}{1 + (12.7\ (f/2)^{1/2}\ (Pr_{tblk}{}^{2/3} - 1))} \qquad \text{B.5.6}$$

$$f = (1.58 \ln[Re_{tblk} - 3.28])^{-2} \qquad \text{B.5.7}$$

For laminar flow of Reynolds number below 2300, Nusselt-Graetz correlation is used where the Nusselt number is set at 3.66:

$$Nu_{tblk} = 3.66$$

The tube side convective heat transfer coefficient for the steam refrigerant in the Superheater can be calculated using the equation below:

$$H_{tspr} = h_t = \frac{Nu_{tblk}\ k_{tref}}{d_{tins}} \qquad \text{B.5.8}$$

Equations B.4.3-6 from PHX Appendix are then used for the superheater overall heat transfer calculations.

Before starting the shell sizing and design stages, the tube conditions below were given existing geometric parameters to conduct preliminary analysis.

Table B.3 Shell and tube heat exchanger design for exhaust loop Superheater (SPR) with recommendations and referencing from Kakac (2002).

Superheater Heat Exchanger Design and Material Selection

Tube inside diameter	0.75 in.
Tube outside diameter	0.68 in.
Square tube pitch	1 in.
Number of Tube Passes	2
Baffle Spacing	0.45 * Shell Diameter
Baffle Cut	25%
Number of Tube Passes	2
Number of Shell Passes	1
Tube Material	Copper
Shell Material	Aluminum
Length	30 in.

Similar to the PHX, the superheater contains unknown geometric parameters such as the diameter size of the cylindrical shaped heat exchanger, number of tubes inside, and velocity of the steam refrigerant inside the tubes. The Kern method using equations B.4.7 and B.4.8 and LMTD method are used to solve for the unknown parameters.

Shell side Heat Transfer Coefficient

Likewise with the PHX analysis, the shell side exhaust gas convection heat transfer coefficient is treated as an ideal gas and under single phase condition. The same equations (B.4.21-24) are used for superheater analysis.

The superheater designed with one shell pass and two tube passes uses Figure B.4.1 to determine its LMTD correction factor. Once F_{spr} is determined, the total heat transfer area can be determined using equation B.5.9.

$$Q_{ref} = U_{spr} A_{spr} F_{spr} \Delta T_{LMTD} \quad \text{B.5.9}$$

The length of superheater is kept constant at 30 inches allowing for the unknown shell diameter and number of tubes to be determined using

$$D_{shell} = 0.637 \sqrt{\frac{CL}{CTP}} \left(\frac{A_{spr} \left(P_{RT}\right)^2 d_{tout}}{L_{spr}} \right)^{1/2} \quad \text{B.5.10}$$

$$N_T = \frac{A_{spr}}{\pi \, d_{tout} \, L_{spr}} \quad \text{B.5.11}$$

The Kern method preliminary design dimensions that determined the heat transfer coefficients used for LMTD analysis are compared with the calculated LMTD's shell diameter, refrigerant velocity and number of tubes dimensions to see if the initial design dimensions match the calculated LMTD results. If the Kern and LMTD shell diameters dimensions are within 7% variance or below, the results are final and the LMTD results are taken. If the dimension didn't fall in the percent difference range, the Kern method's initial dimensions are modified until convergence is reached. Error analysis is conducted also for the superheater on the variance between the LMTD and Kern method.

Tube-side Pressure Drop

The tube side pressure drop for the superheater is calculated using equations B.4.27-29 from Appendix B.4 with superheater's corresponding number of passes for tube-side and shell-side fluids, length of heat exchanger, and velocity of refrigerant.

The results from the tube side pressure drop revealed a 0.20 psi maximum pressure drop and were considered negligible in the pumping power analysis.

Appendix C MATLAB XSteam Function by Magnus Holmgren

The Xsteam function for SI units and the XSteamUS function for British units written by Magnus Holmgren consist of variety of steam thermal and fluid dynamic functions capable of calculate specific properties based on input variables (In1 and In2).

Table C.1 List of functions used from XSteam MATLAB Program to attain steam thermal properties throughout analysis

XSTEAM CALLING FUNCTIONS

Temperature

Function	In1	In2	Out
Tsat_p	p		Saturation temperature
T_ph	p	H	Temperture as a function of pressure and enthalpy
T_ps	p	S	Temperture as a function of pressure and entropy
T_hs	h	S	Temperture as a function of enthalpy and entropy

Enthalpy

Function	In1	In2	Out
hV_p	p		Saturated vapour enthalpy
hL_p	p		Saturated liquid enthalpy
hV_T	T		Saturated vapour enthalpy
hL_T	T		Saturated liquid enthalpy
h_pT	p	T	Entalpy as a function of pressure and temperature.
h_ps	p	s	Entalpy as a function of pressure and entropy.
h_px	p	x	Entalpy as a function of pressure and vapour fraction
h_Tx	T	X	Entalpy as a function of temperature and vapour fraction
h_prho	p	rho	Entalpy as a function of pressure and density. Observe for low temperatures (liquid) this equation has 2 solutions. (Not valid!!)

Density

Function	In1	In2	Out
rhoV_p	p		Saturated vapour density
rhoL_p	p		Saturated liquid density
rhoV_T	T		Saturated vapour density
rhoL_T	T		Saturated liquid density
rho_pT	p	T	Density as a function of pressure and temperature.
rho_ph	p	h	Density as a function of pressure and enthalpy
rho_ps	p	s	Density as a function of pressure and entropy.

Specific entropy

Function	In1	In2	Out
sV_p	p		Saturated vapour entropy
sL_p	p		Saturated liquid entropy
sV_T	T		Saturated vapour entropy
sL_T	T		Saturated liquid entropy
s_pT	p	T	Specific entropy as a function of pressure and temperature (Returns saturated vapour entalpy if mixture.)
s_ph	p	h	Specific entropy as a function of pressure and enthalpy

Specific isobaric heat capacity

Function	In1	In2	Out
CpV_p	p		Saturated vapour heat capacity
CpL_p	p		Saturated liquid heat capacity
CpV_T	T		Saturated vapour heat capacity
CpL_T	T		Saturated liquid heat capacity
Cp_pT	p	T	Specific isobaric heat capacity as a function of pressure and temperature.
Cp_ph	p	h	Specific isobaric heat capacity as a function of pressure and enthalpy
Cp_ps	p	s	Specific isobaric heat capacity as a function of pressure and entropy.

Viscosity

Viscosity is not part of IAPWS Steam IF97. Equations from "Revised Release on the IAPWS Formulation 1985 for the Viscosity of Ordinary Water Substance", 2003 are used.

Viscosity in the mixed region (4) is interpolated according to the density. This is not true since it will be two fases.

Function	In1	In2	Out
my_pT	p	T	Viscosity as a function of pressure and temperature.
my_ph	p	h	Viscosity as a function of pressure and enthalpy
my_ps	p	s	Viscosity as a function of pressure and entropy.

Thermal Conductivity

Revised release on the IAPS Formulation 1985 for the Thermal Conductivity of ordinary water substance (IAPWS 1998)

Function	In1	In2	Out
tcL_p	p		Saturated vapour thermal conductivity
tcV_p	p		Saturated liquid thermal conductivity
tcL_T	T		Saturated vapour thermal conductivity
tcV_T	T		Saturated liquid thermal conductivity
tc_pT	p	T	Thermal conductivity as a function of pressure and temperature.
tc_ph	p	h	Thermal conductivity as a function of pressure and enthalpy
tc_hs	h	s	Thermal conductivity as a function of enthalpy and entropy

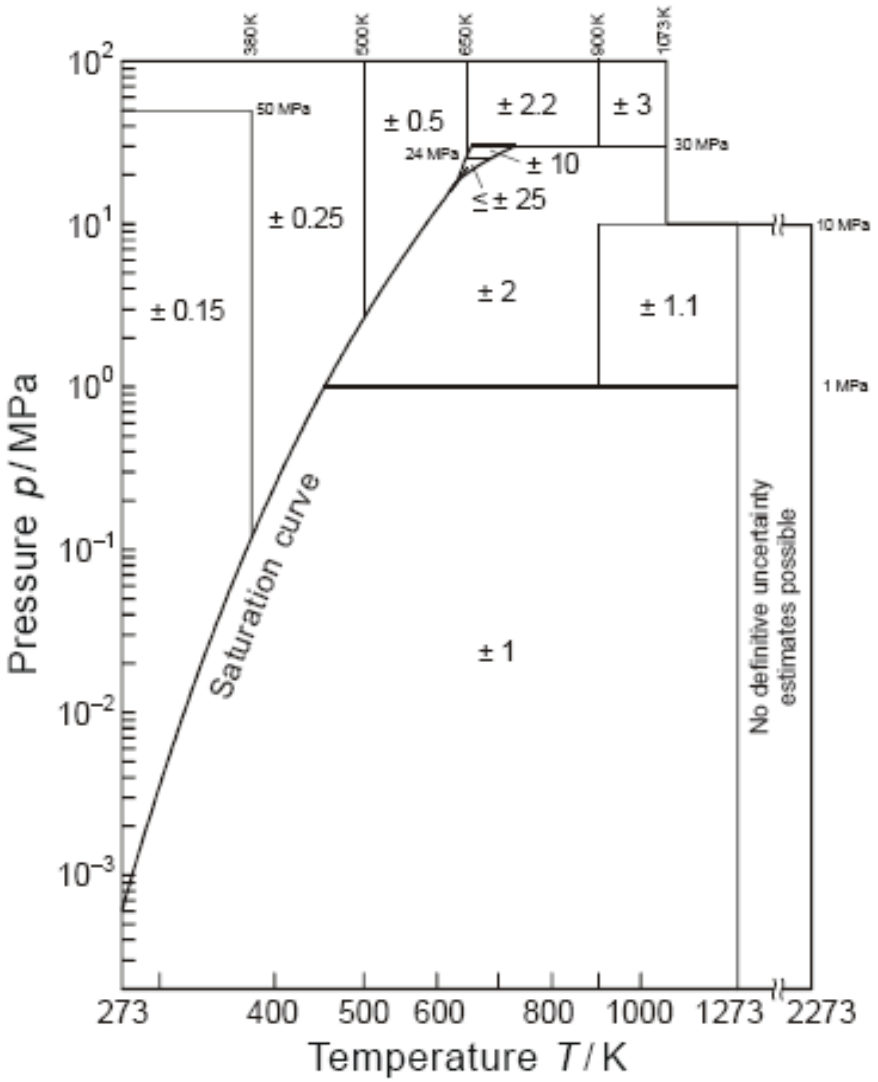

Figure C.1 Absolute uncertainties for specific enthalpy estimated for IAPWS-IF97 comparison in SI units. The position of the lines separating the uncertainty regions, marked by the given values of temperature and pressure are approximate.

Appendix D Steam Pressure Exchange Ejector A/C System Algorithms

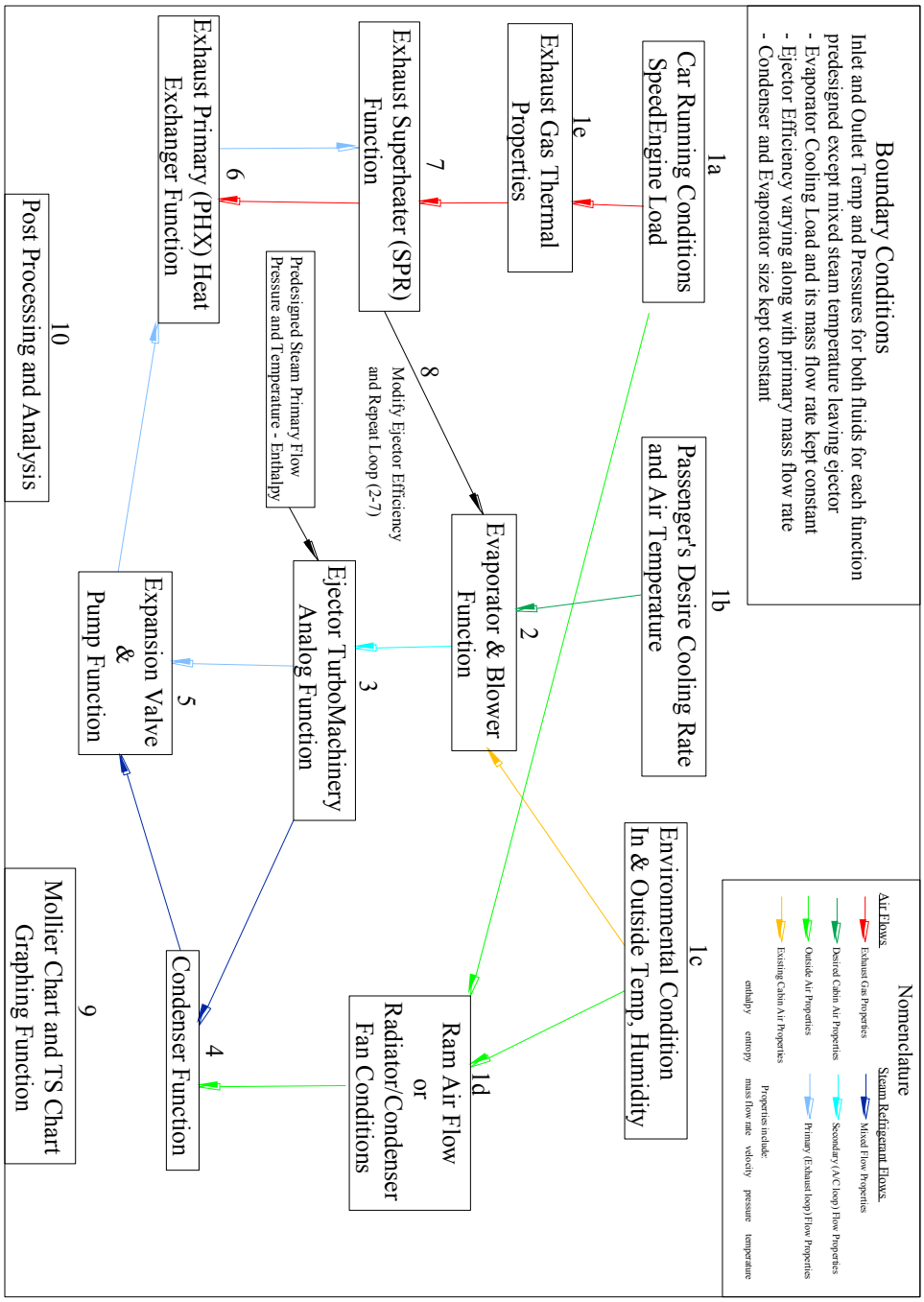

Figue D.1 Algorithm of Steam Ejector Auto A/C System using MATLAB and XSteam function with an interative loop on varying ejector efficiency.

Exhaust Waste Heat Recovery Primary Heat Exchanger Algorithm

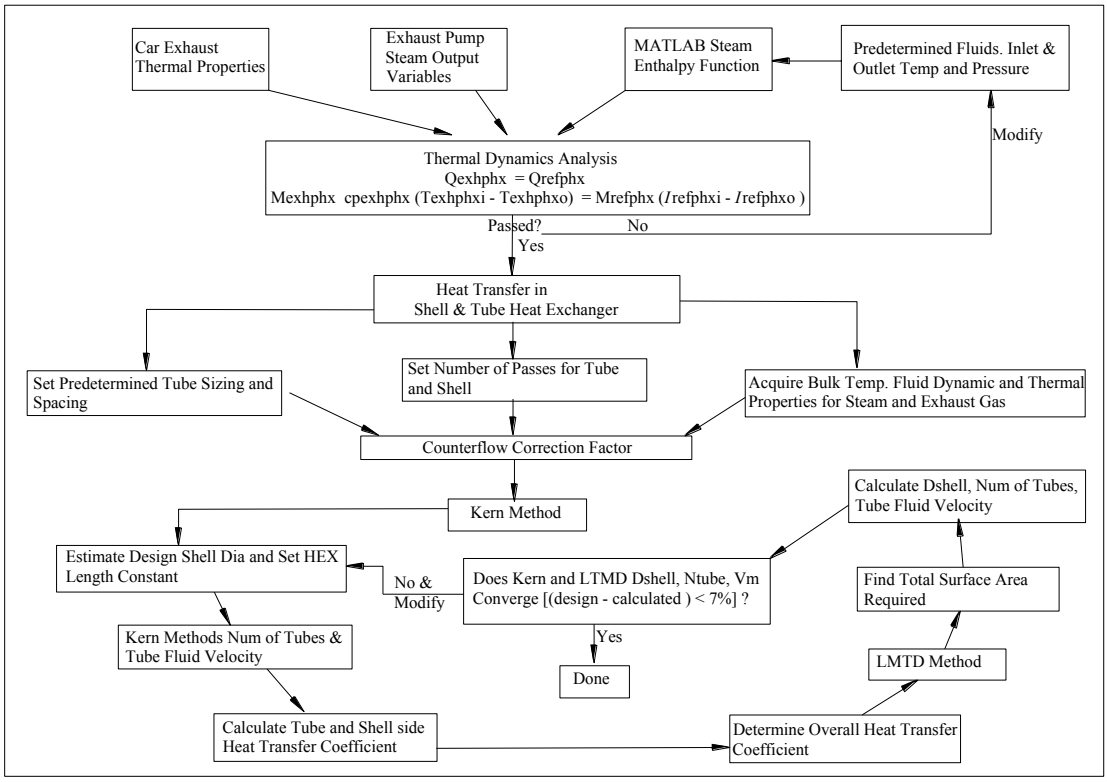

Figure D.2 Primary heat exchanger (PHX) algorithm to determine unknown shell diameter, number of tubes and steam velocity through tubes in the shell and tube heat exchanger design.

Exhaust Waste Heat Recovery Superheater Algorithm

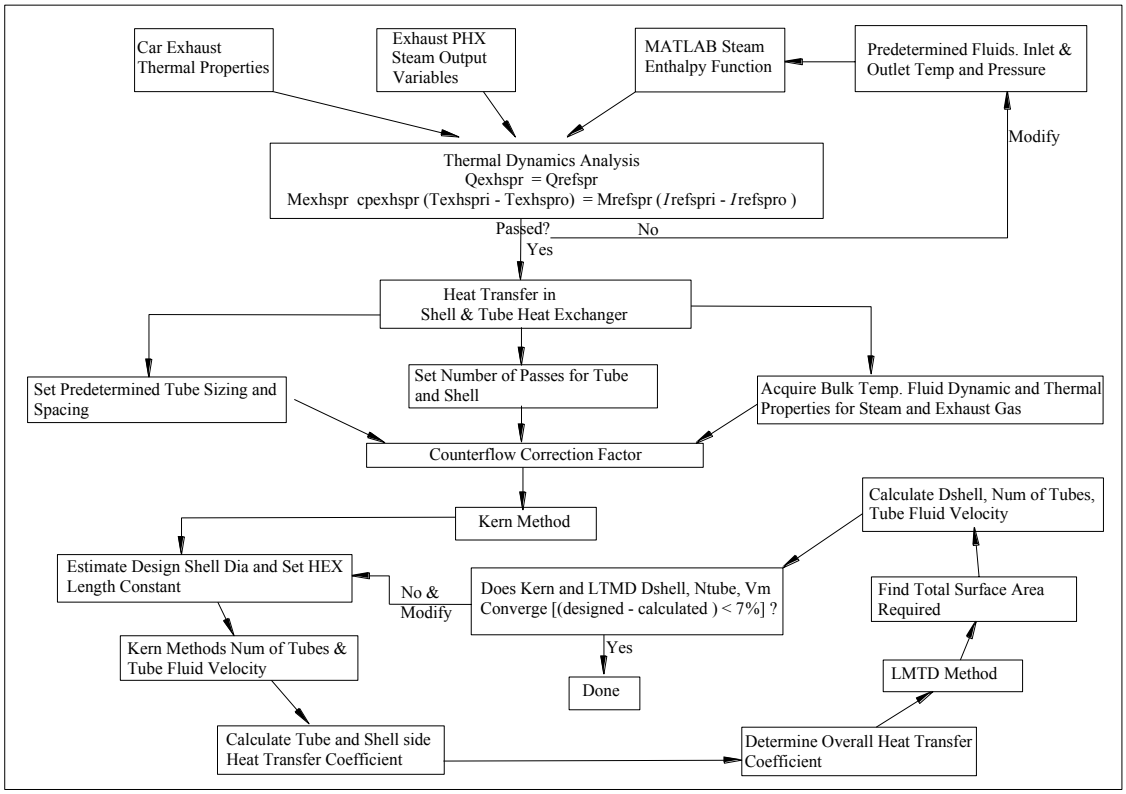

Figure D.3 Superheater (SPR) algorithm to determine unknown shell diameter, number of tubes and steam velocity through tubes in the shell and tube heat exchanger design.